CHEMICAL REVIEWS

pubs.acs.org/CR Review

Single-Cell Nanoencapsulation: Chemical Synthesis of Artificial Cell-in-Shell Spores

Hyeong Bin Rheem, Nayoung Kim, Duc Tai Nguyen, Ghanyatma Adi Baskoro, Jihun H. Roh, Jungkyu K. Lee, Beom Jin Kim,* and Insung S. Choi*

Cite This: https://doi.org/10.1021/acs.chemrev.4c00984 Read Online

ACCESS | Metrics & More | Article Recommendations

ABSTRACT: Nature has evolved adaptive strategies to protect living cells and enhance their resilience against hostile environments, exemplified by bacterial and fungal spores. Inspired by cryptobiosis in nature, chemists have designed and synthesized artificial "cell-in-shell" structures, endowed with the protective and functional capabilities of nanoshells. The cell-in-shells hold the potential to overcome the inherent limitations of biologically naïve cells, enabling the acquisition of exogenous phenotypic traits through the chemical process known as single-cell nanoencapsulation (SCNE). This review highlights recent advancements in the development of artificial spores, with sections organized based on the categorization of material types utilized in SCNE, specifically organic, hybrid, and inorganic types. Particular emphasis is placed on the cytoprotective and multifunctional roles of nanoshells, demonstrating potential applications of SCNEd cells across diverse fields, including synthetic biology, biochemistry, materials science, and biomedical engineering. Furthermore, the perspectives outlined in this review propose future research directions in SCNE, with the goal of achieving fine-tuned precision in chemical modulation at both intracellular and pericellular levels, paving the way for the design and construction of customized artificial spores tailored to meet specific functional needs.

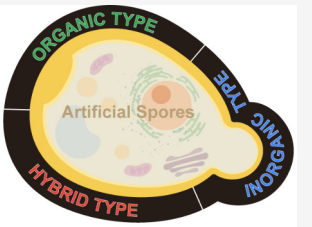

Single-Cell Nanoencapsulation (SCNE)

CONTENTS

1. INTRODUCTION

Nature has biologically evolved diverse adaptive-survival strategies to confront and cope with unpredictable, sporadic environmental challenges that threaten living organisms.[1−3] Notable examples include bacterial endospores, specialized cell-in-shell structures that acquire enhanced resistance to hostile conditions, such as desiccation, radiation, and extreme temperature.[4,5] These metabolically inactive, dormant spores can survive in a quiescent state for extended periods of time and germinate into vegetative cells when environmental conditions become favorable. On the darker side for human beings, the fungus *Cryptococcus neoformans* forms a cytoprotective chitin-

Received: December 18, 2024
Revised: April 15, 2025
Accepted: April 17, 2025

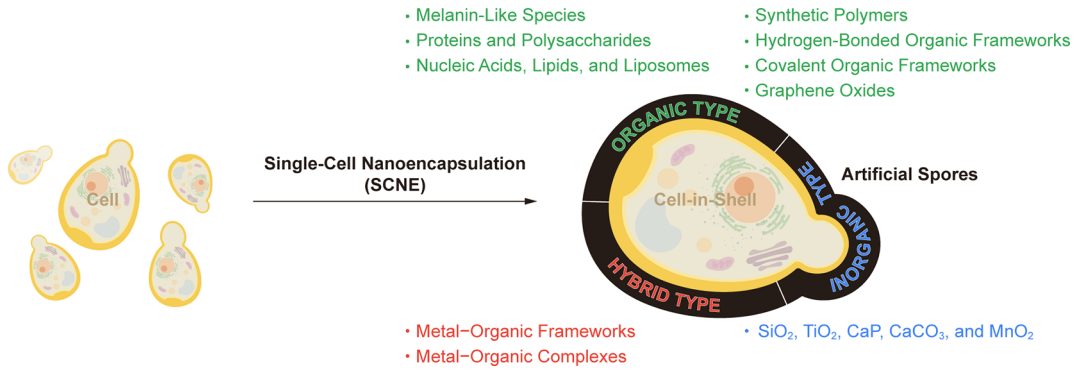

Figure 1. Classification of materials used in single-cell nanoencapsulation (SCNE) for artificial spore formation. The materials are divided into three main categories: organic, hybrid organic–inorganic, and inorganic. Organic materials include melanin-like species, proteins, polysaccharides, nucleic acids, lipids, liposomes, synthetic polymers, hydrogen-bonded organic frameworks, covalent organic frameworks, and graphene oxides. Hybrid materials comprise metal–organic frameworks and metal–organic complexes, and inorganic materials encompass SiO_2, TiO_2, CaP, $CaCO_3$, and MnO_2.

cross-linked melanin shell, utilizing L-3,4-dihydroxyphenylalanine (L-DOPA) from the brain as an exogenous precursor.[6−8] This cell-in-shell structure in *C. neoformans* enhances virulence and resilience against various factors, including UV and γ radiation, enzymatic degradation, and antimicrobial agents. Beyond single-celled organisms, tardigrades (commonly known as water bears) can enter an anhydrobiotic state under dehydrated conditions, contracting into a structure resembling a small tun with extruded wax.[9] In the depths of the ocean, the amphipod *Hirondellea gigas* adapts to high pressure by forming a shell of aluminum hydroxide gel,[10] exemplifying another remarkable adaptation of organisms in extreme environments.

Inspired by the nature's cryptobiosis strategies, chemists, materials scientists, and synthetic biologists have developed a research domain focused on the chemical synthesis of ultrathin (<100 nm), robust artificial shells on the surfaces of nonspore-forming microbial and mammalian cells.[11−17] This pioneering effort in single-cell nanoencapsulation (SCNE) has aims primarily to enhance the protection of cells (aka, cytoprotection) in both in vitro and in vivo environments, drawing inspiration from the remarkable resilience observed in bacterial endospores.[18−20] The resulting cell-in-nanoshell structures, termed artificial spores, emulate the pivotal characteristics of bacterial endospores, including suppressed cell division and heightened tolerance to environmental stressors.[21−23] The cell-in-shell nanobiohybrid structures are also referred to as micrometric "Iron Men", with particular emphasis on chemical sporulation and germination, achievable in a cytocompatible manner.[24] Over the past decade, numerous cytocompatible materials and protocols have been proposed to form artificial spores,[25] demonstrating various potential applications of SCNE, including cell therapy,[26−30] probiotics,[31−34] cell factories,[35] microbial fuel cells and renewable energies,[36,37] biocontrol agents and fertilizers,[38,39] and even cell robotics.[40,41]

In this review, we highlight the materials used to synthesize artificial shells around individual living cells, emphasizing the unique features of cell-in-shell hybrids encased in specific materials, as well as their cytoprotective properties. To date, the concept of chemically synthesized, artificial nanoshells in SCNE has evolved, expanding their roles into active communications with cells and pericellular milieux, with great potential as the extrinsic regulators of cellular activities and behaviors.[40,42] In other words, the careful selection and design of the materials for SCNE enable the synthetic shells to not only protect the nanoencapsulated cells but also endow them with capabilities for exogenous reactions or functionalities that are not biochemically inherent to the wild-type, naïve cells.[40,43,44] The construction of the artificial shells that dynamically interact with cellular metabolisms has opened new avenues for fundamental research, including studies on the origin of life, as well as applications for adaptive cell-survival in unfavorable environments.

Numerous artificial shells with remarkable material-derived functionalities have so far been designed and synthesized for the construction of cell-in-nanoshell structures. In line with the achievements in this direction, this review presents the chronological progress of SCNE, where possible, with a focus on material types, and discusses the current state and future perspectives. The materials used in SCNE are broadly classified into organic, hybrid, and inorganic types (Figure 1). Organic materials are further subdivided into bioorganic molecules and species, synthetic polymers, organic frameworks, and graphene oxides, while hybrid organic–inorganic materials primarily include metal–organic frameworks and complexes. For quick reference, Table 1 presents a summary of reported SCNE studies to date, with particular emphasis on the material types used and their respective features. Several comprehensive reviews on SCNE, with different categorizations of material types, synthetic protocols, cell types, and other aspects, can be found in the literatures, offering complementary insights into the field.[11−25,45] Throughout this review, a cell encapsulated with a material in SCNE is denoted as cell@material, without a space in the nomenclature. For example, *S.cerevisiae*@melanin or *Saccharomyces_cerevisiae*@melanin refers to *Saccharomyces cerevisiae*, which is SCNEd with melanin.

2. ORGANIC TYPE

Organic materials have extensively been used in SCNE because of the structural and functional diversity, as well as high accessibility. section 2.1 covers bioorganic molecules and species, including melanin-like species, proteins (and synthetic peptides), polysaccharides, nucleic acids, and lipids, while section 2.2 focuses on synthetic polymers. sections 2.3 and 2.4 are dedicated to organic frameworks, such as hydrogen-bonded and covalent organic frameworks, and graphene oxides, respectively.

2.1. Bioorganic Molecules and Species

2.1.1. Melanin-Like Species (MLS). Melanin, a group of highly irregular heteropolymers, is ubiquitously found in nature

https://doi.org/10.1021/acs.chemrev.4c00984
Chem. Rev. XXXX, XXX, XXX−XXX

Table 1. Material Types, Features, and Cell Types Used in SCNE

types	materials	features	cells[ref]
organic	melanin-like species (MLS)	advantages: procedural simplicity, shell uniformity, shell durability, shell functionalizability, redox activity disadvantages: irreversibility (nondegradability)	EcN,[27−29,59,65] LAB,[34] *E. coli* BL21,[35] *C. pyrenoidosa*,[44] *S. cerevisiae*,[49,52,55−57] RBC,[50,55] HeLa,[51,55] Jurkat,[56] bone marrow-derived dendritic cell,[58] DC2.4,[58] *R. glutinis*,[60] *S. xiamenensis*,[61] *S. oneidensis*,[62] SV[63,64]
	natural polymers: proteins, polysaccharides, and nucleic acids	advantages: high cytocompatibility, specificity, shell functionalizability, biological activity, shell degradability, customizability disadvantages: procedural laboriousness (e.g., layer-by-layer assembly), low stability	[proteins] HeLa,[74−76] hMSC,[75,85] MIN6,[76,83] fibroblast,[81,85] HepG2,[78,79] HUVEC,[78] cardiomyocyte,[80] iPSC,[80,81] C2C12,[82] *S. cerevisiae*,[84,89,90,94] EcN,[86] *L. acidophilus*,[91] *Chlorella sp.* C-141,[92,93] *Synechocystis sp.* PCC 7002[237] [polysaccharides] *B. coagulans*,[95] *S. epidermidis*,[96] *L. acidophilus*,[97] *L. pentosus*,[98] *S. cerevisiae*,[99] Jurkat,[104] K562,[104] HeLa,[105] HepG2,[105−107] STO cell,[105] 10T1/2,[106] RBC[108] [combinations of proteins and polysaccharides] MSC,[109,111,124] hMSC,[110,113] AML-12,[112] PBMC,[112] PC12,[114] *S. cerevisiae*,[115,116] RBC,[117,118] LLC.OVA,[119] MCA205,[120] NSC,[121] HFSC,[122] C1498,[123] WEHI3B,[123] C2C12,[125] DPC[126] [nucleic acids] *E. coli*,[129,130] MCF-7,[129] *S. cerevisiae*,[129] CCRF-CEM,[131] C166[131]
	lipids and liposomes	advantages: cytocompatibility, biological activity, shell degradability disadvantages: structural instability, procedural complexity (e.g., presynthesis)	Jurkat,[40,136] EcN,[134,135] *E. faecalis*,[135] *S. aureus*[135]
	synthetic polymers	advantages: customizability, shell stability disadvantages: procedural laboriousness (e.g., layer-by-layer assembly), nondegradability, cytotoxicity	*E. coli*,[36,144,160,182] *O. anthropi*,[36] *S. oneidensis*,[36] *S. thermophilus*,[36] *C. pyrenoidosa*,[37,154,155] *S. cerevisiae*,[53,67,138−143,145,147−153,159,161−163,165,169,170,172−174,179,180,184] *A. vinosum*,[71] PCC 6803,[146] *A. baylyi*,[156] HeLa,[157,175,229] *A. borkumensis*,[158] *S. cohnii*,[160] *T. asperellum*,[161] PBCEC,[164] ADSC,[166] *S. epidermidis*,[167] pancreatic islet cell,[171] Jurkat,[173,181,229] BAC,[175] hMSC,[175] MSC,[176−178] NIH 3T3[229]
	organic frameworks	advantages: processability, acid stability (COFs) disadvantages: nondegradability (COFs)	[HOFs] NSC[187] [COFs] *S. cerevisiae*,[188,189] *B. subtilis*,[189] *C. pyrenoidosa*,[189] EcN,[189] *E. coli*[189]
	graphene oxides (GOs)	advantages: mechanical durability, thermal and electric conductivity disadvantages: procedural complexity, nondegradability	*S. cerevisiae*,[150,151,192,193] HeLa[194,195]
hybrid	metal−organic frameworks (MOFs)	advantages: procedural simplicity, shell stability, shell uniformity, shell degradability, shell functionalizability	[MOFs] *M. luteus*,[197] *S. cerevisiae*,[197,200,206] *B. subtilis*,[207] *E. coli*,[208] BMSC,[209,214] *M. thermoacetica*,[210] A549,[211] HeLa,[211] HL-60,[211] sperm[212]
	metal−organic complexes (MOCs)	disadvantages: limited procedural diversity	[MOCs] CVS HPC,[31] EcN,[31] *L. casei*,[31] *B. thetaiotaomicron*,[33] *E. coli*,[33,225] HaCaT,[42,43] *S. cerevisiae*,[42,43,199,215,221,225,228] Jurkat,[43,219] HeLa,[219] NIH 3T3,[219] RBC,[220] *C. reinhardtii*,[222] *E. gracilis*,[223] *L. brevis*,[224] *L. plantarum*,[224] PC12,[225] *L. acidophilus*[227]
inorganic	SiO_2	advantages: mechanical durability, shell degradability (not for SiO_2 and TiO_2), catalytic activity (MnO_2) disadvantages: procedural complexity (priming required; SiO_2, TiO_2, and calcium phosphate (CaP))	[SiO_2] *S. cerevisiae*,[52−54,60,94,145,149,193,234] *Bacillus atrophaeus*,[53] *E. coli*,[53] *R. glutinis*,[60] *Chlorella sp.* C-141,[93] PCC 6803,[146] A549,[211] HeLa,[211,229] hMSC,[213] Jurkat,[229] NIH 3T3,[229] *Synechocystis sp.* PCC 7002[237]
	TiO_2		[TiO_2] *R. glutinis*,[60] *Chlorella sp.* C-141,[92,93] *S. cerevisiae*,[184] Jurkat[230]
	CaP		[CaP] *S. cerevisiae*[147,148]
	$CaCO_3$		[$CaCO_3$] *C. pyrenoidosa*,[37] *S. cerevisiae*,[180] *E. coli*[231]
	MnO_2		[MnO_2] *S. cerevisiae*[233]

https://doi.org/10.1021/acs.chemrev.4c00984
Chem. Rev. XXXX, XXX, XXX−XXX

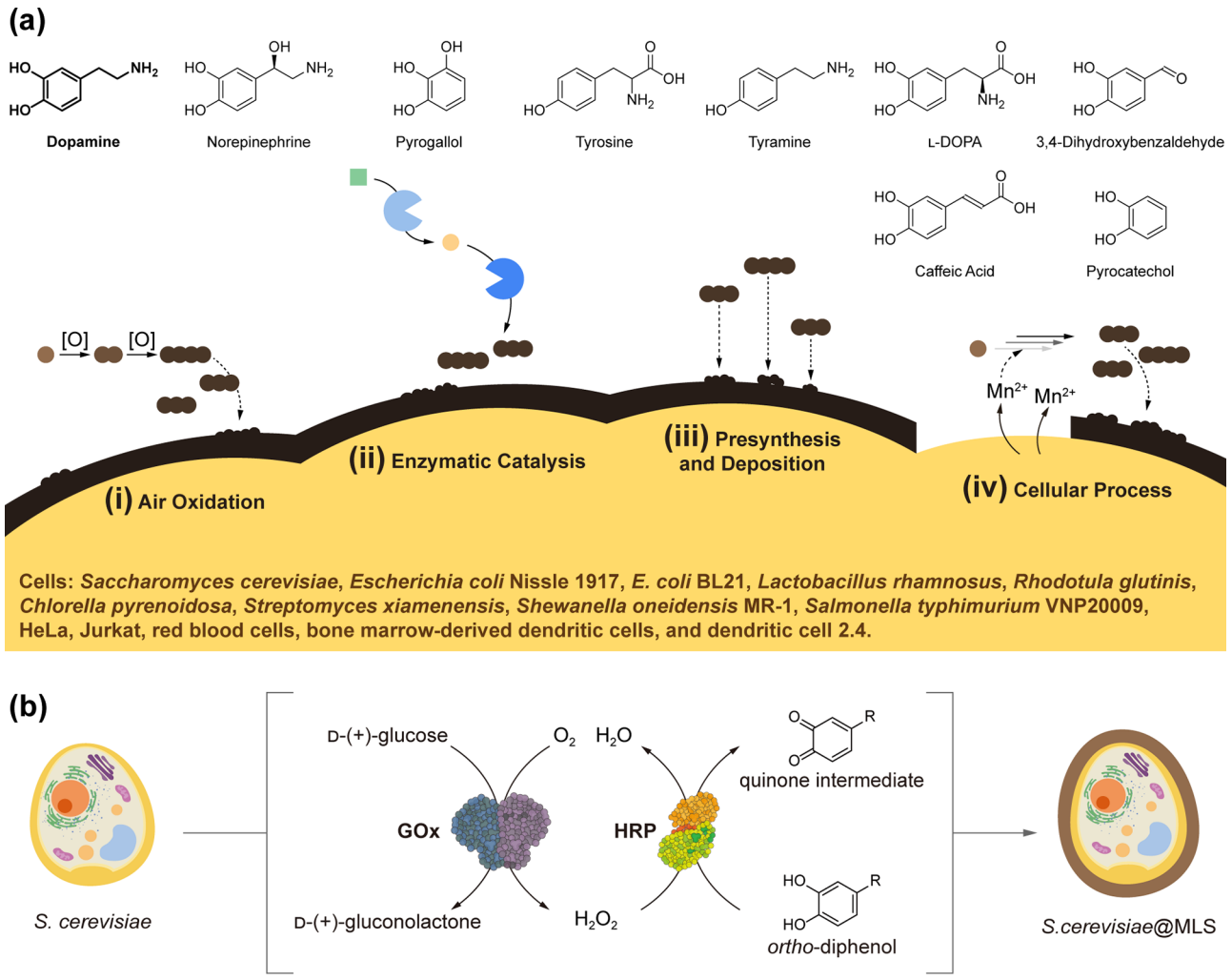

Figure 2. Schematic overview of strategies for synthesizing MLS shells in SCNE. (a) (top) Representative monomers used in MLS synthesis and (bottom) chemical strategies for constructing MLS shells, including (i) air oxidation, (ii) enzyme catalysis, (iii) presynthesis with subsequent deposition, and (iv) cellular process-mediated formation. Examples illustrate each approach, and a list of cells encapsulated within MLS shells is provided. (b) Formation of MLS via a GOx and HRP cascade reaction, demonstrating the conversion of *ortho*-diphenols in the creation of *S.cerevisiae*@MLS.

and imparts a broad range of functionalities to living organisms, including pigmentation, radical scavenging, and radiation protection.[46−48] Melanin is classified into several categories based on its monomer composition, with the biosynthetic pathway of eumelanin being clearly defined by the Raper-Mason pathway. Eumelanin is black or brown in color, and its biosynthesis begins with the oxidation of L-tyrosine (L-Tyr) to L-DOPA, which is then oxidized to DOPAquinone with the aid of tyrosinase. Following this step, intramolecular cyclization, facilitated by the nucleophilic addition of amine groups to quinone moieties in DOPAquinone, results in the formation of DOPAchrome. Its conversion leads to the formation of 5,6-dihydroxyindole (DHI) or 5,6-dihydroxyindole-2-carboxylic acid (DHICA), which, after oxidation and polymerization, are recognized as two representative building units of eumelanin.

Inspired by melanin and its natural synthesis process, melanogenesis, chemical efforts to mimic melanin and synthesize melanin-like species (MLS) in vitro have been undertaken to form cell-in-shell nanobiohybrids, with diverse potential functionalities, including cytoprotection, similar to the protective melanin shell found in nature. For instance, polydopamine (pDA), a synthetic mimic of an adhesive protein found in mussels, displays structural and physicochemical properties similar to eumelanin and has become as a representative example of MLS in SCNE. Analogous to eumelanin, DHI is widely accepted as a key building block of pDA, derived from the oxidation of dopamine (DA), typically by dissolved oxygen (O_2) in a basic solution. While pDA has been the most conventional form of MLS, monomers beyond DA, such as Tyr, L-DOPA, DHICA, DHI, tyramine, epinephrine, and norepinephrine, have also been used for MLS synthesis. The unique properties of MLS, including universal adhesiveness and both in situ and postfunctionalizability, have broadened its range of applications in SCNE since the initial report.[49]

This section begins with the historical development of MLS nanoshells in terms of materials and synthetic protocols (Figure 2a), followed by the examples of their properties and applications.

A report in 2011 demonstrated the synthesis of *S.cerevisiae*@pDA by simply incubating *S. cerevisiae* in a TRIS buffer solution (pH 8.5) containing DA (Figure 2a,i).[49] Uniform pDA nanoshells were firmly formed on the cell wall, retarding cell growth and prolonging the lag phase, while also protecting the cells from digestion by lyticase. Subsequently, the pDA-shell-

https://doi.org/10.1021/acs.chemrev.4c00984
Chem. Rev. XXXX, XXX, XXX−XXX

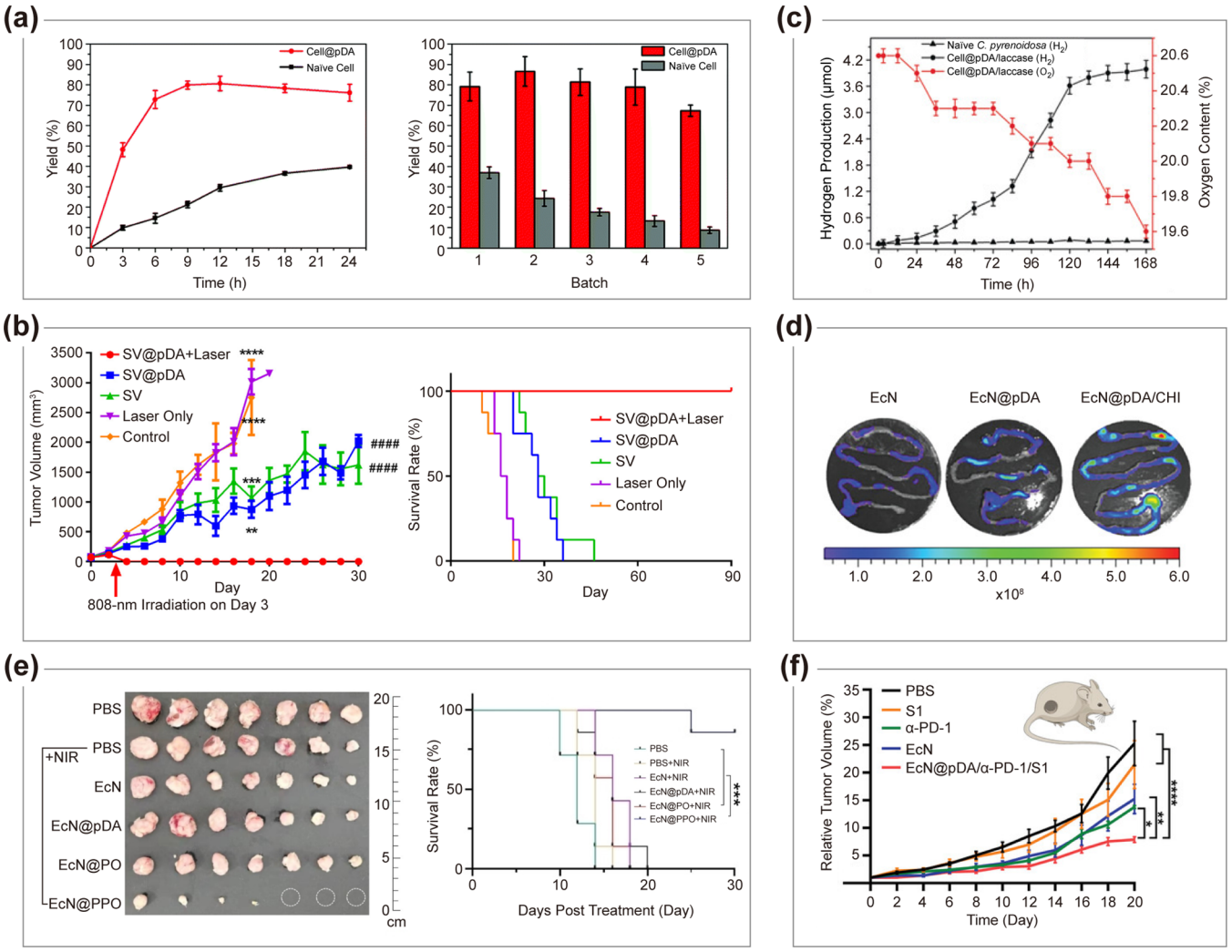

Figure 3. Representative applications of cell-in-MLS shell nanobiohybrids. (a) (left) Yields of (*S*)-1-phenylethanol produced by naïve cells and *R.glutinis*@pDA, and (right) yields of (*S*)-1-phenylethanol upon recycling, showing increased productivity and reusability after SCNE. Reproduced with permission from ref 60. Copyright 2017 Royal Society of Chemistry. (b) (left) Inhibition of tumor growth and (right) enhanced survival rates of tumor-bearing mice after injection of SV@pDA, combined with photothermal treatment. Reproduced with permission from ref 63. Copyright 2018 American Chemical Society. (c) Quantification of H_2 and O_2 produced by naïve *C. pyrenoidosa* and *C.pyrenoidosa*@pDA/laccase, demonstrating the metabolic shift from O_2 photosynthesis to H_2 production in *C.pyrenoidosa*@pDA/laccase. Reproduced with permission from ref 44. Copyright 2019 Wiley-VCH. (d) IVIS images of GI tracts sampled 4 h after oral administration of naïve EcN, EcN@pDA, and EcN@pDA/CHI to a murine model of colitis, showing enhanced accumulation of EcN@pDA/CHI in the inflamed colon. Reproduced with permission from ref 27. Copyright 2021 Wiley-VCH. (e) (left) Digital images of tumors 30 days after subcutaneous inoculation of EcN, EcN@pDA, EcN@pDA/OVA (EcN@PO), and EcN@pDA/*α*-PD-1/OVA (EcN@PPO) in CT26-OVA tumor-bearing mice. (right) Survival rates of CT26-OVA tumor-bearing mice after treatment, showing prolonged survival after inoculation of EcN@PPO combined with NIR irradiation. Reproduced with permission from ref 29. Copyright 2022 Wiley-VCH. (f) Suppressed tumor growth in CT26 tumor-bearing mice after inoculation with EcN@pDA/*α*-PD-1/S1. Reproduced with permission from ref 28. Copyright 2023 Wiley-VCH.

forming strategy has been applied to various cell types, including red blood cells (RBCs) and other mammalian cells.[50,51] For example, pDA nanoshells on RBCs effectively masked the blood-type antigens, and RBC@pDA exhibited comparable in vivo survival profiles to naïve RBCs in a murine model.[50] This demonstration suggests the potential for producing antigenically shielded, universal RBCs for blood transfusion.

Norepinephrine (NE), with an additional hydroxyl (−OH) group on DA, formed the MLS nanoshells that were thinner but smoother than those produced by DA.[52] In this work, poly(ethylenimine) (PEI) was grafted onto the $MLS_{[pNE]}$ shells via the Michael addition, followed by bioinspired silicification under mild conditions,[53,54] resulting in the cytocompatible construction of organic/inorganic double-layered shells. Proteomic analysis indicated that *S.cerevisiae*@pNE/SiO_2, which survived under UV-C irradiation, upregulated the proteins involved in protein folding (e.g., ECM10 and SSA1 from the HSP70 family), demonstrating the biochemical flexibility of *S.cerevisiae*@pNE/SiO_2 in responding to external stresses. As another example, plant-derived pyrogallol (1,2,3-trihydroxybenzene, PG), which undergoes autoxidation under basic conditions analogous to the oxidative polymerization of DA, has been employed for the SCNE of various cells, such as *S. cerevisiae*, RBCs, and human cervical carcinoma cells (HeLa cells).[55]

In addition to the autoxidation-based MLS shell formation, enzyme-mediated strategies have been demonstrated, inspired by the enzymatic cascade reactions involved in melanogenesis

https://doi.org/10.1021/acs.chemrev.4c00984
Chem. Rev. XXXX, XXX, XXX−XXX

(Figure 2a,ii).[56,57] As a first approach, tyrosinase-instructed SCNE was performed on Jurkat cells with Tyr as the substrate.[56] The mild and neutral conditions of the enzymatic reaction allowed Jurkat@pTyr to maintain viability up to 96.5%. In stark contrast, the pDA approach caused detrimental cell death and severe aggregation in Jurkat cells, which are more labile than microbial cells when exposed to chemical treatment. A combination of glucose oxidase (GOx) and horseradish peroxidase (HRP) was also employed to form cell@MLS from *ortho*-diphenols lacking amino ($-NH_2$) groups, a process that could not be achieved with tyrosinase (Figure 2b).[57]

Presynthesized pDA nanoparticles (NPs) have also been used for the construction of MLS shells (Figure 2a,iii).[58,59] *Escherichia coli* Nissle 1917 (EcN), decorated with pDA NPs, showed increased viability after exposure to simulated gastric fluid (SGF) and cholic acid, and successfully colonized in the gastrointestinal (GI) tract when administered to a murine model of colitis. On the other hand, a recent report suggests that innate cellular processes could mediate MLS shell formation, reminiscent of the melanin coat of *C. neoformans* (Figure 2a,iv). Manganese ions (Mn^{2+}), released by probiotic lactic acid bacteria (LAB) strains, catalyze the oxidation of phenolic compounds, such as DA, caffeic acid, and pyrocatechol, resulting in the formation of MLS shells.[34] LAB@pDA exhibited enhanced tolerance to SGF and oxidative stress, higher radical-scavenging activity, and improved adhesion to a model of intestinal epithelial cells compared with naïve LAB.

In addition to the cytoprotective capabilities of MLS shells in the form of artificial spores, other properties of MLS have also been explored for specific applications of cell@MLS in SCNE (Figure 3). Furthermore, the properties of MLS shells have also been enhanced through the incorporation of other functional materials. The potential applications of functionalized bacterium@pDA in bacterial therapeutics are discussed in detail in a recent review.[26]

The redox-active catechol moieties in pDA enabled the pDA nanoshell to function as a redox shuttle in several applications.[60−62] *Rhodotorula glutinis,* widely employed as a whole-cell biocatalyst for the production of chiral alcohols, exhibited a 5-fold increase in productivity and an 8-fold increase in reusability for the asymmetric reduction of acetophenone to (*S*)-1-phenylethanol after SCNE with pDA, compared with naïve cells (Figure 3a).[60] Furthermore, postfunctionalization of the pDA shells with titanium dioxide (TiO_2), SiO_2, and iron oxide NPs conferred high UV and thermal stability to the SCNEd cells and enabled the facile separation during reactions, respectively. The pDA shell on *Streptomyces xiamenensis* collected the electrons near the outer-membrane c-type cytochromes and enhanced direct electron transfer, while also adsorbing cell-secreted flavin at the interface between *S.xiamenensis*@pDA and the electrode, thereby simultaneously facilitating the mediated electron transfer.[61] *Shewanella_oneidensis*@pDA (or *S.oneidensis*@pDA) was developed as a single-cell electron collector to efficiently wire the electronic abiotic/biotic interfaces.[62] The pDA shell formed close contact with the cell's outer membrane, where transmembrane electron conduits are typically embedded, leading to a 1.9-fold increase in current delivery with higher maximum current and power output, compared with naïve *S. oneidensis*.

The photothermal effect of pDA shells has also been utilized to apply cell@pDA in photothermal therapy.[63,64] For example, *Salmonella*_VNP20009@pDA (or SV@pDA) was used in the photothermal treatment of tumor-bearing mice, with laser irradiation significantly inhibiting tumor growth without recurrence or metastasis during the 30-day experiment (Figure 3b).[63] The same research group combined the use of SV@pDA with a local inoculation of a gel containing AUNP-12 for PD-1 blockade in the treatment of advanced melanoma.[64]

In the functionalization of pDA-based nanoshells, a mixture of DA and its lipid derivatives has been used to control the hydrophobicity of cell surfaces for interfacial biocatalysis.[35] *E.coli*@pDA, prepared with DA and *N*-oleoyl DA, emulsified the oil−water media, generating a substantial interfacial area for the reaction, while being protected by the pDA shell against external stresses, including UV exposure, heat, and organic solvents. The SCNEd cells showed enhanced enzymatic activity in the production of optically active α-hydroxy ketone from ethanol and benzaldehyde. This interfacial system can also be expanded to chemoenzymatic synthesis by loading metal catalysts, such as palladium NPs, onto the pDA shell.

In general, multimodal motifs can be incorporated into cell@pDA through the codeposition of functional entities with DA and/or postconjugation after pDA shell formation, as previously demonstrated in ref 49. The incorporated functional entities have shown the potential to modulate metabolic pathways in cells[44] and augment their biological functions.[27−29] As an example of the postfunctionalization, laccase was immobilized onto the pDA shell on *Chlorella pyrenoidosa*, and the oxidation of tannic acid (TA) by *C.pyrenoidosa*@pDA/laccase facilitated the consumption of O_2, creating an isolated anaerobic environment that shifted the metabolic activity from O_2 photosynthesis to H_2 production (Figure 3c).[44] In a similar strategy, hyaluronic acid−poly(propylene sulfide) NPs (HPNs) were conjugated onto mucoadhesive pNE shells of EcN cells, imparting reactive oxygen species (ROS)-scavenging properties.[65] Following oral administration to mice with colitis, EcN@pNE/HPN exhibited enhanced survival and prolonged intestinal retention compared with naïve EcN, likely due to synergistic interactions between the pNE shells and HPNs. These effects led to improved prophylactic and therapeutic efficacy, along with increased gut microbiota abundance and diversity. On the other hand, in the codeposition approach, chitosan (CHI), a widely used excipient for colon-specific drug delivery systems, was incorporated into the pDA shell around individual EcN.[27] EcN@pDA/CHI exhibited a 15-fold higher survival rate after 3 h of exposure to SGF and a 30-fold higher survival rate in the gut after oral administration in a healthy mouse compared with naïve EcN. In vivo imaging system (IVIS) analysis of GI tracts from a murine colitis model treated with naïve EcN, EcN@pDA, and EcN@pDA/CHI demonstrated increased accumulation of EcN@pDA/CHI in the inflamed colon, compared with the others (Figure 3d). Both codeposition and postfunctionalization approaches were combined to create tumor-resident living immunotherapeutics by decorating EcN@pDA with α-PD-1 and ovalbumin (OVA) antigen; α-PD-1 antibody was codeposited with DA, while the OVA antigen was covalently attached to the pDA shell.[29] The SCNEd EcN, combined with NIR irradiation for photothermal therapy, markedly suppressed tumor growth and prolonged the survival of mice in antigen-overexpressing tumor models, specifically the CT26-OVA and MC38-OVA colon tumor models (Figure 3e). Similarly, α-PD-1 antibody and SARS-CoV-2 spike 1 (S1) protein were codeposited with DA, and the SCNEd EcN showed a substantial increase in the production of anti-S1 immunoglobulin G (IgG) titers, contributing to virus neutralization, as well as cytotoxic T lymphocytes, suggesting the activation of both humoral and

https://doi.org/10.1021/acs.chemrev.4c00984
Chem. Rev. XXXX, XXX, XXX−XXX

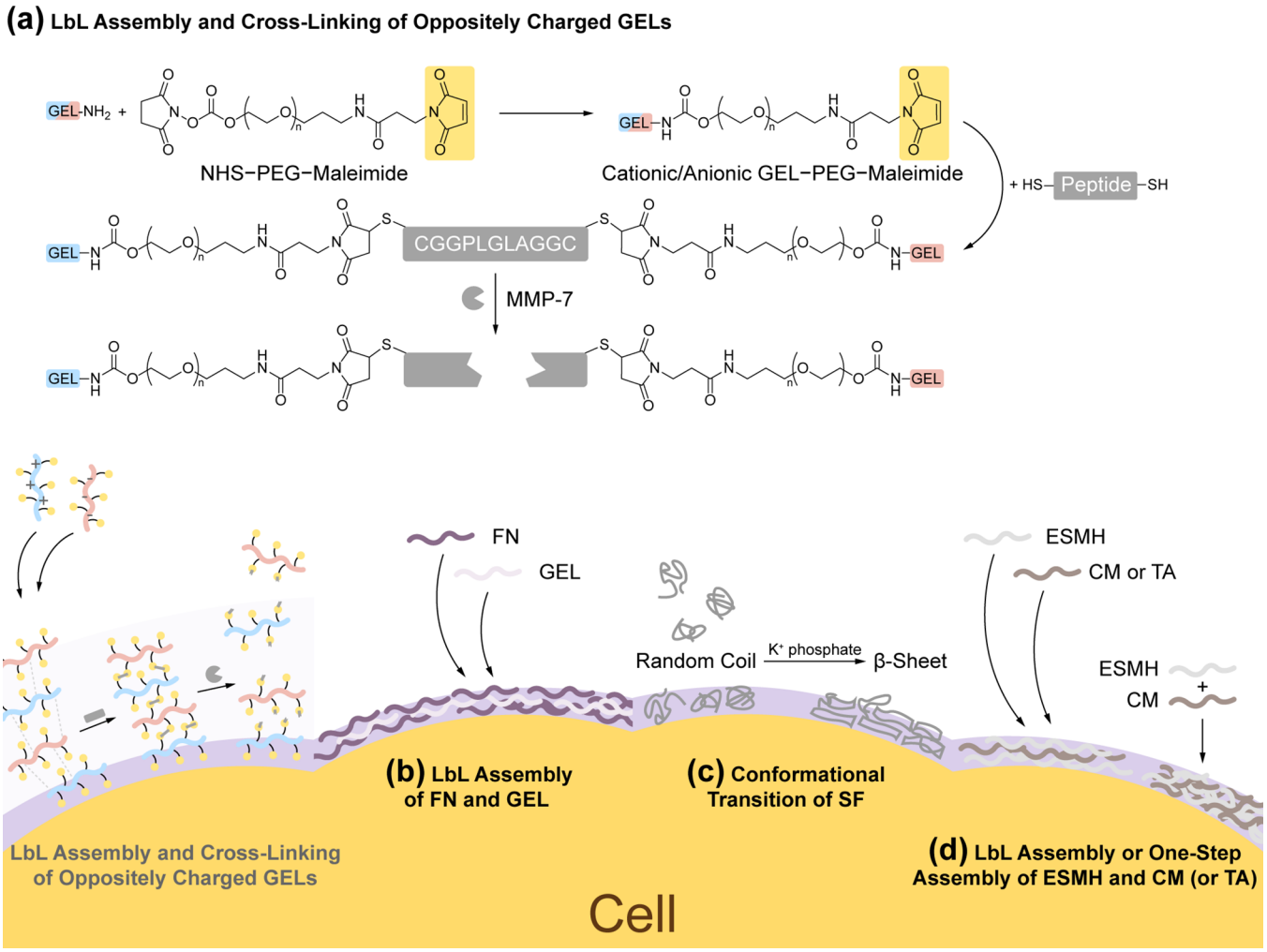

Figure 4. Schematic overview of strategies for forming protein-based nanoshells on individual living cells. (a) LbL self-assembly of oppositely charged GELs, followed by cross-linking with a cysteine-terminated peptide (CGGPLGLAGGC). Treatment of MMP-7 induces enzymatic degradation of the shells, leading to controlled cell release. (b) LbL shell formation from FN and GEL, aided by the collagen binding domain of FN. (c) Conformational transition of SF from a soluble random coil to a β-sheet in the presence of potassium phosphate, resulting in SF shell formation. (d) (left) LbL shell construction with ESMH and CM or TA via hydrogen bonding. (right) One-step assembly of the ESMH/CM complex on the cell surface for ESMH-based shell formation.

cellular immune responses.[28] Tumor growth was significantly inhibited in canonical CT26 colon cancer models and B16 melanoma models, highlighting the promising potential of SCNE in cancer treatment and prevention (Figure 3f).

2.1.2. Proteins. Most nanoshells made from natural polymers, such as proteins, polysaccharides, and nucleic acids, have been assembled around cell surfaces by the well-established layer-by-layer (LbL) technique, since the pioneering work of Lvov and others on LbL-based SCNE.[66,67] LbL nanoshells can be engineered to provide cytoprotection and specific functionality, but they are generally not robust enough to form durable artificial spores.[11]

This section is organized based on the natural proteins used in SCNE to date, such as gelatin, fibronectin, silk fibroin, and eggshell membrane hydrolysate (ESMH). Numerous comprehensive reviews on LbL techniques in cell−material interactions are available for general reference.[68−73]

Gelatin (GEL). GEL-based nanoshells have served as a versatile platform for postfunctionalization to achieve both cytoprotection and on-demand degradation, which are fundamental shell properties required for artificial spores.[21−23] The LbL shells of oppositely charged GELs were constructed around mammalian cells, such as HeLa or mouse insulinoma cells (MIN-6), followed by postfunctionalization utilizing the abundant $-NH_2$ and carboxyl (−COOH) groups in GEL. The postfunctionalization protocols include the coupling of GEL−PEG−thiol/PEG−maleimide (PEG: poly(ethylene glycol))[74] and GEL−PEG−maleimide/cysteine-terminated peptide (CGGPLGLAGGC),[75] as well as transglutaminase-catalyzed cross-linking.[76] In a study, the LbL process ended with GEL−PEG−thiol, and PEG−maleimide was coupled to the outermost layer via the Michael addition, leading to high cell viability, extended persistence period, and enhanced resistance against external physicochemical stresses.[74] Glutathione (GSH)-mediated, controlled shell degradation was also demonstrated in the same study. In another report, the CGGPLGLAGGC peptide was coupled to the GEL−PEG−maleimide LbL shells, and controlled cell release was demonstrated through enzymolysis of the shells by human matrix metalloproteinase-7 (MMP-7), an enzyme overexpressed in various tumors, including those of the breast, prostate, stomach, liver, pancreas, colorectal region, lung, and esophagus (Figure 4a).[75]

https://doi.org/10.1021/acs.chemrev.4c00984
Chem. Rev. XXXX, XXX, XXX−XXX

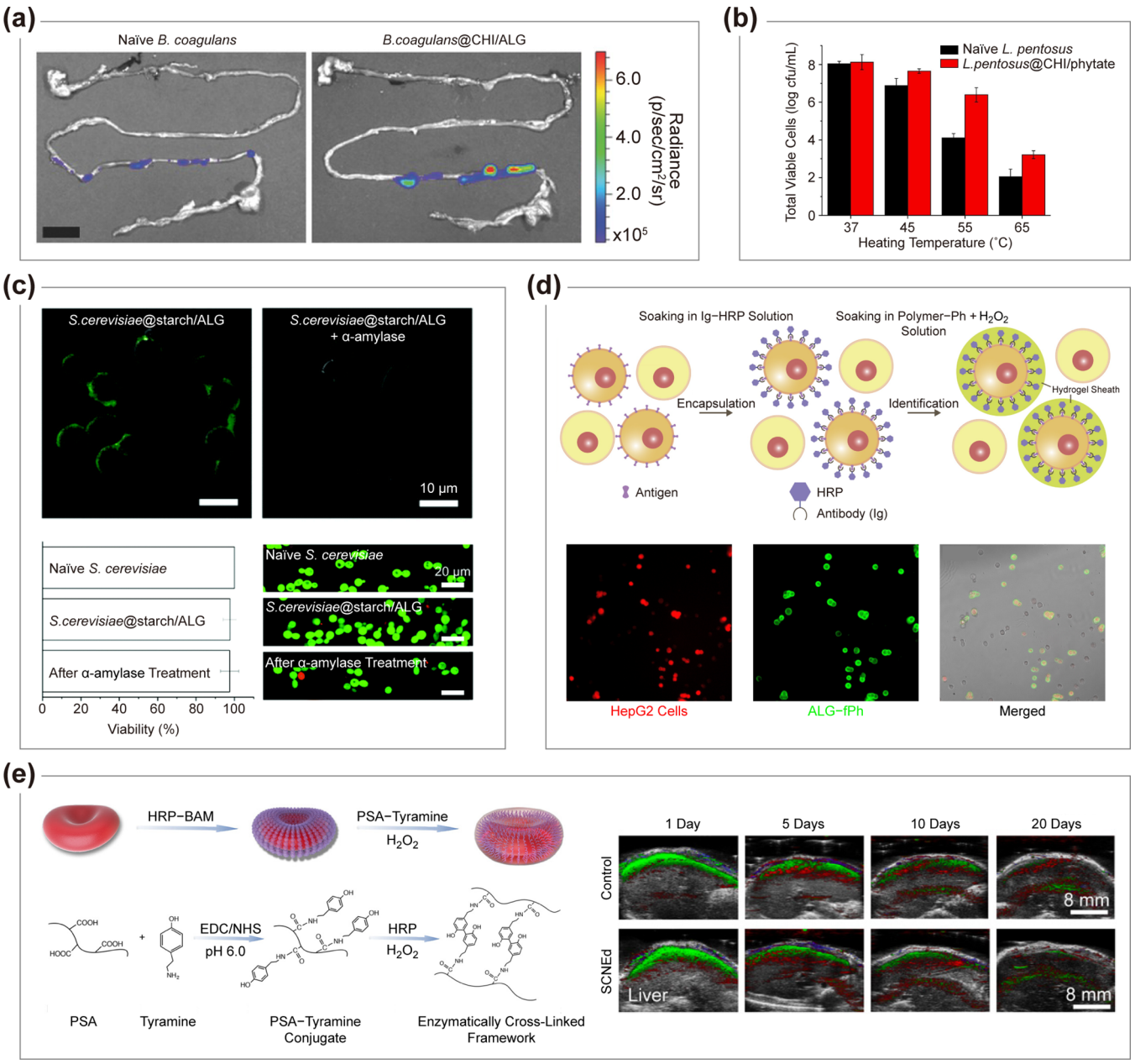

Figure 5. Strategies for encapsulating cells in polysaccharide-based shells and their applications. (a) IVIS images of naïve *B. coagulans* and *B.coagulans*@CHI/ALG 1 h after oral administration, showing enhanced survival of encapsulated cells in the GI tract. Reproduced with permission from ref 95. Copyright 2016 Wiley-VCH. (b) Enhanced thermal stability of *L.pentosus*@CHI/phytate compared with naïve cells. Reproduced with permission from ref 98. Copyright 2019 Elsevier. (c) (top) Confocal laser scanning microscopy (CLSM) images of *S.cerevisiae*@starch/ALG, before and after shell degradation with α-amylase, using fluorescein-linked ALG (green) as a shell component for visualization. (bottom) Cell viability assessments after shell formation and shell degradation with α-amylase. Green, live; red, dead. Reproduced with permission from ref 99. Copyright 2020 Royal Society of Chemistry. (d) (top) Schematic illustration of cell-specific hydrogel shell formation via antigen-antibody interactions. (bottom) Fluorescent images and merged phase-contrast image of a mixture of CD326-expressing HepG2 cells and nonexpressing 10T1/2 cells after sequential incubation in IgCD326−HRP solution and a solution of ALG derivatives bearing phenolic hydroxyl groups and fluorescein moieties (ALG−fPh) and H_2O_2. Red, HepG2 cells stained with Cell Tracker Orange; green, ALG−fPh. Reproduced with permission from ref 107. Copyright 2015 Elsevier. (e) (left) Schematic illustration of hydrogel sheath formation on RBCs using the HRP−BAM-based strategy. (right) Photoacoustic images of a mouse liver after injection of DiR dye-labeled naïve and SCNEd RBCs. Red, oxyhemoglobin; blue, deoxyhemoglobin; green, DiR dye. Reproduced with permission from ref 108. Copyright 2020 American Association for the Advancement of Science.

Gelatin (GEL) and Fibronectin (FN). Protein-based SCNE of mammalian cells has found applications in tissue engineering, cell-fate alteration, drug delivery systems, and cell-cycle control, in addition to cytoprotection.[77−83] For example, some protein-based shells have facilitated the formation of cell clusters, spheroids, 3D tissues, and artificial organs due to their pivotal roles in cell−cell interactions and the extracellular matrix (ECM). Matsusaki and co-workers demonstrated the LbL shell formation of FN and GEL on fibroblasts and constructed dense 3D tissue structures (Figure 4b).[77] The protocol has been applied to other mammalian cells, such as human umbilical vein endothelial cells (HUVECs) and human hepatocellular

https://doi.org/10.1021/acs.chemrev.4c00984
Chem. Rev. XXXX, XXX, XXX−XXX

carcinoma (HepG2) cells.[78] The FN/GEL shells protected the cells against extreme shear stress during 10,000 rpm centrifugation and preserved cell growth during cell culture.[79] Furthermore, coculture of different SCNEd cells led to the formation of complex cellular structures, including regenerative tissues such as cardiomyocytes,[80,81] skeletal muscle,[82] and pancreatic β-cell tissues.[83] As an example, human cardiomyocyte tissues, generated by coculturing FN/GEL-encapsulated human induced pluripotent stem cells (hiPSCs) with FN/GEL-encapsulated normal human cardiac fibroblasts and normal human cardiac microvascular endothelial cells, developed a blood capillary-like 3D network, which significantly increased the viability of the resulting cardiomyocyte microtissues.[80,81] Pancreatic β-cell spheroids, based on the FN/GEL SCNE strategy, secreted significantly higher amounts of insulin, with a 2- to 2.5-fold increase in the expression of insulin and glucose transporter 2 genes, and immediately alleviated glycemia in diabetic mice and significantly improved glucose sensitivity in in vivo experiments, compared with naïve-cell spheroids.[83]

Silk Fibroin (SF). SF has widely been used in tissue engineering to develop cellular scaffolds, matrices, and artificial tissues due to its biocompatibility, biodegradability, high mechanical strength, and therapeutic effects. Notably, SF exhibits low inflammatory reactions and immune responses in vivo, making SF scaffolds and networks suitable materials for tissue engineering and SCNE. In an early study, Tsukruk and co-workers utilized the salting-out and crystallization of SF β-sheets, involving the conformational transition from a soluble random coil to a β-sheet in the presence of potassium phosphate, for the SCNE of *S. cerevisiae* (Figure 4c).[84] Intriguingly, the SF shells could undergo autonomous degradation via endocytosis, restoring the cells with full functionality and leaving no visible trace of the shell. Kaplan and co-workers used LbL assembly for the SCNE of mammalian cells. They modified SF by carboxylation and amination to synthesize anionic and cationic SF, respectively, and formed the SF LbL shells on murine fibroblasts and human mesenchymal stem cells (MSCs).[85] SF-based SCNE has also been applied to probiotics, where EcN@SF was demonstrated as a potential candidate for probiotic therapy due to the protective and therapeutic features of SF shells.[86] The SF shells protected EcN from harmful aggressors, such as pH, bile salts, and pepsins, as well as SGF and simulated intestinal fluid (SIF). Both in vitro and in vivo experiments showed the potent anti-inflammatory effect of EcN@SF in the treatment of intestinal mucositis in murine models, attributed to the anti-inflammatory properties of SF and the biotherapeutic activities of the delivered EcN.

Eggshell Membrane Hydrolysate (ESMH). As an upcyclable natural resource, ESMH has been widely exploited for anti-inflammatory therapy and protective medicine due to its bioactivities, such as antimicrobial and antioxidative effects.[87,88] In the SCNE field, ESMH has been utilized to form nanoshells around microbial cells, such as *S. cerevisiae* and *L. acidophilus*, where hydrogen-bonding-based LbL assembly with TA[89] or coffee melanoidins (CM),[90] as well as one-step assembly of the ESMH/CM complex,[91] were employed (Figure 4d). The ESMH-based shells provided cytoprotection against various factors, such as pH fluctuations, cationic PEI, and heavy metals. Furthermore, the shells were postfunctionalizable via click reactions, owing to the $-NH_2$ and $-SH$ moieties in ESMH, and also acted as a biosilicification mediator for the construction of ESMH/SiO_2 double-layered shells.[89]

Others. Short peptides have also been used in SCNE, though their application remains relatively rare, typically serving as a secondary role. For example, $(RKK)_4D_8$ (R, arginine; K, lysine; D, aspartic acid) has been utilized as a catalytic template for the formation of TiO_2 nanoshells after being grafted onto cell surfaces.[92,93] In addition, $R_4C_{12}R_4$ (C, cysteine), electrostatically adsorbed onto the surface of *S. cerevisiae*, has been shown to catalyze the formation of SiO_2 nanoshells from tetraethyl orthosilicate.[94]

2.1.3. Polysaccharides. Polysaccharides are abundant polymeric carbohydrates, composed of long chains of monosaccharide units bonded by glycosidic linkages. They contain various functional groups, such as $-COOH$, $-NH_2$, and sulfate ($-OSO_3^-$), which render them either positively or negatively charged under physiological conditions, thereby facilitating efficient LbL assembly via electrostatic interactions. Most of the work in this section highlights the cytoprotective capabilities of nanoshells.

As cytocompatible and edible materials, polysaccharide-based nanoshells have extensively been utilized to protect probiotic cells in applications for probiotic delivery and therapy. Probiotics, commonly used in nutritional and dietary products, often undergo harsh industrial processes, such as elevated temperature and repeated freeze−thaw processes, before consumption. Microencapsulation has been used to immobilize multiple probiotic cells in a microbead, but this approach has drawbacks, including large size, low stability, and limited permeability. SCNE offers a more versatile strategy that maintains or controls cell viability, growth, proliferation, surface recognition, and interactions with extracellular molecules and other cells.[20] In this regard, the SCNE strategy with polysaccharides has achieved unprecedented results in cytoprotection against the harsh conditions of the GI tract. For example, the multiple LbL bilayers of CHI and alginate (ALG) significantly enhanced the tolerance of therapeutic *Bacillus coagulans* against bile salts and acidic conditions in the GI tract (Figure 5a).[95] The same polysaccharide pair has also been applied to *Staphylococcus epidermidis*.[96]

CHI was also paired with carboxymethyl cellulose (CEL) to form more stable bilayers compared with CHI/ALG shells, which are relatively unstable under acidic conditions. The pK_a of CEL shifted to below 4.5, inducing collective hydrogen-bonding interactions even at low pH. The CHI/CEL shells (and CHI/phytate shells) acted as impermeable protection barriers against several proteases, such as pepsin and pancreatin in SGF and SIF, reduced the viability loss of *Lactobacillus acidophilus* during the freeze−thaw process,[97] and increased the survival rate of *Lactobacillus pentosus* after thermal treatment during food production (Figure 5b).[98]

Starch, composed of amylose and amylopectin, has also been used for the construction of cell-in-shell structures after functionalization with glycidyltrimethylammonium chloride. The synthesized cationic starch was paired with ALG to form α-amylase-degradable LbL shells around *S. cerevisiae,* which can be degraded on demand by enzymatic cleavage (Figure 5c).[99] The enzyme-triggered degradation of starch-based shells loaded with therapeutic drugs could be applied to drug delivery systems targeting α-amylase-rich sites in the body, such as the mouth and pancreas.

In studies related to this section, enzymes were utilized for the construction of polysaccharide-based hydrogel shells, where HRP or tyrosinase catalyzes the oxidative coupling of the phenolic hydroxyl moieties grafted onto polysaccharide chains

https://doi.org/10.1021/acs.chemrev.4c00984
Chem. Rev. XXXX, XXX, XXX−XXX

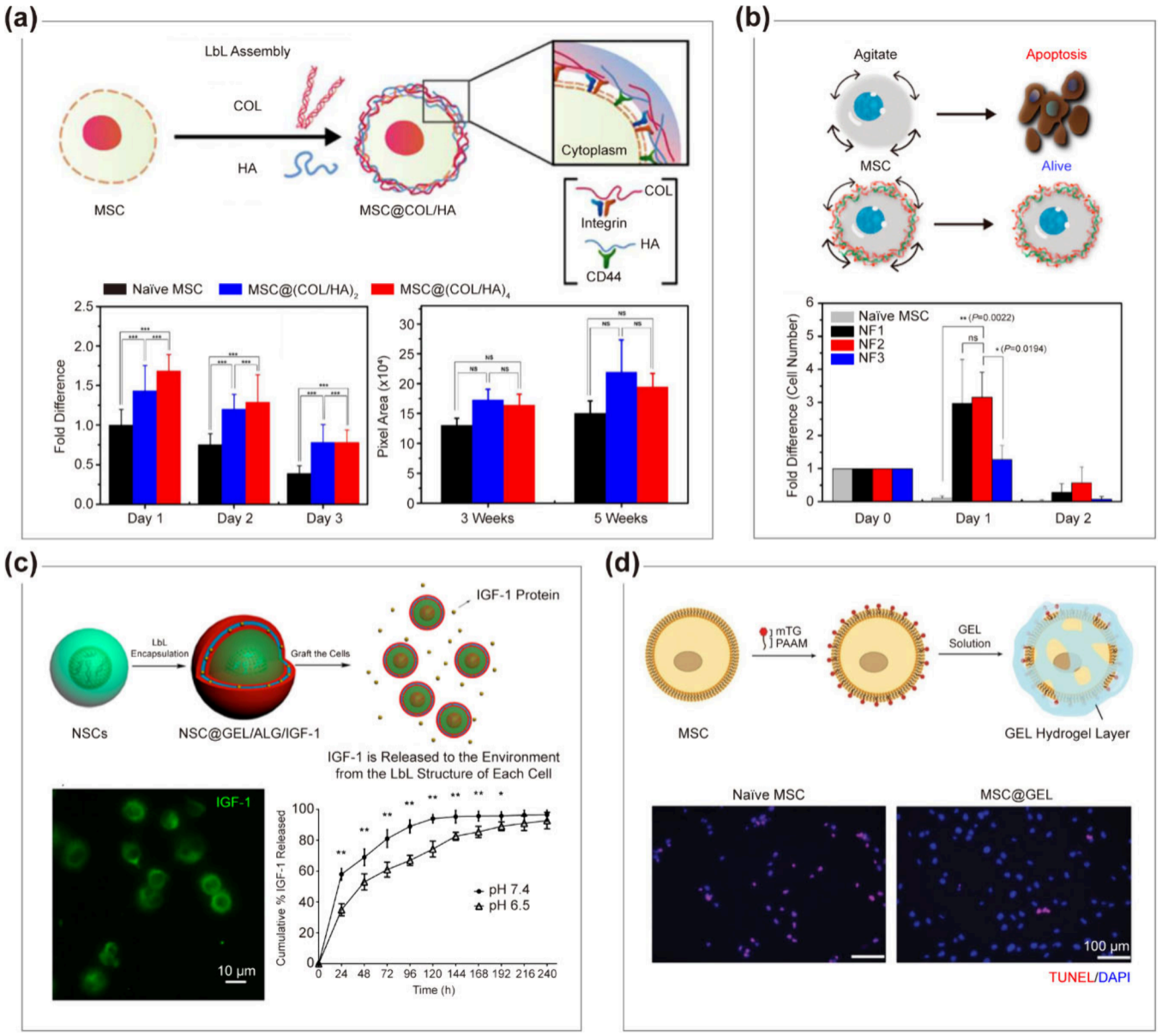

Figure 6. Strategies for constructing nanoshells on cells using combinations of proteins, synthetic peptides, and polysaccharides, and properties of SCNEd cells. (a) (top) Schematic illustration of COL/HA shell formation on MSCs via LbL assembly. (bottom, left) Normalized proportion of viable MSCs cultured for 3 days without attachment, showing enhanced resistance of MSC@COL/HA to anoikis under nonattached conditions. (bottom, right) Graph showing alizarin-red stained areas after in vitro incubation of MSCs in osteogenesis induction medium for 3 and 5 weeks, indicating upregulated osteogenic differentiation of the SCNEd cells. Reproduced with permission from ref 109. Copyright 2017 American Chemical Society. (b) (top) Schematic illustration depicting the different responses of naïve and SCNEd MSCs to shear stress. (bottom) Cell viability after exposure to spinner culture under nonattachment conditions, showing the cytoprotective properties of PLL/RGD and PLL/HA shells. NF1, $(PLL/RGD)_3$ shells; NF2, $(PLL/HA)/(PLL/RGD)_2$ shells; NF3, $(PLL/HA)_3$ shells. Reproduced with permission from ref 113. Copyright 2017 American Chemical Society. (c) (top) A scheme illustrating SCNE of NSCs within GEL/ALG shell containing IGF-1, with controlled release functionality. (bottom, left) Fluorescence image of NSCs SCNEd with GEL/ALG shells loaded with IGF-1, labeled by anti-IGF-1 (green). (bottom, right) Release profiles of IGF-1 from shells under different pH conditions. Reproduced with permission from ref 121. Copyright 2015 American Chemical Society. (d) (top) Schematic illustration of mTG incorporation into the MSC membrane using PSA-based anchor molecules, catalyzing cross-linking of GEL to form nanogel sheaths. PAAM: PSA anchor for cell membranes. PAAM−mTG was formed by linking PAAM and mTG in the presence of NHS. (bottom) CLSM images of cell viability assays for naïve MSCs and MSC@GEL cultured in serum- and sugar-free medium under hypoxic conditions. Cell viability and apoptosis were evaluated using terminal deoxynucleotidyl transferase dUTP nick end labeling (TUNEL) staining (red). DAPI: 4′,6-diamidino-2-phenylindole (blue). Reproduced with permission from ref 124. Copyright 2021 Wiley-VCH under CC BY 4.0.

in the presence of hydrogen peroxide (H_2O_2) or O_2, respectively.[100−104] Sakai and co-workers demonstrated the formation of hydrogel sheaths on various mammalian cells, including mouse embryonic fibroblast cell line STO cells, human hepatoma HepG2 cells, and human cervical cancer HeLa cells, with phenolic hydroxyl-modified ALG, hyaluronic acid (HA), and others.[105] The hydrogel sheath formation process was highly cytocompatible, and the ALG shells were degradable by alginase. The protocol was further used to identify H_2O_2-secreting cells through selective encapsulation.[106] In addition,

https://doi.org/10.1021/acs.chemrev.4c00984
Chem. Rev. XXXX, XXX, XXX−XXX

cell-specific shell formation was also achieved through antigen-antibody interactions. Only cells expressing target antigens were identified by HRP-conjugated antibodies and selectively encased in hydrogel sheaths (Figure 5d).[107] Furthermore, Wang, Tang, and co-workers applied the HRP−biocompatible anchor for cell membrane (BAM)-based strategy to form nanothin hydrogel sheaths on Rhesus D (RhD)-positive RBCs for the production of RhD-negative RBCs (Figure 5e).[108] The HRP-catalyzed cross-linking of polysialic acid (PSA)−tyramine conjugates resulted in the construction of flexible 3D framework structures on cell membranes, while preserving their fluidity. The PSA shells completely shielded the RhD antigen, as confirmed by blood transfusion tests performed in a mouse model and immunostimulation with RhD-positive human RBCs conducted in a rabbit model.

2.1.4. Combinations of Proteins (or Synthetic Peptides) and Polysaccharides. The coutilization of proteins, such as GEL, collagen (COL), and β-lactoglobulin (BLB), along with polysaccharides, such as ALG and HA, has been employed in SCNE to anticipate synergistic effects between the two components. For instance, the durability of polysaccharides and the specificity of protein−protein interactions are significantly beneficial for harnessing the potential of therapeutic cells, particularly stem cells and immune cells, which require careful handling to preserve not only cell viability but also the ability to differentiate or be activated through specific surface interactions. This section addresses the various application potentials of the combined SCNE approach, including the use of synthetic (poly)peptides, such as arginine-glycine-aspartic acid (RGD) and poly(L-lysine) (PLL), when needed. The focus is on key nanoshell properties in artificial spores: cytoprotection, permselectivity, and shell functionalizability.[21−23]

The initial SCNE of protein−polysaccharide pairs has been used in mammalian cells primarily to protect the cells from external stresses. For example, stem cell therapy holds great promise for treating various diseases, including nervous system disorders. However, the outcomes of stem cell transplantation, particularly through direct intravenous injection, have been limited by the low survival rates of transplanted cells due to apoptosis. In addition, the production processes can also be damaging to fragile stem cells. In this context, the construction of cytoprotective cell-in-shell structures would offer a powerful solution, providing cytoprotection both in vitro and in vivo.

The COL/HA LbL shells on MSCs not only improved their viability against anoikis under nonattached conditions, but also promoted osteogenic differentiation (Figure 6a).[109] Similar enhancement in osteogenic differentiation was also observed with the COL/ALG pair, and systematic studies of various LbL pairs suggested a correlation between the mechanical properties of the nanoshells and the regulation of osteogenesis through mechanotransduction pathways.[110] The PLL/HA pair was also used for the SCNE of various mammalian cells, including immune cells, while maintaining their viability and immunoactivities.[111,112] Furthermore, the nanoshells of the PLL/RGD and PLL/HA pairs provided significant cytoprotective effects on MSCs in suspension, safeguarding them against extreme shear stresses (Figure 6b).[113] Mechanistic studies suggested that the interactions between the RGD/HA components of the shells and cell surface receptors triggered downstream survival signals, such as the FAK-PI3K-Akt pathway, preventing the cells from entering anoikis. Furthermore, GEL/HA nanoshells served as a shield for transplanted cells, blocking interactions between tumor necrosis factor-α (TNF-α) and TNF-receptor 1 (TNF-R1), which initiate downstream signals for apoptosis.[114] Rat pheochromocytoma cells, SCNEd within the GEL/HA nanoshells, showed a 60% blockade effect against TNF-α antagonists compared with naïve cells, presumably due to the permselectivity of the shells—one of the essential shell properties required for artificial spores.[21−23]

Cryopreservation is another promising example of cytoprotection in SCNE. For instance, 71% of *S. cerevisiae* SCNEd with the BLB/ALG multilayers survived freezing at −80 °C.[115] The observed cryopreservation was attributed to the formation of hydrogen bonds between the $-NH_2$ or −COOH groups of BLB or ALG and water, which likely hindered the formation of large ice crystals that could damage cellular structures. The BLB/ALG nanoshells also protected the cells from repeated dehydration/rehydration cycles, presumably by physically slowing the kinetics of water transfer during the cycles, leading to high cell survival.[116] Immunocamouflage is also achievable through the SCNE of protein−polysaccharide combinations, as demonstrated in an early study on the construction of potential universal RBCs based on the nanoshells of ALG and HA, pairing with CHI-*g*-phosphorylcholine or PLL-*g*-PEG.[117,118] Although not alive, whole dead cancer cells were encapsulated in dextran sulfate (DexS)/poly(L-arginine) shells doped with mannitol for the development of cancer vaccines.[119] The doped mannitol enhanced protease influx and degradation of the shells upon uptake by dendritic cells (DCs), while also increasing the recovery yield of the SCNEd cells, preventing the protein denaturation, and generating porosity in the shells. Furthermore, the nanoshells protected cell proteins from leaking into the supernatant and enhanced antigen cross-presentation on DCs. DexS/poly(L-arginine) shells doped with gold (Au) NPs were also used to remotely influence the cells.[120] Upon exposure to an NIR laser beam, the Au NPs generated localized heat-induced rapid necrosis, accompanied by swelling of the cell morphology.

In therapeutic applications, drug loading into and release from the nanoshells have been demonstrated with the GEL/ALG pair, in addition to cytoprotection. Neural stem cells (NSCs) were SCNEd within the shells containing insulin-like growth factor-1 (IGF-1), without significantly affecting cell viability, proliferation, and differentiation (Figure 6c).[121] IGF-1 remarkably enhanced the cell viability, and its controlled release allowed for the manipulation of cell proliferation and differentiation in neuronal cell culture. The GEL/ALG pair has also been applied to hair follicle stem cells (HFSCs), where transforming growth factor TGF-β2 was loaded into the shell. While $CD34^+$HFSC@GEL/ALG/TGF-β2 was activated, leading to the transformation into highly proliferative $Lgr5^+$HFSCs and promoting hair follicle regeneration, $CD34^+$HFSC@GEL/ALG remained in an undifferentiated state, demonstrating the potential of SCNE in controlling cell fate.[122] In addition, transplantation of SCNEd cells has shown potential in various therapeutic applications. In allogeneic hematopoietic stem cell transplantation for the treatment of acute myeloid leukemia, the transplantation of SCNEd T cells reduced graft-versus-host disease, with GEL/ALG nanoshells acting as barriers to minimize immune responses between donor T cells and recipient antigen-presenting cells.[123] SCNE with GEL nanogel sheaths has also been applied to reduce cell death in MSC transplantation. Microbial transglutaminase (mTG) was incorporated into the MSC membrane using PSA-based anchor molecules, where mTG catalyzed the cross-linking of adjacent GEL molecules, leading to the formation of nanogel sheaths (Figure 6d).[124] These nanogel sheaths reduced apoptosis by

https://doi.org/10.1021/acs.chemrev.4c00984
Chem. Rev. XXXX, XXX, XXX−XXX

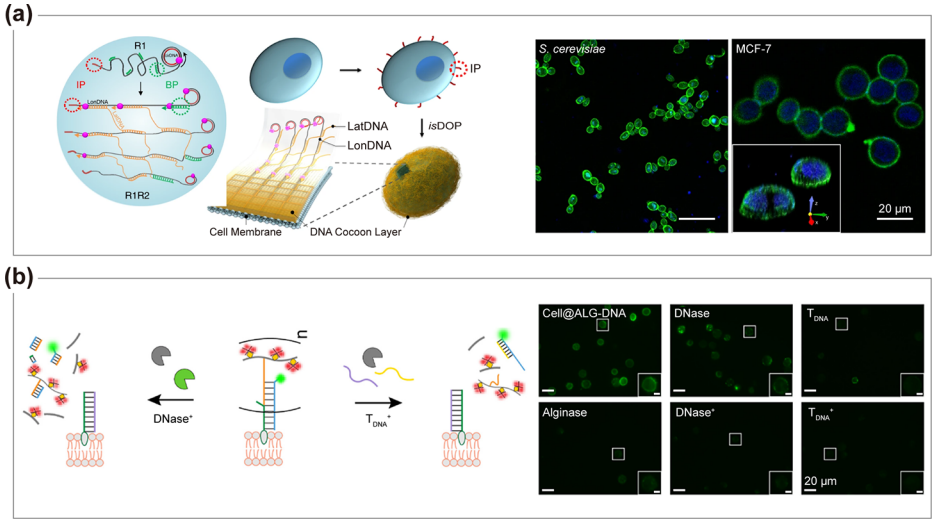

Figure 7. Strategies for constructing nucleic acid-based nanoshells and their properties. (a) (left) Schematic illustration of *is*DOP for SCNE. Rolling cycling replication (R1) is initiated by primer−PEG−BAM (initiating primers, IP), producing longitude initial polymers (LonDNA, gray). Branched replication (R2) is initiated by branching primers (BPs), synthesizing latitude DNA polymers (LatDNA, yellow). DNA cocoons are assembled on the cell surface using LonDNA and LatDNA. (right) CLSM images of *S. cerevisiae* and MCF-7 SCNEd with DNA polymer cocoons, with cocoons labeled with 6-carboxy-fluorescein-modified oligonucleotides (green) and cell nuclei stained with Hoechst 33342 (blue). Reproduced with permission from ref 129. Copyright 2019 Springer Nature under CC BY 4.0. (b) (left) Schematic illustration of ALG−DNA shell degradation via complementary oligonucleotides or enzyme treatment. T_{DNA}^{+}, combination of T_{DNA} (complementary oligonucleotide) and alginase; DNase^{+}, combination of DNase and alginase. (right) CLSM images showing fluorescein signals before and after treatment with shell-degrading agents on fluorescein-labeled shells. Inset scale bars: 5 μm. Reproduced with permission from ref 131. Copyright 2022 American Chemical Society.

blocking TNF-α and TNF receptor interactions, as well as downstream signaling, under both hypoxic and normoxic conditions. In tissue engineering applications, the COL/ALG shells have also been used to enhance the mechanical durability of cell sheets.[125] In another study, 3D spheroids of dermal papilla cells (DPCs) were constructed with DPC@GEL/ALG by cross-linking with Ca^{2+} ions.[126]

2.1.5. Nucleic Acids. Compared with proteins and polysaccharides, nucleic acids (DNA and RNA) are underexplored for SCNE, largely due to challenges in storage, preservation, and handling. In addition to biocompatibility, abundance, protein-binding ability, and other biofunctionalities, DNA and RNA offer the unique advantage of precise, programmable self-assembly through complementary base pairing, as exemplified by DNA origami.[127,128] Therefore, nucleic acids have the potential in the creation of nanoshells with specific, customizable functions. In SCNE, nucleic acids have been utilized in both grafting-from[129] and grafting-to approaches.[130,131] In the grafting-from (or surface-initiated polymerization, SIP) approach, nucleic acids are synthesized directly from the cell surfaces with primers. In the grafting-to approach, the LbL method is typically used with positively charged polymers.

Grafting-From Approaches. The method of in situ DNA-oriented polymerization (*is*DOP) was developed for the creation of DNA-based nanoshells (Figure 7a).[129] In brief, primer−PEG−BAM[132] or primer−diazirine was used to introduce the primer onto the surfaces of mammalian and microbial cells, respectively, allowing DNA chains to grow from the cell surfaces in the DNA replication media, along with simultaneous cross-linking via branching primers. These nanoshells were referred to as DNA polymer cocoons. Furthermore, three cleavage sites of three restriction endonucleases, *Eco*RI-HF, *Hind*III-HF, and *Pst*I-HF, were encoded within the DNA polymer cocoons of three different *S. cerevisiae* samples, respectively. Analysis showed that the release of encoded cells by endonucleases exhibited over 90% specificity, demonstrating the potential of SCNE for cell encoding and postmanipulation.

Grafting-To Approaches. An early example is the nanoencapsulation of *E. coli* HB101 within CHI/DNA shells via the LbL approach.[130] In another study, ALG−oligonucleotide conjugates were assembled to the complementary oligonucleotides predeposited to cell surfaces (Figure 7b).[131] The ALG−DNA shells were degradable on demand through strand displacement by other complementary oligonucleotides or by enzyme degradation with DNase or alginase, which could be applied to the control over cell−cell and cell−material interactions.

2.1.6. Lipids and Liposomes. Lipids are ubiquitous in all living organisms, making up a significant portion of cellular membranes. Amphiphilic lipids, in particular, self-assemble into various structures in water, such as micelles and vesicles, and can interact with various biomolecules, such as proteins and other lipids via noncovalent interactions. In this regard, lipids could act as versatile, cytocompatible materials for SCNE, although further research is needed to finely control and manipulate the interplay between lipids and the cytospace.

Unlike liposome fusion with mammalian cells,[133] the Ca^{2+}-assisted self-assembly of dioleoylphosphatidic acid and cholesterol on the EcN surfaces resulted in the formation of lipid nanoshells (Figure 8a).[134] In this process, Ca^{2+} ions assisted the self-assembly of lipids on the negatively charged cell surfaces, while cholesterol provided additional stabilization for the lipid shells. The lipid shells were cytoprotective. For instance, the number of SCNEd EcN that survived 3 h of exposure to ampicillin and apramycin was 50 times higher than that of naïve EcN. Cytoprotection was also observed against ethanol, extreme pH levels (2 and 11), SIF with trypsin, and SGF with pepsin. Furthermore, in vivo treatment of an ulcerative colitis mouse with the SCNEd EcN significantly reduced inflammation,

https://doi.org/10.1021/acs.chemrev.4c00984
Chem. Rev. XXXX, XXX, XXX−XXX

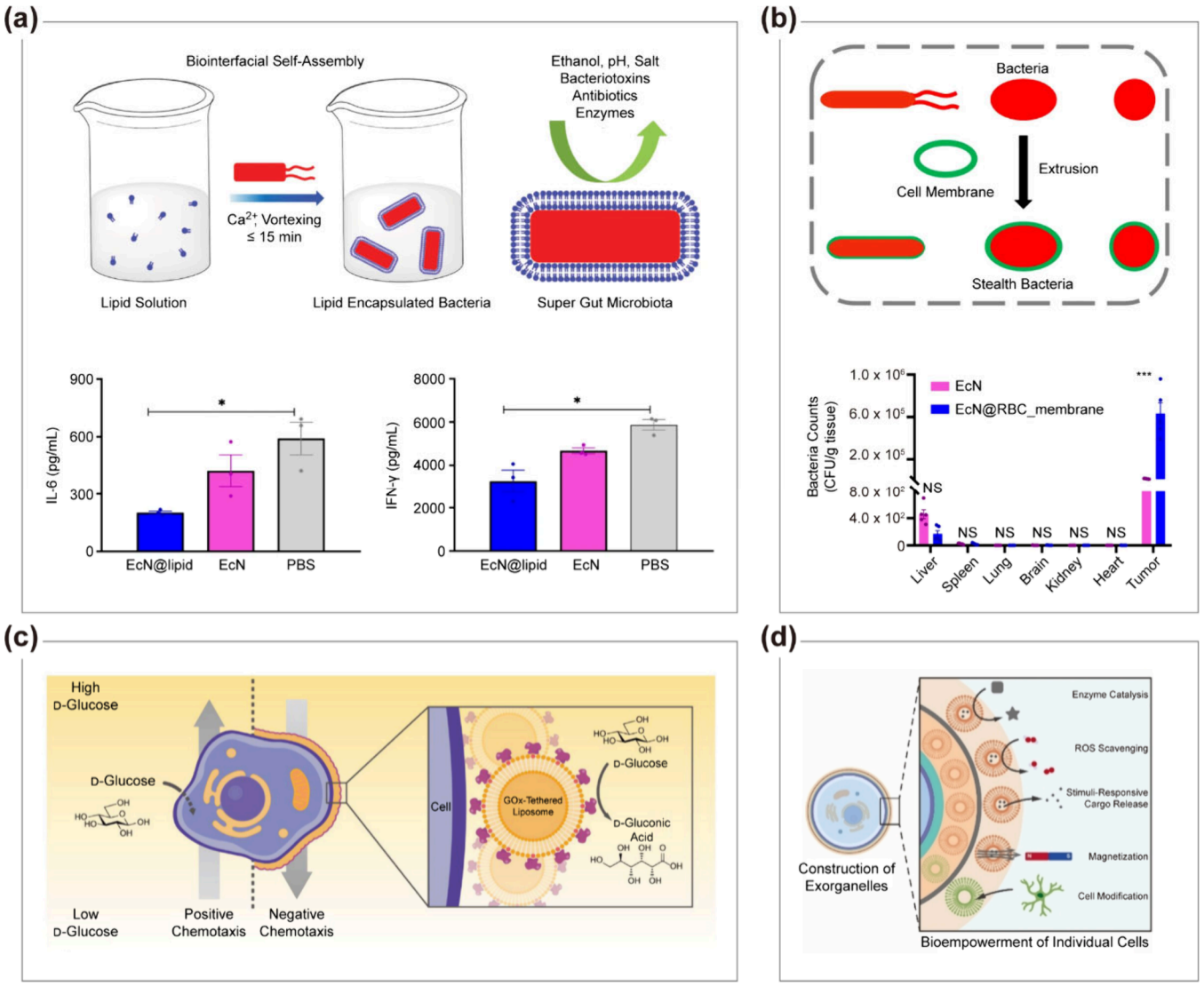

Figure 8. Schematic illustration of strategies for forming nanoshells from lipids and liposomes. (a) (top) Schematic of Ca^{2+}-assisted self-assembly of lipid nanoshells on cell surfaces. (bottom) Cytokine levels in serum after treating a *Salmonella typhimurium*-induced mouse model of colitis with EcN@lipid. Reproduced with permission from ref 134. Copyright 2019 Springer Nature under CC BY 4.0. (b) (top) Schematic of RBC-membrane nanoshell formation on cells via coextrusion. (bottom) Biodistribution of RBC-membrane nanoshell-encapsulated EcN and naïve EcN 12 days postinjection in tumor-bearing mice. Reproduced with permission from ref 135. Copyright 2019 Springer Nature under CC BY 4.0. (c) Schematic of enzymatic reaction-driven redirection of cell chemotaxis in Jurkat@liposome$_{[GOx]}$. Reproduced with permission from ref 40. Copyright 2023 Wiley-VCH. (d) Schematic of cells encapsulated within multilayers of functional liposomes, exorganelles. Reproduced with permission from ref 136. Copyright 2024 Wiley-VCH.

indicated by lower levels of cytokines such as interleukin-6 (IL-6) and tumor necrosis factor-γ compared with naïve EcN, attributed to the cytoprotective capability of the lipid shells that increased the amount of living EcN delivered to the target sites.

The immunocamouflaging capability of nanoshells has also been demonstrated with RBC membranes as shell materials (Figure 8b).[135] RBC membranes were chosen because membrane-bound CD47, a self-marker, reduces immunogenicity, leading to lower nonspecific adsorption, an antiphagocytic effect, and prolonged blood circulation time; thus, this approach would reduce the side effects of bacteria transplantation. The RBC-membrane nanoshell was formed on EcN by coextruding EcN with RBC membranes extracted from 6-to-8-week-old male mice. The anti-CD47-antibody experiment showed a 10-fold increase in CD47 intensity in the SCNEd EcN compared with naïve EcN, indicating that the SCNEd EcN carried extra CD47 of RBC membranes. Furthermore, the SCNEd EcN exhibited a 14-fold increase in blood circulation time, even 48 h after treatment, a significant reduction in inflammatory cytokines, a 42-fold increase in accumulation at tumor sites, and minimal accumulation in normal organs.

On the other hand, liposomes, rather than lipids themselves, have been used to impart active, exogenous functions to cells.[40,136] For instance, the nanoshell of GOx-tethered liposomes redirected the movement of Jurkat@liposome$_{[GOx]}$ in a D-glucose gradient through a GOx-catalyzed reaction of D-glucose, causing fugetactic movement opposite to that of their naïve counterparts (Figure 8c).[40] This demonstration provides a straightforward, efficient, and bioorthogonal tool to control the chemotactic behavior of cells in response to varying clinical environments. In addition, individual cells were encased with

https://doi.org/10.1021/acs.chemrev.4c00984
Chem. Rev. XXXX, XXX, XXX−XXX

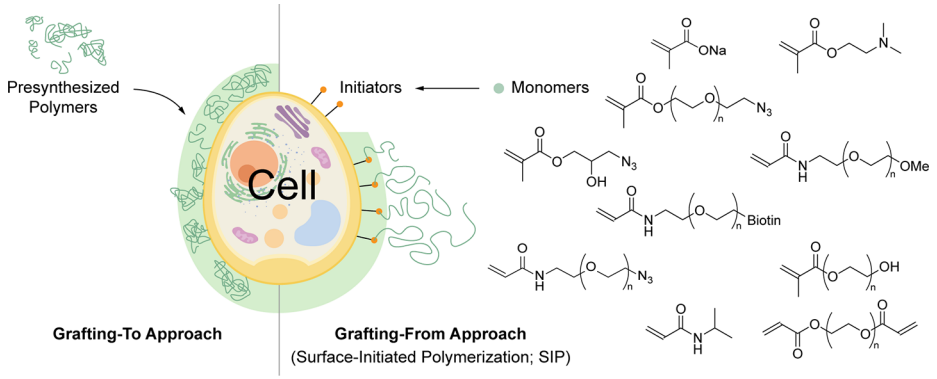

Figure 9. Schematic illustration of "grafting-to" and "grafting-from" synthetic strategies for cell-in-shell structures. In the "grafting-to" approach, presynthesized polymers are deposited onto the cell surfaces. In the "grafting-from" approach, also known as surface-initiated polymerization (SIP), polymers are synthesized directly from the polymerization initiators present on the cell surfaces. Representative monomers used for SIP: sodium methacrylate, 2-(dimethylamino)ethyl methacrylate, 3-azido-2-hydroxypropyl methacrylate, PEGMA-N_3, methoxy-PEG-acrylamide, ω-azido-PEG-acrylamide, ω-biotin-PEG-acrylamide, PEGMA, *N*-isopropylacrylamide, and PEGDA.

multilayers of functional liposomes, referred to as extracellular artificial organelles (exorganelles) (Figure 8d).[136]

2.2. Synthetic Polymers

Synthetic polymers have both advantages and limitations when used in SCNE. They offer greater diversity in composition and function, with the potential for customization in design. While numerous studies have demonstrated their use in shell formation, particularly via the LbL method, their application to mammalian cells remain limited due to cytotoxicity concerns.[69,137]

LbL Approaches. Early related work involves the alternating deposition of poly(allylamine hydrochloride) (PAH) and poly(sodium 4-styrenesulfonate) (PSS) on *S. cerevisiae*, where the cells remained viable after the formation of polyelectrolyte multilayers (PEMs).[67,138−141] These early studies primarily focused on the physicochemical properties of the PEMs, such as permeability,[71] rather than the cells themselves. However, MLS-inspired cross-linking of the PEMs, composed of catechol-grafted PEI and catechol-grafted HA, at pH 8.5 demonstrated that the durability of LbL shells could be enhanced, enabling the control of cell division as well as cytoprotection.[142] The thiol-exchange reaction was also utilized for cross-linking the PEMs of poly(2-(dimethylamino)ethyl methacrylate-*co*-2-(pyridyl disulfide)ethyl methacrylate) (PDMAEM-*co*-PPDEM) and poly(methacrylate-*co*-2-mercaptoethyl methacrylate) (PMA-*co*-PMEM), and the cross-linked nanoshells were degraded in response to GSH.[143]

The properties of LbL shells were utilized for enhanced cytoprotection and postmodification. UV-absorbing polymers, such as PSS, poly(vinyl sulfate) (PVS), and humic acid (HMA), were incorporated as anionic components in PEMs, and the SCNEd R34(pGFPuv)_*E. coli* exhibited increased resistance to UV-C irradiation, while maintaining GFPa1 expression rates and maximum GFPa1 fluorescence.[144] In addition, the outmost layer in PEMs served as an initiation site for bioinspired mineralization, enabling the nanoshell formation of SiO_2 (with PDADMA in PDADMA/PSS PEMs)[53,145,146] and calcium phosphate (CaP; with PAA in PDADMA/PAA PEMs).[147,148] As a method for achieving the control over the thickness of SiO_2 shells, a cycle of PDADMA deposition and bioinspired silicification was also repeated.[149] Furthermore, LbL SCNE approaches have incorporated a variety of organic and inorganic materials into the PEM shells, such as graphene oxide (GO),[150,151] multiwalled carbon nanotubes (MWCNTs),[152] magnetic NPs (MNPs),[153−159] Au NPs,[160,161] Ag NPs,[160,161] indium phosphide NPs,[162] and hydroxylated boron nitride nanotubes.[163]

Considering the potential toxicity of cationic polymers in electrostatic-based LbL construction,[164−168] Tsukruk and co-workers proposed a hydrogen-bonding-based approach for SCNE, where the nanoshells of TA and poly(*N*-vinylpyrrolidone) (PVPON) were constructed on *S. cerevisiae* with no noticeable decrease in viability.[169] A pH-responsive LbL nanoshell was also developed based on hydrogen bonding.[170] The LbL shells, made from PVPON and poly(methacrylic acid-*co*-amine) (PMAA-*co*-NH_2), were cross-linked with 1-ethyl-3-(3-dimethylaminopropyl)carbodiimide (EDC). The resulting nanoshells showed a remarkable capacity for reversible swelling/deswelling within a narrow pH range (pH 5.0−6.0), enabling the controlled cell growth. The hydrogen-bonding approach was also applied to pancreatic islet cells.[171]

Grafting-From Approaches. In surface-initiated polymerization (SIP), polymerization initiators, including chain transfer agents (CTAs), should be present on the cell surfaces prior to the initiation of SIP (Figure 9). In an early study, an initiator moiety for activator regenerated by electron transfer, atom transfer radical polymerization (ARGET-ATRP) was introduced to the surfaces of *S. cerevisiae* based on the pDA method, described in section 2.1.1.[172] A mixture of DA and a DA derivative bearing 2-bromoisobutyryl group, the initiator moiety, was used for the formation of pDA nanoshells. Compared with the direct conjugation of 2-bromoisobutanoic acid *N*-hydroxysuccinimide ester (BIB−NHS) to the cell surfaces, the pDA-mediated method resulted in a 2.4-fold increase in viability after SI-ARGET-ATRP with biocompatible sodium methacrylate as a monomer, demonstrating the protective ability of the pDA shell from radical species and the successful formation of polymer shells. Other monomers, such as 2-(dimethylamino)ethyl methacrylate, 3-azido-2-hydroxypropyl methacrylate, and azide-bearing PEG methacrylate (PEGMA-N_3), were also employed in the SI-ARGET-ATRP. The dense polymer shells physically prevented the agglutination of *S. cerevisiae* with *E. coli*. On the other hand, photoinduced electron transfer-reversible addition−fragmentation chain-transfer polymerization (PET-RAFT) was also employed for SIP from cell surfaces after CTA conjugation to *S. cerevisiae* or Jurkat cells.[173] In SI-PET-RAFT, PEG-based acrylamides were

https://doi.org/10.1021/acs.chemrev.4c00984
Chem. Rev. XXXX, XXX, XXX−XXX

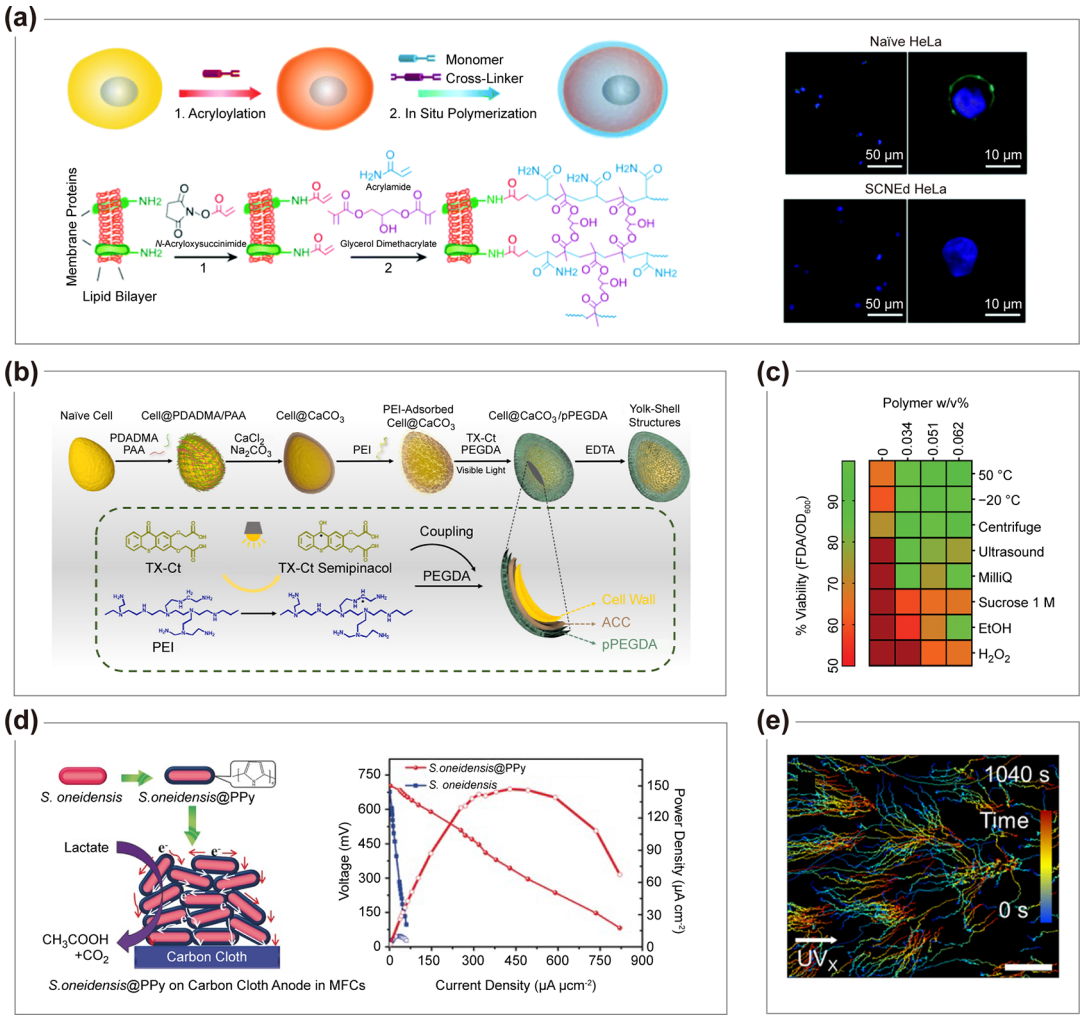

Figure 10. Strategies for constructing cells SCNEd in shells comprised of synthetic polymers, and properties of the SCNEd cells. (a) (left) Schematic of the procedure for constructing a cross-linked polymeric shell on mammalian cells through acryloylation of the cell membrane, followed by in situ polymerization. (right) CLSM images of naïve and SCNEd HeLa cells after immunoreaction. Green, FITC−anti-CD44; blue, DAPI. Reproduced with permission from ref 175. Copyright 2016 Royal Society of Chemistry. (b) Schematic illustration of constructing yolk-shell-type cell-in-shell structures via subsequent construction of $CaCO_3$ and pPEGDA shells, followed by removal of the $CaCO_3$ layer. Cell: *S. cerevisiae*. Reproduced with permission from ref 180. Copyright 2023 American Chemical Society. (c) Cell viabilities of naïve and SCNEd bacteria after exposure to harsh conditions. Reproduced with permission from ref 182. Copyright 2023 Wiley-VCH under CC BY 4.0. (d) (left) Schematic of the procedure for forming *S.oneidensis*@PPy on a carbon cloth anode. (right) Polarization and power density curves for MFCs with anodes of naïve bacteria films and *S.oneidensis*@PPy films. Reproduced with permission from ref 36. Copyright 2017 Wiley-VCH. (e) Tracking trajectories of *S.cerevisiae*@TiO_2/PPy during UV irradiation, showing collective behaviors of *S.cerevisiae*@TiO_2/PPy. Reproduced with permission from ref 184. Copyright 2023 American Chemical Society.

employed with eosin Y as a catalyst. In a recent study, HRP was copresented with BIB or CTA moiety on the surface of *S. cerevisiae*, and the performances of bio-ATRP and bio-RAFT were compared in the formation of PEGMA shells.[174] The bio-ATRP copolymerization of PEGMA and PEGMA-N_3 enabled on-surface bioorthogonal postfunctionalization, as demonstrated by click reactions with β-galactosidase−dibenzylcyclooctyne (DBCO), alkaline phosphatase−DBCO, and Cy5−DBCO.

Conceptually similar approaches have been utilized to form cross-linked hydrogel shells on individual cells. In one study, *N*-acryloxysuccinimide was coupled to the surfaces of various mammalian cells, including HeLa cells, MSCs, and bovine articular chondrocytes, followed by radical polymerization with acrylamide and glycerol dimethacrylate (Figure 10a).[175] The hydrogel shell prevented the penetration of anti-CD44 antibodies and Au NPs (diameter: 76.5 nm), not small molecules, while allowing the passage of amino acids and vitamins, demonstrating permselectivity. In other reports, GEL/PEG hydrogel shells were formed on MSCs primed with eosin, through photo-induced polymerization using GEL−methacrylamide and PEG diacrylate (PEGDA).[176,177] MSC@GEL/PEG exhibited enhanced retention in ischemic myocardium after transplantation to WT BL/6 mice subjected to myocardial infarction (MI), compared with naïve cells.[176] In addition, the shells were degradable by metalloproteinases, which are highly expressed in the ischemic heart. The GEL/PEG-based hydrogel shell was also formed after preconditioning in hypoxic culture, and MSC@GEL/PEG showed improved cell retention 7 days after injection into a murine MI model, compared with naïve cells. Furthermore, the enhanced retention after transplantation led to better cardioprotection, as demonstrated by improved recovery of cardiac function, smaller scar size, and enhanced

https://doi.org/10.1021/acs.chemrev.4c00984
Chem. Rev. XXXX, XXX, XXX−XXX

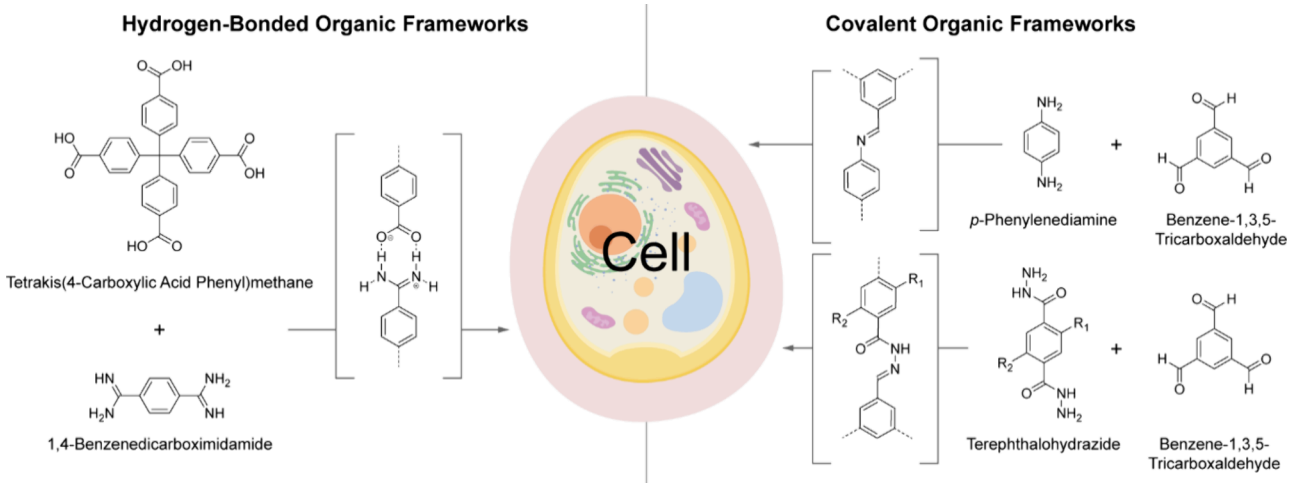

Figure 11. Schematic illustration of the formation of HOF shells and COF shells on individual living cells. HOF shells were constructed using 1,4-benzenedicarboximidamide and tetrakis(4-carboxylic acid phenyl)methane through hydrogen-bonding interactions. Two types of COF shells were formed: one using *p*-phenylenediamine and benzene-1,3,5-tricarboxaldehyde, and the other using 2-(but-3-en-1-yloxy)-5-(2-methoxyethoxy)-terephthalohydrazide and benzene-1,3,5-tricarboxaldehyde, both relying on covalent bond formation (R_1, 2-methoxyethoxy group; R_2, but-3-en-1-yloxy group).

angiogenesis compared with control groups.[177] A similar approach, using different strategies for eosin immobilization in the formation of MSC@GEL/PEG, was also reported by the same research group.[178]

As another approach to the photoinitiator introduction, the surface of *S. cerevisiae* was primed with PEI, and thioxanthone catechol-*O*,*O*-diacetic acid (TX-Ct) was electrostatically attached, leading to the formation of PEGDA shells.[179] This protocol was then modified to construct yolk-shell-type cell-in-shell structures (Figure 10b).[180] Prior to PEGDA shell formation, calcium carbonate ($CaCO_3$) shells were formed, followed by the subsequent attachment of PEI and TX-Ct. PEGDA polymerization and ethylenediaminetetraacetic acid (EDTA) treatment resulted in yolk-shell structures. Cell-specific shell formation has also been achieved with PEGDA hydrogel shells. For example, Jurkat cells, which express abundant CD45, were primed with eosin through subsequent coupling with a biotinylated anti-CD45 antibody and streptavidin-eosin isothiocyanate.[181] Jurkat@PEGDA showed cytoprotection (e.g., against sodium dodecyl sulfate (5%)), permselectivity, and degradability upon exposure to UV light.

Bruns, Belluati, and co-workers have recently reported a coextrusion method for forming a shell of Pluronic L-121 (PEG_5-*b*-PPG_{62}-*b*-PEG_5; PPG: poly(propylene glycol)), in which *E. coli* was coextruded with giant unilamellar vesicles of Pluronic L-121.[182] The Pluronic L-121 shell not only protected the cells from osmotic pressure, temperature shock, and lysozyme, but enabled postfunctionalization, exemplified by α-amylase conjugation (Figure 10c).

On the other hand, the nanoshells of polypyrrole (PPy), a synthetic conducting polymer, were formed around various bacterial cells, such as *S. oneidensis* MR-1, *Ochrobactrum anthropi*, *Streptococcus thermophilus*, and *E. coli*.[36] Fe^{3+} ions, electrostatically deposited on the cell surfaces, acted as oxidative initiators to form the PPy nanoshells in the presence of Py. In the study, *S. oneidensis* MR-1 was used as a model exoelectrogen. Exoelectrogens have been employed in microbial fuel cells (MFCs) to harvest electricity from organic substrates. However, the low power density, caused by poor extracellular electron transfer between exoelectrogens and anodes, has hindered the practical application in MFCs.[183] The PPy shells facilitated direct contact-based extracellular electron transfer through c-type cytochromes at outer membrane, and *S.oneidensis*@PPy exhibited a 14.1-fold increase in power output, compared with their naïve counterparts (Figure 10d). The same protocol for PPy shell formation was applied to *C. pyrenoidosa* in another study, aimed at augmenting the hypoxic photosynthesis of *C. pyrenoidosa* for H_2 production.[37] The PPy/$CaCO_3$ organic–inorganic hybrid shells were formed. The hypoxic conditions were induced by the Fe^{3+}/O_2-mediated oxidation of ascorbate, leading the activation of hydrogenase. The conductive PPy shells enhanced the rate of H_2 production by capturing and transferring extracellular electrons from *C.pyrenoidosa*@PPy/$CaCO_3$. The SCNE system enabled sustained H_2 production for 14 days, and photosynthesis-independent H_2 evolution for 200 days when extracellular electrons were periodically supplied. In addition, the manipulation of collective behaviors of individual *S. cerevisiae* was achieved by constructing the double-layered shells of TiO_2 NPs and PPy, where aldehyde-modified TiO_2 NPs were attached to the cell surface via Schiff base formation, followed by Fe^{3+} adsorption for PPy polymerization.[184] The conductive PPy layer was formed to enhance the photocatalytic activity of TiO_2 NPs under UV irradiation by lowering the recombination rate of photogenerated electrons and holes. Changes in the collective behaviors of *S.cerevisiae*@TiO_2/PPy in response to various inputs have been demonstrated. For example, upon UV irradiation of a solution containing *S.cerevisiae*@TiO_2/PPy and ferrocenemethanol (MFc), the SCNEd cells showed the collective negative phototaxis movement, which was attributed to the electroosmotic flow generated by the photoinduced redox reaction of MFc and the electric field produced by the diffusion of MFc^+ (Figure 10e).

2.3. Hydrogen-Bonded Organic Frameworks (HOFs) and Covalent Organic Frameworks (COFs)

HOFs and COFs are the 3D structures formed from organic building units interconnected via hydrogen bonds and covalent bonds, respectively (Figure 11). Unlike the more amorphous organic materials discussed in previous sections, they are relatively crystalline and can be intricately designed. In addition, the degree of cross-linking within the frameworks can be fine-

https://doi.org/10.1021/acs.chemrev.4c00984
Chem. Rev. XXXX, XXX, XXX−XXX

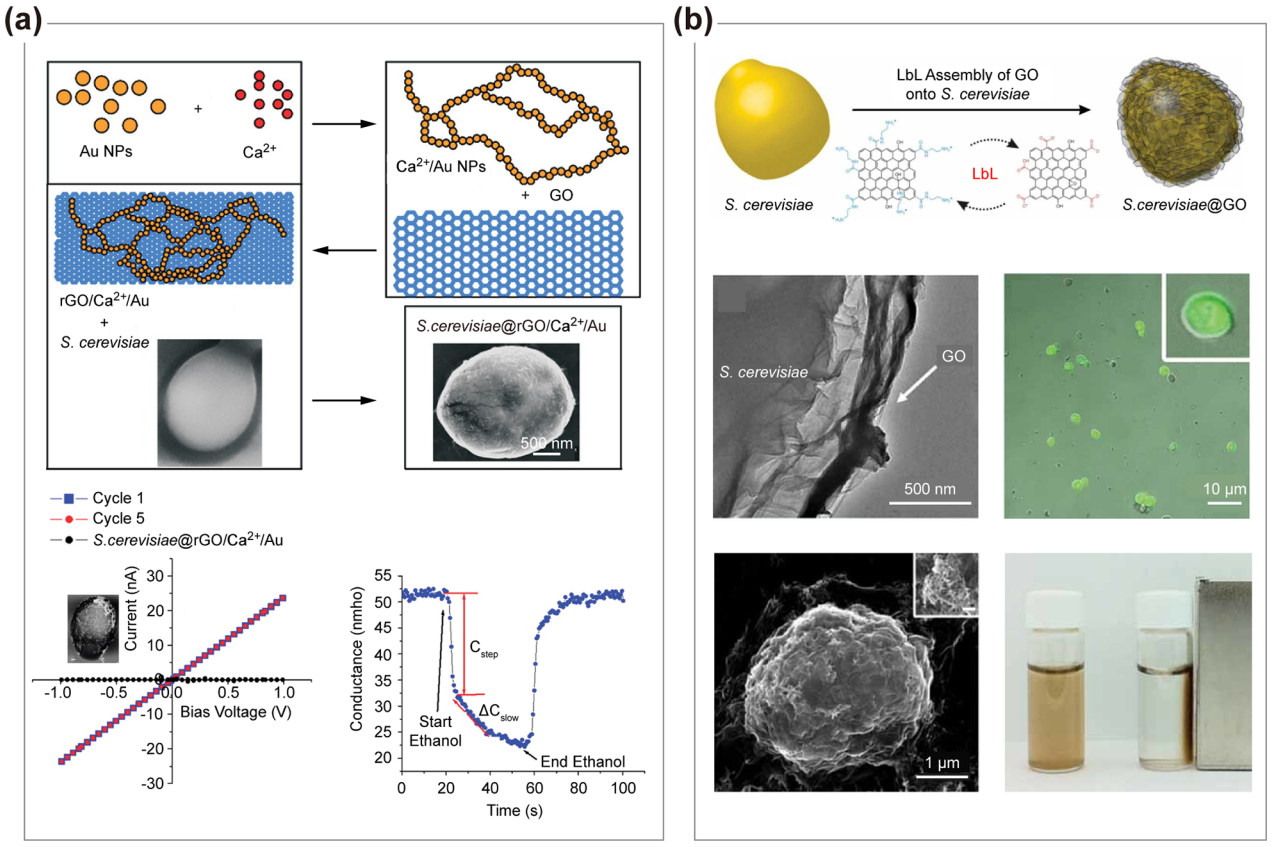

Figure 12. Strategies for constructing GO shells on living cells, and properties of the SCNEd cells. (a) (top) Schematic of *S.cerevisiae*@rGO/Ca^{2+}/Au construction. (bottom, left) Current and voltage characteristics of naïve and SCNEd cells. (bottom, right) Conductance of SCNEd cells upon ethanol exposure. Reproduced with permission from ref 192. Copyright 2011 American Chemical Society. (b) (top) LbL SCNE of GO nanosheets. (middle) Transmission electron microscopy and CLSM images of *S.cerevisiae*@GO, with cells stained with fluorescein diacetate for viability test. (bottom) Scanning electron microscopy and optical images of *S.cerevisiae*@GO/MNP. Reproduced with permission from ref 150. Copyright 2012 Wiley-VCH.

tuned on the specific selection of building units. Their metal-free nature promotes compatibility with biomolecules[185,186] and living cells,[187−189] making them highly promising candidates for SCNE.

The reversible and flexible nature of hydrogen-bonding interactions in HOFs facilitates high crystallinity, excellent solution processability, and mild synthesis conditions. Catalytically active HOF shells were formed around individual NSCs while preserving both their viability and multipotency, using 1,4-benzenedicarboximidamide, tetrakis(4-carboxylic acid phenyl)-methane, and porous carbon nanospheres (PCNs).[187] The PCNs were incorporated into the shells due to their catalase (CAT)- and superoxide dismutase (SOD)-like activities, which protected NSC@PCN/HOF from cytotoxic ROS. Furthermore, the porous PCNs served as carriers for retinoic acid (RA) in the formation of NSC@PCN/RA/HOF. The sustained release of RA from PCNs increased the proportion of NSCs differentiated into neurons. In vivo administration of NSC@PCN/RA/HOF into an Alzheimer's disease mouse model improved memory function and alleviated cognitive deficits, as demonstrated by the Morris water maze test and immunohistochemical analysis of brain tissues. These results highlight the potential of SCNE for customized, cell-based therapeutics against intractable diseases.

Compared with HOFs, COFs are constructed through stronger interactions, specifically covalent bonds, which are expected to provide more durable shells with diverse properties for living cells. Notably, the physicochemical characteristics of COFs, including acidic stability, water retention, ion-chelating effects, and the adsorption of organic molecule through $\pi-\pi$ and hydrogen-bonding interactions, effectively protected *S.cerevisiae*@COF from external aggressors, such as elevated temperatures, low pH, and organic pollutants (e.g., bisphenol A).[188] In this study, the COF was synthesized using *p*-phenylenediamine and benzene-1,3,5-tricarboxaldehyde, with acetic acid as the catalyst. The adsorption of CAT onto the cell surface prior to COF nanoshell formation further improved cellular survival under severe oxidative stress (100 mM H_2O_2). Another example of cell@COF/enzyme has been recently reported.[189] To a mixture of inulinase (INU) and *E. coli*, expressing D-allulose 3-epimerase, were added subsequently 2-(but-3-en-1-yloxy)-5-(2-methoxyethoxy)-terephthalohydrazide and benzene-1,3,5-tricarboxaldehyde in acetic acid, after the −COOH activation of INU and *E. coli*. *E.coli*@COF/INU exhibited higher resistance, when exposed to harsh environments, including heat, organic solvents, and enzymatic attack by chymotrypsin, as well as improved recyclability, compared with the mixture of free INU and *E. coli*. The cascade reaction of INU in the shell and D-allulose 3-epimerase in the cell for the production of D-allulose from inulin was demonstrated. The strategy was also applicable to various cell types, including EcN, *B. subtilis*, *C. pyrenoidosa*, and *S. cerevisiae*.

2.4. Graphene Oxides and Others

Graphene and its derivatives, such as graphene oxide (GO) and reduced graphene oxide (rGO), are promising candidates for

https://doi.org/10.1021/acs.chemrev.4c00984
Chem. Rev. XXXX, XXX, XXX−XXX

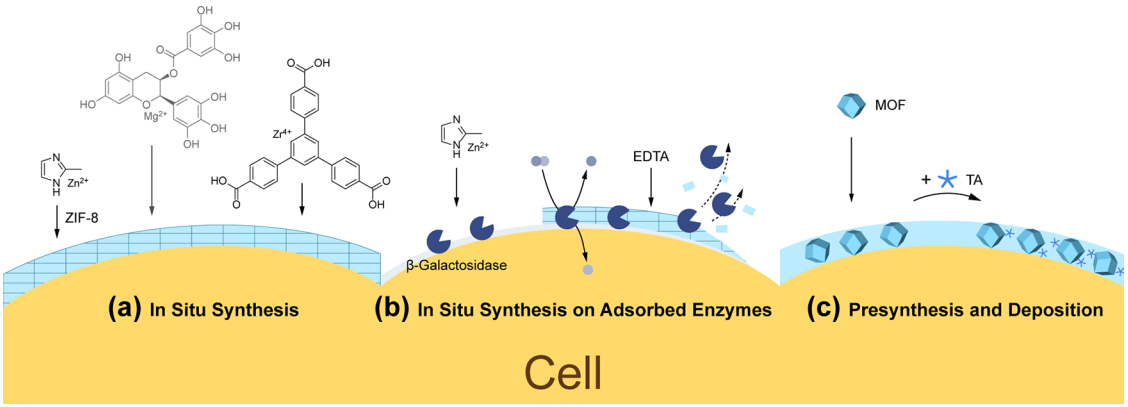

Figure 13. Schematic overview of strategies for forming MOF shells. (a) In situ synthesis of MOF shells on cell surfaces using Zn^{2+} ion and 2-methylimidazole, Mg^{2+} ion and EGCG, or Zr^{4+} ion and BTB. (b) In situ formation of ZIF-8 shells on cell surfaces preadsorbed with β-gal. The embedded β-gal enabled cell survival in lactose-containing media by cleaving lactose into glucose and galactose. Exposure to EDTA resulted in shell degradation and release of embedded enzymes. (c) Presynthesized MOF NPs are deposited onto cell surfaces and cross-linked with TA to construct MOF shells.

biological applications, including drug delivery systems, bioanalysis, and biosensors, due to their remarkable physicochemical properties.[190,191] Both GO and rGO exhibit high mechanical strength, with rGO demonstrating higher thermal and electrical conductivity as a result of the partial restoration of the π-bonding network. In SCNE, the graphene-based shells confer the electrical conductivity and robustness to cells.[150,151,192−194]

An early study leveraged the electrical conductivity of rGO sheets to monitor cellular responses by correlating mechanical changes in cells with alterations in the conductance of the rGO sheets (Figure 12a).[192] A complex of rGO, Au NP, and Ca^{2+} ions was deposited onto *S. cerevisiae*, leading to the formation of *S.cerevisiae*@rGO/Ca^{2+}/Au. As a demonstration, *S.cerevisiae*@rGO/Ca^{2+}/Au was exposed to ethanol, resulting in structural changes, such as a decrease in cell volume and an increase in surface roughness, which were tracked by a decline in conductance. In another study, the incorporation of graphene into the SiO_2 shell encapsulating *S. cerevisiae* led to a 9-fold increase in electrical conductivity compared with naïve cells.[193]

The nanoshell formation with GO has primarily been achieved through the LbL method, exemplified by the early work with negatively charged (GO−COO^-) and positively charged GO nanosheets (GO−NH_3^+) (Figure 12b).[150] The cytoprotective capability of GO shells against various harmful stresses was demonstrated for *S. cerevisiae* and HeLa cells,[151,194] but not against heavy metals (e.g., Cu^{2+} and Cd^{2+}).[195] For example, HeLa@GO demonstrated higher membrane integrity, reduced ROS levels, and inhibited apoptosis compared with naïve cells, when exposed to organic solvents, such as DMSO, acetone, ethanol, and glycerin.

3. HYBRID TYPE

Crystalline metal−organic frameworks (MOFs) and amorphous metal−organic complexes (MOCs) are the representative examples of hybrid coordination materials, widely used in SCNE. The organic and inorganic building blocks readily self-assemble into semi-infinite networks through coordination interactions between organic ligands and metal cations or clusters. MOFs and MOCs have recently gained widespread recognition as robust components in nanofilms for interface engineering and in nanoshells for SCNE, due to their uniformity and cytocompatibility.[196−199] Distinct from organic materials, the precise design and selection of components enable the modulation of pore sizes and network dimensions in specific hybrid shells. In addition, the degradability of these coordination materials under mild conditions allows for the restoration of cellular activities and proliferation after temporal but necessary cytoprotection, leading to the creation of micrometric Iron Men,[24] further empowered catalytically by the enzyme embedment within the nanoshells.[43,200]

3.1. Metal−Organic Frameworks (MOFs)

Over the past few decades, MOFs have garnered significant attention as a class of crystalline, porous materials. Their tunable, hierarchical, and functionalizable properties stem from the coordination interactions between inorganic and organic components, giving rise to one-, two-, or three-dimensional structures. The exceptional properties and large surface areas of MOFs offer great potential for various applications, including CO_2 capture and conversion,[201] as well as gas storage and separation.[202] In the realm of biomaterials, MOFs have taken a central role in SCNE as well as drug delivery systems, due to their thermal and chemical stability, cytocompatibility, and biodegradability.[14,203]

Encapsulation with MOF shells, pioneered by Falcaro and coworkers for the protection of biomacromolecules, including enzymes,[204,205] has recently been extended to individual living cells, such as *S. cerevisiae* and *Micrococcus luteus*.[197] The tunable pore sizes and modular structures of MOF shells offer size-specific designs that provide cytoprotection against various external stresses. For example, the ZIF-8 nanoshells around *S. cerevisiae* functioned as cytoprotective exoskeletons, allowing the selective transport of nutrients for cell metabolism while shielding the SCNEd cells from lyticase (Figure 13a). *S.cerevisiae*@ZIF-8 was further engineered to survive the oligotrophic microenvironments (e.g., lactose-based media) by embedding β-galactosidase (β-gal) between the cell wall and the ZIF-8 layer (Figure 13b).[200] The catalytically empowered *S.cerevisiae*@ZIF-8 retained over 70% viability after 7 days of culture in lactose-containing media, owing to the β-gal-catalyzed conversion of lactose into glucose. In contrast, over 90% of naïve cells lost their viability. In another study, MOF nanoshells, as cargo carriers, facilitated cytoprotection through the controlled release of exogenous biomolecules or drugs.[206] Specifically, cargo was released upon shell degradation, thereby inducing

https://doi.org/10.1021/acs.chemrev.4c00984
Chem. Rev. XXXX, XXX, XXX−XXX

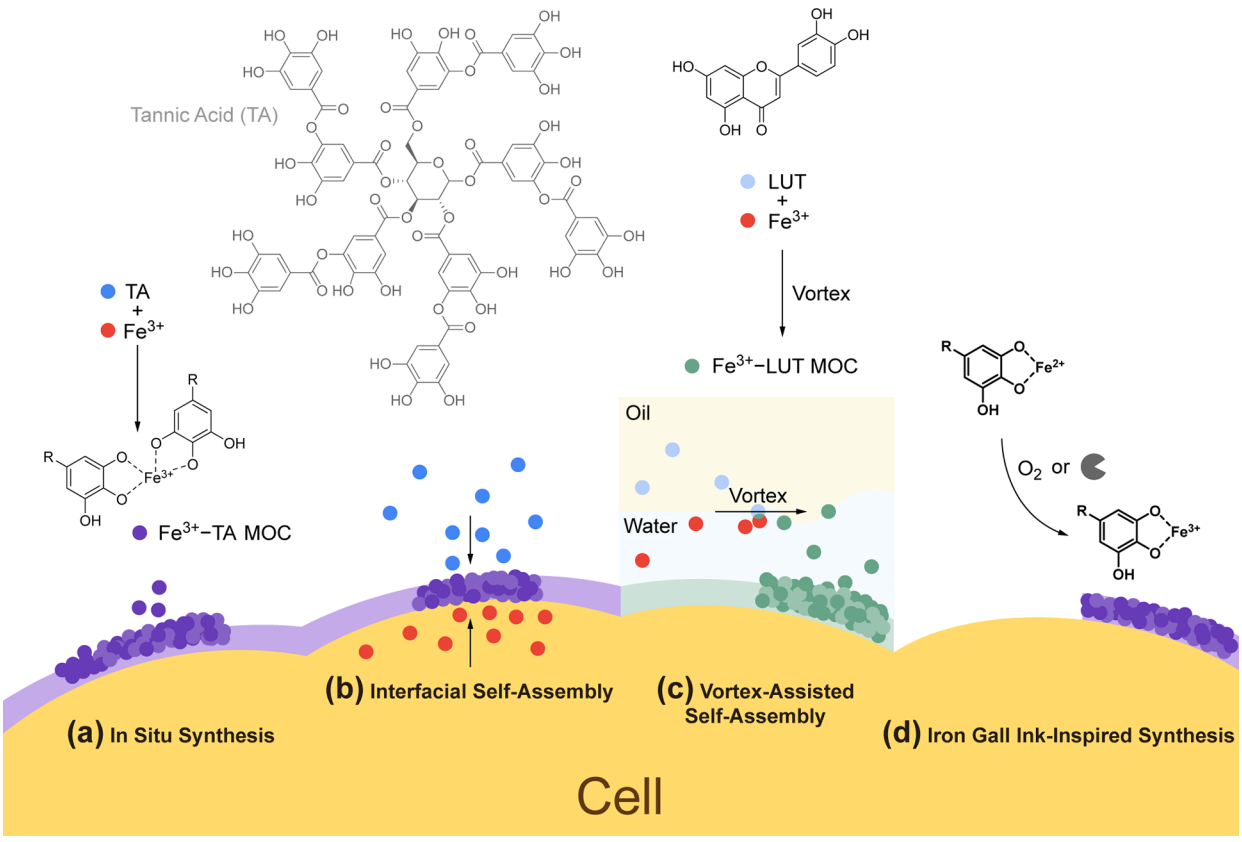

Figure 14. Schematic overview of strategies for constructing MOC shells. (a) Supramolecular assembly of Fe^{3+}−TA complexes enables the in situ synthesis of Fe^{3+}−TA MOC shells. (b) Biphasic interfacial supramolecular self-assembly of Fe^{3+} ions, prefed to cells, and TA from a TA solution results in Fe^{3+}−TA MOC shell formation. (c) Vortex-assisted, biphasic water−oil systems facilitate MOC shell formation of Fe^{3+} ions and water-insoluble LUT. (d) Inspired by iron gall ink, Fe^{2+} ions are used for Fe^{3+}−TA MOC shell formation, with Fe^{2+} oxidized to Fe^{3+} by O_2 or GOx.

cytoprotection through the actions of the released entity. As an example, *S.cerevisiae*@ZIF-8 was encased with antitrypsin and ZIF-C. Since the ZIF-C layer degraded more rapidly than the ZIF-8 layer when exposed to EDTA, ZIF-8 continued to serve as the cytoprotective shell, while the released antitrypsin deactivated trypsin in the medium.

The use of ZIF-8 is substantial in MOF-based SCNE applications, primarily due to its cytocompatibility and degradability. In biocatalysis, *B. subtilis*, genetically engineered to overexpress trehalose synthase, was SCNEd within ZIF-8 nanoshells containing glucose isomerase.[207] *B.subtilis*@ZIF-8 functioned as reusable whole-cell biocatalysts in the production of trehalose and fructose from maltose, demonstrated by a maximal conversion rate of trehalose synthase as 68%, while maintaining over 50% efficiency after 20-reaction cycles, with the concomitant production of fructose mediated by glucose isomerase. In whole-cell vaccines and cell-based therapies, it was reported that even when dosed to a lethal dose of uropathogenic *E. coli* CFT073 (CFT), model mice vaccinated with CFT@ZIF-8 survived without developing urosepsis.[208] Such vaccination effects were absent with vaccines made from fixed or heat-treated CFT. The serum level of anti-CFT073 IgG in splenocytes from mice immunized with CFT@ZIF-8 increased 5-fold compared with the control, likely due to the formation of larger germinal centers in the draining lymph nodes, which may account for the improved survival rate of vaccinated mice. Furthermore, CFT@ZIF-8 remained at the injection sites for 4 days longer than the fixed CFT, suggesting superior vaccine efficacy. In addition to ZIF-8, a MOF shell of Mg^{2+} and epigallocatechin-3-gallate (EGCG) was formed around bone marrow stem cells (BMSCs) in situ for cell therapy applications, demonstrating that BMSC@Mg^{2+}−EGCG alleviated ionizing radiation-induced hematopoietic damage and reduced apoptosis and ferroptosis via the regulation of ROS generated by IR-induced lipid peroxidation in vivo (Figure 13a).[209]

On the other hand, catalytic MOF nanoshells were constructed around anaerobic microbes to protect them under aerobic conditions. Exposure of anaerobic bacteria to air has a lethal impact on cell survival, as O_2 is converted to H_2O_2 by NADH oxidase, and subsequently into cytotoxic hydroxyl radicals through Fenton reactions. Yang, Yaghi, and co-workers encapsulated anaerobic *Moorella thermoacetica* within the MOF shells composed of Zr^{4+} and 1,3,5-benzenetribenzoate (BTB), which possessed catalytic capability to decompose ROS (Figure 13a).[210] When subjected to 21% O_2 conditions for 2 days, naive *M. thermoacetica* experienced a 33% reduction in viability, whereas *M.thermoacetica*@Zr^{4+}−BTB exhibited only a 7% decrease. Furthermore, in a 1 μM H_2O_2 solution for 2 days, the viability of *M.thermoacetica*@Zr^{4+}−BTB was more than twice that of naïve *M. thermoacetica*. These results promise the potential of MOF shells to serve as both extrinsic catalysts and active carriers for functional cargo, endowing cells with exogenous capabilities.

In addition to the in situ synthesis of MOFs on the cell surfaces, presynthesized MOF NPs were deposited onto the cell surfaces with cross-linking, endowing the cell with the properties of NPs, as well as cytoprotection in the construction of SupraCells (Figure 13c).[211,212] In a recent study, ZIF-8 NPs

https://doi.org/10.1021/acs.chemrev.4c00984
Chem. Rev. XXXX, XXX, XXX−XXX

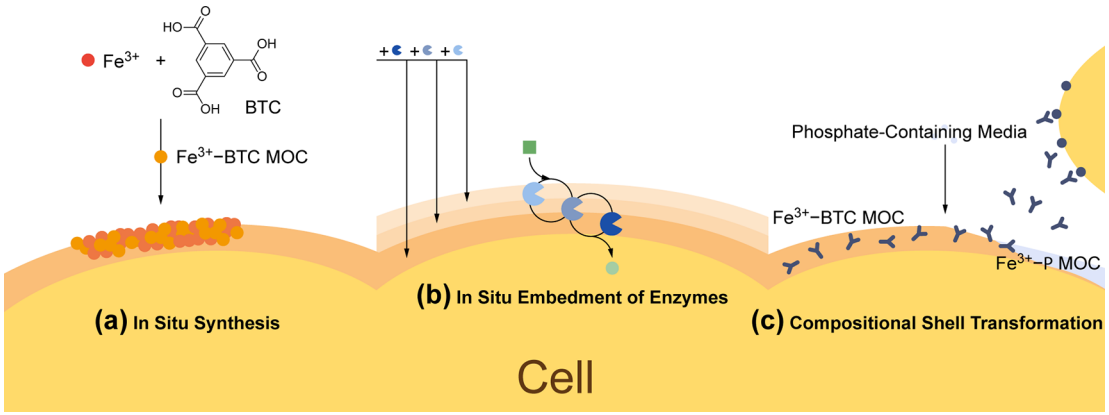

Figure 15. Schematic illustration of the formation of Fe^{3+}−BTC MOC shells and their properties. (a) In situ supramolecular assembly of Fe^{3+} and BTC results in the formation of Fe^{3+}−BTC MOC shells. (b) The inclusion of enzymes during the shell formation enables the simultaneous embedment of multiple enzymes within the shell, facilitating multienzymatic cascade reactions. (c) Exposure to phosphate-containing media transforms the Fe^{3+}−BTC shells into Fe^{3+}−P shells, accompanied by the release of embedded functional cargos.

were deposited only on the exposed surfaces of BMSCs adhered to the culture dish, leading to the formation of Janus-type cell-in-shell structures.[213,214] The Janus-type ZIF-8 nanoshell maintained cellular integrity and viability even after cell detachment, allowing the suspended BMSCs to preserve metabolic activities and secrete functional biomolecules essential for cell therapies. Drug loading into the ZIF-8 shells was also achievable. Notably, the partial ZIF-8 shell provided cytoprotection against detrimental environmental conditions, including ROS, pH changes, and osmotic pressure.

3.2. Metal−Organic Complexes (MOCs)

MOCs are broadly amorphous networks composed of metal ions and organic ligands.[215] They are typically produced spontaneously at ambient temperature, whereas crystalline MOFs require precisely controlled conditions for synthesis. The mild conditions in the synthesis of MOCs have facilitated in situ encapsulation strategies in various fields, including bioaugmentation, interface engineering, antimicrobial applications, and even cosmetics.[43,216−218] In SCNE, the cytocompatibility and degradability of MOC nanoshells, in particular, have catalyzed the widespread use of MOCs in nanoshell formation.

As an initial example of degradable nanoshells, the MOC shell composed of Fe^{3+} and TA was constructed around *S. cerevisiae* in 2014 (Figure 14a).[199] Later, the protocol was adapted to various cell types, including labile mammalian cells, with modifications as needed.[219,220] The degradation processes of Fe^{3+}−TA MOC shells, as well as the SCNE conditions, proved mild enough to maintain cell viability and activity.[221−223] It was recently reported that anaerobic *Bacteroides_thetaiotaomicron*@Fe^{3+}−TA was protected from O_2 exposure and harsh processing conditions, such as lyophilization, even in the absence of a canonical cryoprotectant like trehalose.[33] In another study, the Fe^{3+}−TA MOC nanoshell protected EcN from antibiotics, as indicated by a significantly recovered growth rate after incubation in simulated GI conditions including the antibiotic levofloxacin.[31] Moreover, antibiotic-induced diarrhea was alleviated in model mice experiments. Furthermore, a recent study demonstrates the enhanced in vivo wound healing efficacy of hydrogel dressing incorporating *Lactobacillus*@Fe^{3+}−TA in rat models.[224] Overall, the cytoprotective and on-demand degradative properties of Fe^{3+}−TA MOC shells, or MOC shells in general, would facilitate the use of SCNEd cells in various application sectors.

Departing from the extensive use of Fe^{3+}−TA MOC, a new type of MOC, composed of Fe^{3+} and 1,3,5-benzenetricarboxylic acid (BTC), has recently been developed and adapted for application in cytocompatible SCNE of both microbial and mammalian cells (Figure 15a).[43] This system, in particular, enabled simultaneous enzyme embedment during multilayered shell formation, along with cytoprotection and degradation, as its key characteristics (Figure 15b). The controlled embedment of a series of enzymes in the Fe^{3+}−BTC MOC shells supported exogenous cascade reactions without any loss of enzymatic activities. As a demonstration, β-glucosidase (β-glu) in a set of β-glu, GOx, and HRP embedded in the shell cleaved octyl-β-D-glucopyranoside, a toxic nonionic detergent, into D-glucose, which then served as a substrate for subsequent GOx−HRP reactions. Furthermore, the Fe^{3+}−BTC shells transformed into Fe^{3+}−phosphate (Fe^{3+}−P) shells in phosphate-containing media, concomitant with the release of the cargo from the Fe^{3+}−BTC MOC shell, Fe^{3+}−$BTC_{[cargo]}$ (Figure 15c).[42] For example, *S.cerevisiae*@Fe^{3+}−$BTC_{[lysozyme]}$ effectively killed *E. coli* upon its shell transformation into Fe^{3+}−P. Anti-CD3 and anti-CD28 antibodies, released from *S.cerevisiae*@Fe^{3+}−$BTC_{[anti-CD3/anti-CD28]}$, activated Jurkat cells, leading to the secretion of IL-2 at the level approximately 600% higher compared with Jurkat cells alone. These demonstrations highlight the potential of SCNEd cells to actively control and modulate external environments.

In terms of fabrication strategies, unlike MOF-based SCNE, which requires the localized concentration of MOF precursors near or on cell surfaces, the formation of MOC shells can be achieved through various strategic approaches, each with its own advantages. For example, LbL-like processes enabled the formation of MOC nanoshells incorporating functional entities, such as DNA, MNPs, and magnetic resonance imaging agents.[225] Another method is biphasic interfacial supramolecular self-assembly (BI-SMSA),[215] in which *S. cerevisiae*, prefed with Fe^{3+} ions, were incubated in a TA solution (Figure 14b). In this system, the efflux of Fe^{3+} ions induced interfacial self-assembly with TA on cell surfaces, resulting in the formation of *S.cerevisiae*@Fe^{3+}−TA.[226] Vortex-assisted, biphasic water−oil systems were also developed in MOC SCNE for water-insoluble ligands, where a simple vortexing of the biphasic system of Fe^{3+} ions and *L. acidophilus* in water and water-insoluble luteolin (LUT) in oil rapidly encapsulated *L. acidophilus* (Figure 14c).[227]

https://doi.org/10.1021/acs.chemrev.4c00984
Chem. Rev. XXXX, XXX, XXX−XXX

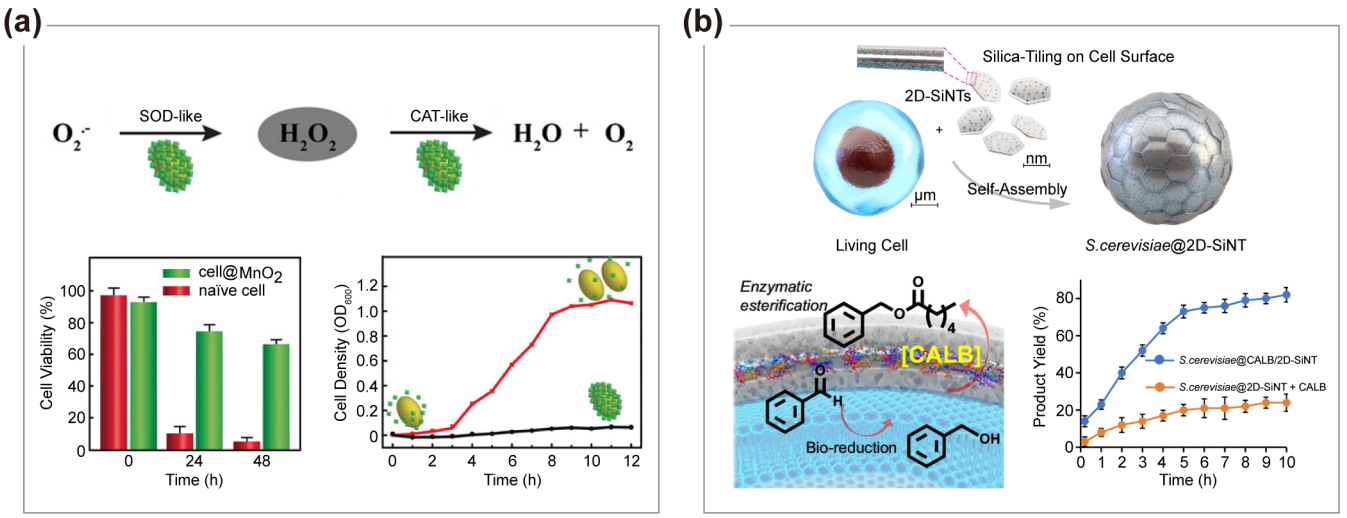

Figure 16. Construction of cell-in-shell hybrids from inorganic materials. (a) (top) Schematic of SOD- and CAT-like activities of MnO_2 nanoshells. (bottom, left) Cell viabilities of naïve and *S.cerevisiae*@MnO_2 cells after incubation in H_2O_2 solution for different durations. (bottom, right) Growth profile of *S.cerevisiae*@MnO_2 before and after shell degradation with GSH. Reproduced with permission from ref 233. Copyright 2017 Wiley-VCH. (b) (top) Schematic of silica-tiling on the surface of *S. cerevisiae*. (bottom, left) Schematic showing the combination of intracellular ketoreductase activity of *S. cerevisiae* with shell-embedded-CALB-mediated esterification reactions and (bottom, right) reaction kinetics of final ester product formation. Reproduced with permission from ref 234. Copyright 2024 Springer Nature under CC BY 4.0.

Alternatively, Fe^{2+} ions, rather than Fe^{3+} ions, have been employed for the formation of Fe^{3+}−TA MOC shells, inspired by iron gall ink,[216] and applied to SCNE (Figure 14d). In one study, the oxidation of Fe^{2+}, mediated by GOx, led to the formation of *S.cerevisiae*@Fe^{3+}−TA, with the simultaneous embedment of GOx in the shell.[228]

4. INORGANIC TYPE

Nature offers numerous examples of using inorganic materials for cytoprotection and adaptability, such as diatoms and radiolarians with SiO_2-based cell walls, and coccolithophores and foraminifera with $CaCO_3$ exoskeletons. These natural systems inspired researchers to develop mineral-based nanoshells in the early stages of SCNE research. Inorganic materials, compared with the organic counterparts, provide superior mechanical durability and thermal stability, along with additional functionalities such as catalytic activity and magnetism, making them suitable for the creation of artificial spores. For instance, bioinspired mineralization has enabled the formation of SiO_2−TiO_2 nanoshells, which function as thermal barriers to protect the SCNEd cells.[93] TiO_2 nanoshells have also been used to confer exogeneous photocatalytic activities to *S. cerevisiae* under UV irradiation, which would otherwise cause detrimental effects to naïve cells.[184] $CaCO_3$ shells[231] have served as platforms for the construction of artificial yolk-shell spores[180,232] and for metabolic switching from O_2 to H_2 production in algal cell bionics.[37] Since reports on certain mineral nanoshells (i.e., SiO_2 (refs 52−54, 60, 94, 145, 146, 149, 193, 229), TiO_2 (refs 60, 92, 93, 184, 230), CaP (refs 147, 148), and $CaCO_3$ (refs 37, 180, 231, 232)) have been discussed in previous sections in conjunction with other material types, this section highlights additional examples involving other inorganic materials for SCNE.

MnO_2 nanoshells, acting as nanozymes, were constructed on *S. cerevisiae* through a biomineralization approach, where the cells were incubated in a solution containing $MnCl_2$, followed by the addition of NaOH, to mimic the activities of SOD and CAT (Figure 16a).[233] *S.cerevisiae*@MnO_2 exhibited cytoprotection against prolonged exposure to high H_2O_2 levels, in addition to resistance to dehydration and lytic enzymes, due to nanozyme activity. Furthermore, the MnO_2 nanoshell could be degraded by GSH, a feature also observed in other inorganic shells, such as CaP under acidic conditions[147] or $CaCO_3$ in the presence of EDTA.[180]

Recently, *S. cerevisiae* was SCNEd with 2D-bilayer porous silica nanotiles (2D-SiNTs), which could host various catalytic entities, such as enzymes and NPs, in their nanospace, enabling exogenous reactions in concert with the cell's innate bioreactions (Figure 16b).[234] For instance, *S.cerevisiae*@2D-SiNT incorporated with *Candida antarctica* lipase B (CALB) performed esterification reactions that were coupled with the endogenous intracellular ketoreductase activity of *S. cerevisiae*. The SCNEd *S.cerevisiae*@CALB/2D-SiNT achieved significantly higher yield of an ester product compared with a physical mixture of *S.cerevisiae*@2D-SiNT and CALB.

5. APPLICATIONS AND CHALLENGES

Although this review primarily focuses on the material types of nanoshells utilized in SCNE, this emerging field has already shown substantial potential across a wide range of disciplines, spanning foundational areas such as bioorganic chemistry, biochemistry, and chemical biology, as well as applied fields including synthetic biology, materials science, and biomedical engineering. As a platform for fundamental research, SCNE enables the precise manipulation of cellular processes through the nanoencapsulation of individual cells with engineered nanomaterials, allowing for the investigation of intracellular interactions at the single-cell level. SCNE has also proven to be a valuable tool for examining cellular responses to specific stimuli, thereby facilitating the elucidation of complex biochemical pathways. Moreover, SCNE permits the isolation and observation of single cells within chemically controlled microenvironments, contributing to studies of cellular heterogeneity and underlying molecular mechanisms.[21−24]

On the applied side, the potential of SCNE is even more expansive. For instance, in materials science, SCNE enables the

https://doi.org/10.1021/acs.chemrev.4c00984
Chem. Rev. XXXX, XXX, XXX−XXX

design of advanced nanomaterials capable of interacting with and modulating cellular functions in a cytocompatible manner, thereby supporting the development of next-generation, cell-based biomaterials. SCNE also facilitates the construction of self-contained synthetic cellular systems capable of executing complex tasks, including the production of biofuels and pharmaceuticals, as well as environmental sensing. Furthermore, SCNE provides a means to enhance drug delivery systems, cancer therapies, regenerative medicine, and agricultural innovation by protecting labile biological components and enabling precise control over their fate.[12−16]

Despite the remarkable potential of SCNE demonstrated at the laboratory scale, several challenges remain—particularly in the development of processing technologies that enable seamless integration into real-world applications. A primary hurdle is the need for practically efficient SCNE methods capable of reliably nanoencapsulating and purifying individual cells at scale, ideally in conjunction with existing industrial processes, such as lyophilization and cold storage.[33,38] While certain demonstrated approaches, including those based on pDA and MOCs, show promise for scalability, practical large-scale implementation has yet to be achieved. Homogeneity is another concern, as variations in the SCNE process and inherent cellular activities could result in structural and functional heterogeneity among SCNEd cells. Addressing these challenges requires continued technological innovation, along with a deeper understanding of how various SCNE materials and strategies influence cellular behavior.

6. REMARKS AND PERSPECTIVES

This review provides a general overview of the developments and progress achieved over the past decade, with a focus on the materials used in SCNE. The materials are categorized into organic, hybrid, and inorganic types for clarity in discussion. It should be noted, however, that many studies have employed combinations of materials to achieve specific goals, highlighting the versatility of SCNE approaches.

SCNE has emerged as a transformative tool and burgeoning research field, marked by monumental breakthroughs. Initially inspired by cryptobiosis in nature, chemists have developed physiochemically and mechanically durable shells around individual living cells in a cytocompatible manner, with the aim of creating artificial spores.[21−23] The nanoshells provide robust physical and chemical protection, shielding the cells inside from external, often sporadic, stressors, also known as cytoprotection, which is a hallmark of SCNE.[235,236] Advances such as on-demand shell degradation and compositional transformation have led to the development of micrometric "Iron Men"[24,199] and "Transformers"[42,43] in the construction of artificial spores. The nanoshells of micrometric Iron Men provide robust protection for cells and are designed to degrade or disassemble on demand, allowing for controlled release or modification of the SCNEd cells. In addition to cytoprotectability and permselectivity, degradability is another key property for artificial spore shells, enabling adaptive responses to environmental changes, therapeutic interventions, or metabolic processes. It balances the durable protective function of the shell with the ability to be dismantled when necessary. In contrast, micrometric Transformers are engineered to undergo chemical changes or adaptive transformations, allowing them to adjust their shell composition or properties in response to external stimuli or environmental conditions. The shell transformation can be activated to enhance cellular functionality and enable control over the external environment according to the cell's needs. Aside from the methodological and strategic developments, innumerable potential applications of SCNE have been demonstrated, particularly benefiting from shell functionalizability, including cell theranostics, microbial biotherapeutics, probiotics for health, cell factories for chemical production and renewable energy, biosensing, environmental remediation, tissue engineering, regenerative medicine, and drug delivery.

In addition to a general overview of past research achievements, this review offers insight into the next significant advancements in fundamental SCNE research, such as the chemical manipulation of cellular metabolism, states, and fates, as well as the enhancement of cellular capacity.[18] Notable early examples in this direction include metabolic rewiring from O_2 to H_2 synthesis in *C. pyrenoidosa*[37,44] and metabolic coupling with external chemical reactions in *S. cerevisiae*.[234] Structurally, the yolk-shell construction is particularly noteworthy,[237] as it creates internal free space, analogous to egg architecture before hatching. This design would offer distinct advantages in the preservation of cellular functionality, while also providing cytoprotection and enabling controlled interactions with the external environment. Furthermore, research demonstrates that SCNE can be extended to chemically control dynamic cellular processes like cytotaxis, alongside the regulation of "static" cellular metabolism,[40] enhancing the adaptive survivability of cell-in-shells.

From a chemical perspective, the next frontier in SCNE is anticipated to involve the creation of metabolically coupled, "all-in-one" artificial spores with advanced self-sustaining functionalities (Figure 17). Inspired by myriad examples in nature, including the melanin coat of *C. neoformans*, upcoming studies in SCNE are proposed to center on the establishment of a cyclic, self-regenerating process of chemical shell formation and degradation, seamlessly integrated with intrinsic cellular reactions to support adaptive cellular survival at every stage—from alpha to omega. In this all-in-one framework, individual cells gain the ability to autonomously sense and respond to external conditions, dynamically forming and breaking down

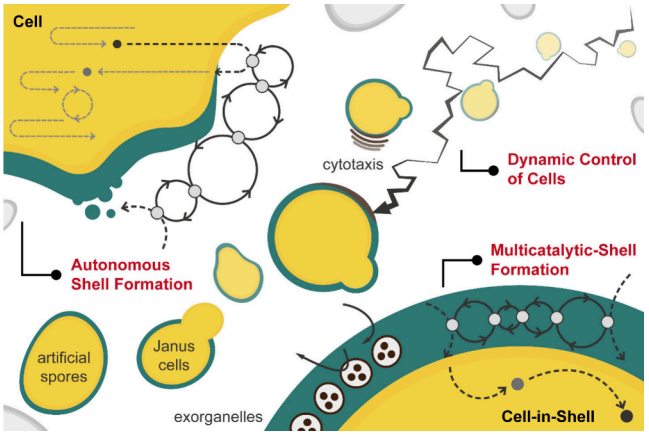

Figure 17. A schematic illustrating the next frontier in single-cell nanoencapsulation: "all-in-one" artificial spores. These artificial spores autonomously detect and respond to external environments, dynamically assembling and disassembling functional nanoshells through a precise interplay of endogenous and exogenous reactions. Functional entities embedded within nanoshells of varied forms and shapes empower cell-in-shell hybrids with the capability of enhanced adaptive survival, environmental manipulation, and dynamic cell movement.

https://doi.org/10.1021/acs.chemrev.4c00984
Chem. Rev. XXXX, XXX, XXX−XXX

reconfigurable nanoshells through a finely tuned interplay of endogenous and exogenous reactions. The nanoshells incorporate functional entities—such as enzymes, antibodies, and nanoparticles—during shell formation, and strategically release them upon shell degradation or transformation to enhance adaptive survival, regulate external conditions, or execute specific missions for diverse applications. Moreover, the shell structures are not limited to uniformly closed shells but include open-shell structures, such as Janus-type shells, alongside yolk-shell-type structures, which enable precisely controlled, autonomous cell movement.

Living cells have transcended their traditional role as mere subjects of biochemical and biological study. The SCNE strategies introduced in this review present a compelling approach for the chemical synthesis of on-demand, tailor-made cell-in-shell spores. Future research in SCNE holds substantial promise for foundational studies on the origin of life and cellular evolution, including phenomena like microchimerism and symbiogenesis. In addition, they offer a "top-down" paradigm for constructing synthetic cells and bioreactors. Furthermore, all-in-one artificial spores contribute to the development of multicellular structures such as organoids, expanding their applications across various sectors.

AUTHOR INFORMATION

Corresponding Authors

Insung S. Choi − *Center for Cell-Encapsulation Research, Department of Chemistry and Department of Bio and Brain Engineering, KAIST, Daejeon 34141, Korea;* orcid.org/0000-0002-9546-673X; Email: ischoi@kaist.ac.kr

Beom Jin Kim − *Department of Chemistry, University of Ulsan, Ulsan 44776, Korea; Basic-Clinic Convergence Research Institute, University of Ulsan, Ulsan 44033, Korea;* orcid.org/0000-0003-1526-6445; Email: kimbj@ulsan.ac.kr

Authors

Hyeong Bin Rheem − *Center for Cell-Encapsulation Research, Department of Chemistry, KAIST, Daejeon 34141, Korea*

Nayoung Kim − *Center for Cell-Encapsulation Research, Department of Chemistry, KAIST, Daejeon 34141, Korea*

Duc Tai Nguyen − *Center for Cell-Encapsulation Research, Department of Chemistry, KAIST, Daejeon 34141, Korea*

Ghanyatma Adi Baskoro − *Department of Chemistry, University of Ulsan, Ulsan 44776, Korea*

Jihun H. Roh − *Department of Chemistry, University of Ulsan, Ulsan 44776, Korea*

Jungkyu K. Lee − *Department of Chemistry, Kyungpook National University, Daegu 41566, Korea;* orcid.org/0000-0001-9508-1488

Complete contact information is available at: https://pubs.acs.org/10.1021/acs.chemrev.4c00984

Author Contributions

H.B.R. and N.K. contributed equally. CRediT: **H.B.R.** writing - original draft, writing - review and editing; **N.K.** writing - original draft, writing - review and editing; **D.T.N.** writing - original draft; **G.A.B.** writing - original draft; **J.H.R.** writing - original draft; **J.K.L.** writing - review and editing; **B.J.K.** writing - original draft, writing - review and editing; **I.S.C.** writing - original draft, writing - review and editing.

Notes

The authors declare no competing financial interest.

Biographies

Hyeong Bin Rheem is a Ph.D. candidate in the Department of Chemistry at KAIST. He joined Prof. Choi's group as a graduate student after obtaining his B.S. degree in Chemistry at KAIST. His research interest includes biomimetic chemistry and supramolecular chemistry for the applications in bioreactors, biocatalysts, as well as enzyme-powered nano/micromotors.

Nayoung Kim is a Ph.D. candidate in the Department of Chemistry at KAIST. She joined Prof. Choi's group as a graduate student after obtaining her B.S. degree in Chemistry at KAIST. Her research interests lie in enzyme-mediated systems for biomimetic chemistry and supramolecular chemistry.

Duc Tai Nguyen is a Ph.D. candidate in the Department of Chemistry at KAIST. He joined Prof. Choi's group as a graduate student after obtaining his B.S. degree in Chemistry with a double major in Biology at KAIST. His research interests span biomaterials, supramolecular chemistry, cell encapsulation, and biphasic systems.

Ghanyatma Adi Baskoro is a Ph.D. candidate in the Department of Chemistry at the University of Ulsan. He joined Prof. Beom Jin Kim's research group as a graduate student after earning his B.S. in Chemistry from the University of Indonesia. His research interest lies in the light-mediated control of molecular assemblies.

Jihun H. Roh earned his B.S. in Chemistry from the University of Ulsan in 2023. He is currently pursuing an M.S. degree at the University of Ulsan under the guidance of Prof. Beom Jin Kim. His research interest is the enzyme-catalyzed self-assembly.

Jungkyu K. Lee is a professor of Chemistry at Kyungpook National University (KNU). After completing his Ph.D. degree (with Prof. Zhenan Bao) at Stanford University, he worked as a postdoctoral researcher (with Prof. Hadley D. Sikes) at MIT. His current research interest is photoredox catalysis for polymerization.

Beom Jin Kim is an assistant professor of Chemistry at the University of Ulsan. He earned his B.S. in Chemistry from Sungkyunkwan University in 2012 and his Ph.D. in Chemistry from KAIST in 2018 under the supervision of Prof. Insung S. Choi. Following a postdoctoral fellowship with Prof. Bing Xu at Brandeis University, he began his independent research career at the University of Ulsan in 2020. His current research centers on the dynamic regulation of macromolecular assemblies within cellular niches.

Insung S. Choi is a professor of Chemistry and of Bio and Brain Engineering of KAIST. He earned his B.S. and M.S. degrees in Chemistry under the supervision of Prof. Eun Lee at Seoul National University and his Ph.D. in Chemistry and Chemical Biology under Prof. George M. Whitesides at Harvard University. He conducted postdoctoral research in Prof. Robert Langer's laboratory in the Department of Chemical Engineering of MIT before joining the KAIST faculty in 2002. He is currently focused on the development of chemical, biological, and computational tools for deciphering the cytosociety.

ACKNOWLEDGMENTS

This work was supported by the Basic Science Research Program through the National Research Foundation of Korea (NRF) (RS-2024-00335713).

ABBREVIATIONS

2D-SiNT = 2D-bilayer porous silica nanotile

https://doi.org/10.1021/acs.chemrev.4c00984
Chem. Rev. XXXX, XXX, XXX−XXX

ALG = alginate
ARGET-ATRP = activator regenerated by electron transfer, atom transfer radical polymerization
BAM = biocompatible anchor for cell membrane
BIB = 2-bromoisobutanoic acid
BLB = β-lactoglobulin
BMSC = bone marrow stem cell
BTB = 1,3,5-benzenetribenzoate
BTC = 1,3,5-benzenetricarboxylic acid
CALB = *Candida antarctica* lipase B
CaP = calcium phosphate
CAT = catalase
CEL = carboxymethyl cellulose
CFT = *Escherichia coli* CFT073
CHI = chitosan
CM = coffee melanoidin
COF = covalent organic framework
COL = collagen
CTA = chain transfer agent
DA = dopamine
DAPI = 4′,6-diamino-2-phenylindole
DBCO = dibenzylcyclooctyne
DC = dendritic cell
DexS = dextran sulfate
DHI = 5,6-dihydroxyindole
DHICA = 5,6-dihydroxyindole-2-carboxylic acid
DPC = dermal papilla cell
ECM = extracellular matrix
EcN = *Escherichia coli* Nissle 1917
EDC = 1-ethyl-3-(3-(dimethylamino)propyl)carbodiimide
EDTA = ethylenediaminetetraacetic acid
ESMH = eggshell membrane hydrolysate
Fe^{3+}−P = Fe^{3+}−phosphate
FN = fibronectin
GEL = gelatin
GI = gastrointestinal
GO = graphene oxide
GOx = glucose oxidase
GSH = glutathione
HA = hyaluronic acid
HFSC = hair follicle stem cell
hiPSC = human induced pluripotent stem cell
HMA = humic acid
HOF = hydrogen-bonded organic framework
HPN = hyaluronic acid-poly(propylene sulfide) nanoparticle
HRP = horseradish peroxidase
HUVEC = human umbilical vein endothelial cell
IGF-1 = insulin-like growth factor-1
IgG = immunoglobulin G
IL = interleukin
INU = inulinase
*is*DOP = in situ DNA-oriented polymerization
IVIS = in vivo imaging system
LAB = lactic acid bacteria
LbL = layer-by-layer
L-DOPA = L-3,4-dihydroxyphenylalanine
Lgr5 = leucine-rich repeat-containing G-protein coupled receptor 5
LUT = luteolin
MFc = ferrocenemethanol
MI = myocardial infarction
MIN-6 = mouse insulinoma cell
MLS = melanin-like species
MMP-7 = matrix metalloproteinase-7
MNP = magnetic nanoparticle
MOC = metal−organic complex
MOF = metal−organic framework
MR = magnetic resonance
MSC = mesenchymal stem cell
MWCNT = multiwalled carbon nanotube
NE = norepinephrine
NHS = *N*-hydroxysuccinimide
NIR = near infrared
NP = nanoparticle
NSC = neural stem cell
OVA = ovalbumin
PAH = poly(allylamine hydrochloride)
PCN = porous carbon nanosphere
PD-1 = programmed cell death protein 1
pDA = polydopamine
PDADMA = poly(diallyldimethylammonium chloride)
PDMAEM-*co*-PPDEM = poly(2-(dimethylamino)ethyl methacrylate-*co*-2-(pyridyl disulfide)ethyl methacrylate)
PEG = poly(ethylene glycol)
PEGDA = poly(ethylene glycol) diacrylate
PEGMA = poly(ethylene glycol) methacrylate
PEI = poly(ethylenimine)
PEM = polyelectrolyte multilayer
PET-RAFT = photoinduced electron transfer-reversible addition−fragmentation chain-transfer polymerization
PG = 1,2,3-trihydroxybenzene; pyrogallol
PLL = poly(L-lysine)
PMA-*co*-PMEM = poly(methacrylate-*co*-2-mercaptoethyl methacrylate)
PMAA-*co*-NH_2 = poly(methacrylic acid-*co*-amine)
pNE = polynorepinephrine
PPG = poly(propylene glycol)
PPy = polypyrrole
PSA = polysialic acid
PSS = poly(sodium 4-styrenesulfonate)
PVPON = poly(*N*-vinylpyrrolidone)
PVS = poly(vinyl sulfate)
RA = retinoic acid
RBC = red blood cell
RGD = arginine-glycine-aspartic acid
rGO = reduced graphene oxide
RhD = rhesus D
ROS = reactive oxygen species
S1 = SARS-CoV-2 spike 1
SCNE = single-cell nanoencapsulation
SF = silk fibroin
SGF = simulated gastric fluid
SI-ARGET ATRP = surface-initiated activator regenerated by electron transfer, atom transfer radical polymerization
SIF = simulated intestinal fluid
SIP = surface-initiated polymerization
SOD = superoxide dismutase
SV = *Salmonella* VNP20009
TA = tannic acid
TGF-β2 = transforming growth factor-β2
TNF-R1 = TNF-receptor 1
TNF-α = tumor necrosis factor-α
TUNEL = terminal deoxynucleotidyl transferase dUTP nick end labeling
TX-Ct = thioxanthone catechol-*O*,*O*-diacetic acid
L-Tyr = L-tyrosine

https://doi.org/10.1021/acs.chemrev.4c00984
Chem. Rev. XXXX, XXX, XXX−XXX

α-PD-1 = antiprogrammed cell death protein 1
β-gal = β-galactosidase
β-glu = β-glucosidase

REFERENCES

(1) Sun, J. C.; Beilke, J. N.; Lanier, L. L. Adaptive Immune Features of Natural Killer Cells. *Nature* **2009**, *457*, 557−561.
(2) Foster, E. A.; Franks, D. W.; Mazzi, S.; Darden, S. K.; Balcomb, K. C.; Ford, J. K. B.; Croft, D. P. Adaptive Prolonged Postreproductive Life Span in Killer Whales. *Science* **2012**, *337*, 1313.
(3) Russo, M.; Sogari, A.; Bardelli, A. Adaptive Evolution: How Bacteria and Cancer Cells Survive Stressful Conditions and Drug Treatment. *Cancer Discovery* **2021**, *11*, 1886−1895.
(4) Driks, A. Maximum Shields: The Assembly and Function of the Bacterial Spore Coat. *Trends Microbiol.* **2002**, *10*, 251−254.
(5) Nicholson, W. L.; Fajardo-Cavazos, P.; Rebeil, R.; Slieman, T. A.; Riesenman, P. J.; Law, J. F.; Xue, Y. Bacterial Endospores and Their Significance in Stress Resistance. *Antonie van Leeuwenhoek* **2002**, *81*, 27−32.
(6) Wang, Y.; Aisen, P.; Casadevall, A. *Cryptococcus neoformans* Melanin and Virulence: Mechanism of Action. *Infect. Immun.* **1995**, *63*, 3131−3136.
(7) Nosanchuk, J. D.; Casadevall, A. Budding of Melanized *Cryptococcus neoformans* in the Presence or Absence of L-Dopa. *Microbiol.* **2003**, *149*, 1945−1951.
(8) Eisenman, H. C.; Casadevall, A. Synthesis and Assembly of Fungal Melanin. *Appl. Microbiol. Biotechnol.* **2012**, *93*, 931−940.
(9) Sømme, L. Anhydrobiosis and Cold Tolerance in Tardigrades. *Eur. J. Entomol.* **1996**, *93*, 349−357.
(10) Kobayashi, H.; Shimoshige, H.; Nakajima, Y.; Arai, W.; Takami, H. An Aluminum Shield Enables the Amphipod *Hirondellea gigas* to Inhabit Deep-Sea Environments. *PLoS One* **2019**, *14*, No. e0206710.
(11) Park, J. H.; Yang, S. H.; Lee, J.; Ko, E. H.; Hong, D.; Choi, I. S. Nanocoating of Single Cells: From Maintenance of Cell Viability to Manipulation of Cellular Activities. *Adv. Mater.* **2014**, *26*, 2001−2010.
(12) Hasturk, O.; Kaplan, D. L. Cell Armor for Protection against Environmental Stress: Advances, Challenges and Applications in Micro- and Nanoencapsulation of Mammalian Cells. *Acta Biomater.* **2019**, *95*, 3−31.
(13) Pires-Santos, M.; Nadine, S.; Mano, J. F. Unveiling the Potential of Single-Cell Encapsulation in Biomedical Applications: Current Advances and Future Perspectives. *Small Sci.* **2024**, *4*, 2300332.
(14) Guo, Z.; Richardson, J. J.; Kong, B.; Liang, K. Nanobiohybrids: Materials Approaches for Bioaugmentation. *Sci. Adv.* **2020**, *6*, No. eaaz0330.
(15) Lee, H.; Kim, N.; Rheem, H. B.; Kim, B. J.; Park, J. H.; Choi, I. S. A Decade of Advances in Single-Cell Nanocoating for Mammalian Cells. *Adv. Healthc. Mater.* **2021**, *10*, 2100347.
(16) Yang, S.; Choi, H.; Nguyen, D. T.; Kim, N.; Rhee, S. Y.; Han, S. Y.; Lee, H.; Choi, I. S. Bioempowerment of Therapeutic Living Cells by Single-Cell Surface Engineering. *Adv. Therap.* **2023**, *6*, 2300037.
(17) Thirumalai, A.; Girigoswami, K.; Harini, K.; Pallavi, P.; Gowtham, P.; Girigoswami, A. A Review of the Current State of Probiotic Nanoencapsulation and Its Future Prospects in Biomedical Applications. *Biocatal. Agric. Biotechnol.* **2024**, *57*, 103101.
(18) Youn, W.; Kim, J. Y.; Park, J.; Kim, N.; Choi, H.; Cho, H.; Choi, I. S. Single-Cell Nanoencapsulation: From Passive to Active Shells. *Adv. Mater.* **2020**, *32*, 1907001.
(19) Xue, Z.; Mei, D.; Zhang, L. Advances in Single-Cell Nano-encapsulation and Applications in Diseases. *J. Microencapsul.* **2022**, *39*, 481−494.
(20) Centurion, F.; Basit, A. W.; Liu, J.; Gaisford, S.; Radim, Md. A.; Kalantar-Zadeh, K. Nanoencapsulation for Probiotic Delivery. *ACS Nano* **2021**, *15*, 18653−18660.
(21) Yang, S. H.; Hong, D.; Lee, J.; Ko, E. H.; Choi, I. S. Artificial Spores: Cytocompatible Encapsulation of Individual Living Cells within Thin. *Tough Artificial Shells. Small* **2013**, *9*, 178−186.
(22) Hong, D.; Park, M.; Yang, S. H.; Lee, J.; Kim, Y.-G.; Choi, I. S. Artificial Spores: Cytoprotective Nanoencapsulation of Living Cells. *Trends Biotechnol.* **2013**, *31*, 442−447.
(23) Hong, D.; Ko, E. H.; Choi, I. S. Artificial Spores. In *Cell Surface Engineering: Fabrication of Functional Nanoshells*; RSC Smart Materials; Fakhrullin, R. F., Choi, I. S., Lvov, Y. M., Eds.; The Royal Society of Chemistry: Cambridge, 2014; pp 142−161.
(24) Park, J. H.; Hong, D.; Lee, J.; Choi, I. S. Cell-in-Shell Hybrids: Chemical Nanoencapsulation of Individual Cells. *Acc. Chem. Res.* **2016**, *49*, 792−800.
(25) Kim, B. J.; Cho, H.; Park, J. H.; Mano, J. F.; Choi, I. S. Strategic Advances in Formation of Cell-in-Shell Structures: From Syntheses to Applications. *Adv. Mater.* **2018**, *30*, 1706063.
(26) Wang, L.; Liu, J. Dopamine Polymerization-Mediated Surface Functionalization toward Advanced Bacterial Therapeutics. *Acc. Chem. Res.* **2024**, *57*, 945−956.
(27) Pan, C.; Li, J.; Hou, W.; Lin, S.; Wang, L.; Pang, Y.; Wang, Y.; Liu, J. Polymerization-Mediated Multifunctionalization of Living Cells for Enhanced Cell-Based Therapy. *Adv. Mater.* **2021**, *33*, 2007379.
(28) Liu, Y.; Zhang, M.; Wang, X.; Yang, F.; Cao, Z.; Wang, L.; Liu, J. Dressing Bacteria with a Hybrid Immunoactive Nanosurface to Elicit Dual Anticancer and Antiviral Immunity. *Adv. Mater.* **2023**, *35*, 2210949.
(29) Li, J.; Xia, Q.; Guo, H.; Fu, Z.; Liu, Y.; Lin, S.; Liu, J. Decorating Bacteria with Triple Immune Nanoactivators Generates Tumor-Resident Living Immunotherapeutics. *Angew. Chem., Int. Ed.* **2022**, *61*, No. e202202409.
(30) Guo, H.; Cao, Z.; Li, J.; Fu, Z.; Lin, S.; Wang, L.; Liu, J. Integrating Bacteria with a Ternary Combination of Photosensitizers for Monochromatic Irradiation-Mediated Photoacoustic Imaging-Guided Synergistic Photothermal Therapy. *ACS Nano* **2023**, *17*, 5059−5071.
(31) Pan, J.; Gong, G.; Wang, Q.; Shang, J.; He, Y.; Catania, C.; Birnbaum, D.; Li, Y.; Jia, Z.; Zhang, Y.; Joshi, N. S.; Guo, J. A Single-Cell Nanocoating of Probiotics for Enhanced Amelioration of Antibiotic-Associated Diarrhea. *Nat. Commun.* **2022**, *13*, 2117.
(32) Geng, Z.; Wang, X.; Wu, F.; Cao, Z.; Liu, J. Biointerface Mineralization Generates Ultraresistant Gut Microbes as Oral Biotherapeutics. *Sci. Adv.* **2023**, *9*, No. eade0997.
(33) Fan, G.; Wasuwanich, P.; Rodriguez-Otero, M. R.; Furst, A. L. Protection of Anaerobic Microbes from Processing Stressors Using Metal−Phenolic Networks. *J. Am. Chem. Soc.* **2022**, *144*, 2438−2443.
(34) Centurion, F.; Merhebi, S.; Baharfar, M.; Abbasi, R.; Zhang, C.; Mousavi, M.; Xie, W.; Yang, J.; Cao, Z.; Allioux, F.-M.; Harm, G. F. S.; Biazik, J.; Kalantar-Zadeh, K.; Rahim, Md. A. Cell-Mediated Biointerfacial Phenolic Assembly for Probiotic Nano Encapsulation. *Adv. Funct. Mater.* **2022**, *32*, 2200775.
(35) Sun, Z.; Hübner, R.; Li, J.; Wu, C. Artificially Sporulated *Escherichia coli* Cells as a Robust Cell Factory for Interfacial Biocatalysis. *Nat. Commun.* **2022**, *13*, 3142.
(36) Song, R.-B.; Wu, Y.; Lin, Z.-Q.; Xie, J.; Tan, C. H.; Loo, J. S. C.; Cao, B.; Zhang, J.-R.; Zhu, J.-J.; Zhang, Q. Living and Conducting: Coating Individual Bacterial Cells with *In Situ* Formed Polypyrrole. *Angew. Chem., Int. Ed.* **2017**, *56*, 10516−10520.
(37) Xu, Z.; Qi, J.; Wang, S.; Liu, X.; Li, M.; Mann, S.; Huang, X. Algal Cell Bionics as a Step towards Photosynthesis-Independent Hydrogen Production. *Nat. Commun.* **2023**, *14*, 1872.
(38) Burke, B.; Fan, G.; Wasuwanich, P.; Moore, E. B.; Furst, A. L. Self-Assembled Nanocoatings Protect Microbial Fertilizers for Climate-Resilient Agriculture. *JACS Au* **2023**, *3*, 2973−2980.
(39) Peil, S.; Beckers, S. J.; Fischer, J.; Wurm, F. R. Biodegradable, Lignin-Based Encapsulation Enables Delivery of *Trichoderma reesei* with Programmed Enzymatic Release against Grapevine Trunk Diseases. *Mater. Today Bio* **2020**, *7*, 100061.
(40) Rheem, H. B.; Choi, H.; Yang, S.; Han, S.; Rhee, S. Y.; Jeong, H.; Lee, K.-B.; Lee, Y.; Kim, I.-S.; Lee, H.; Choi, I. S. Fugetaxis of Cell-in-Catalytic-Coat Nanobiohybrids in Glucose Gradients. *Small* **2023**, *19*, 2301431.

https://doi.org/10.1021/acs.chemrev.4c00984
Chem. Rev. XXXX, XXX, XXX−XXX

(41) Tang, S.; Zhang, F.; Gong, H.; Wei, F.; Zhuang, J.; Karshalev, E.; Esteban-Fernández de Ávila, B.; Huang, C.; Zhou, Z.; Li, Z.; Yin, L.; Dong, H.; Fang, R. H.; Zhang, X.; Zhang, L.; Wang, J. Enzyme-Powered Janus Platelet Cell Robots for Active and Targeted Drug Delivery. *Sci. Robot.* **2020**, *5*, No. eaba6137.
(42) Park, J.; Kim, N.; Han, S. Y.; Rhee, S. Y.; Nguyen, D. T.; Lee, H.; Choi, I. S. A Micrometric Transformer: Compositional Nanoshell Transformation of Fe^{3+}−Trimesic-Acid Complex with Concomitant Payload Release in Cell-in-Catalytic-Shell Nanobiohybrids. *Adv. Sci.* **2024**, *11*, 2306450.
(43) Lee, H.; Park, J.; Kim, N.; Youn, W.; Yun, G.; Han, S. Y.; Nguyen, D. T.; Choi, I. S. Cell-in-Catalytic-Shell Nanoarchitectonics: Catalytic Empowerment of Individual Living Cells by Single-Cell Nanoencapsulation. *Adv. Mater.* **2022**, *34*, 2201247.
(44) Su, D.; Qi, J.; Liu, X.; Wang, L.; Zhang, H.; Xie, H.; Huang, X. Enzyme-Modulated Anaerobic Encapsulation of *Chlorella* Cells Allows Switching from O_2 to H_2 Production. *Angew. Chem., Int. Ed.* **2019**, *58*, 3992−3995.
(45) Lee, J. K.; Choi, I. S.; Oh, T. I.; Lee, E. A. Cell-Surface Engineering for Advanced Cell Therapy. *Chem.—Eur. J.* **2018**, *24*, 15725.
(46) Cordero, R. J. B.; Casadevall, A. Functions of Fungal Melanin Beyond Virulence. *Fungal. Biol. Rev.* **2017**, *31*, 99−112.
(47) Simon, J. D.; Peles, D. N. The Red and the Black. *Acc. Chem. Res.* **2010**, *43*, 1452−1460.
(48) Cao, W.; Zhou, X.; McCallum, N. C.; Hu, Z.; Ni, Q. Z.; Kapoor, U.; Heil, C. M.; Cay, K. S.; Zand, T.; Mantanona, A. J.; Jayaraman, A.; Dhinojwala, A.; Deheyn, D. D.; Shawkey, M. D.; Burkart, M. D.; Rinehart, J. D.; Gianneschi, N. C. Unraveling the Structure and Function of Melanin through Synthesis. *J. Am. Chem. Soc.* **2021**, *143*, 2622−2637.
(49) Yang, S. H.; Kang, S. M.; Lee, K.-B.; Chung, T. D.; Lee, H.; Choi, I. S. Mussel-Inspired Encapsulation and Functionalization of Individual Yeast Cells. *J. Am. Chem. Soc.* **2011**, *133*, 2795−2797.
(50) Wang, B.; Wang, G.; Zhao, B.; Chen, J.; Zhang, X.; Tang, R. Antigenically Shielded Universal Red Blood Cells by Polydopamine-Based Cell Surface Engineering. *Chem. Sci.* **2014**, *5*, 3463−3468.
(51) Liu, Y.; Yan, G.; Gao, M.; Zhang, X. Magnetic Capture of Polydopamine-Encapsulated HeLa Cells for the Analysis of Cell Surface Proteins. *J. Proteomics* **2018**, *172*, 76−81.
(52) Hong, D.; Lee, H.; Ko, E. H.; Lee, J.; Cho, H.; Park, M.; Yang, S. H.; Choi, I. S. Organic/Inorganic Double-Layered Shells for Multiple Cytoprotection of Individual Living Cells. *Chem. Sci.* **2015**, *6*, 203−208.
(53) Yang, S. H.; Lee, K.-B.; Kong, B.; Kim, J.-H.; Kim, H.-S.; Choi, I. S. Biomimetic Encapsulation of Individual Cells with Silica. *Angew. Chem., Int. Ed.* **2009**, *48*, 9160−9163.
(54) Yang, S. H.; Ko, E. H.; Jung, Y. H.; Choi, I. S. Bioinspired Functionalization of Silica-Encapsulated Yeast Cells. *Angew. Chem., Int. Ed.* **2011**, *50*, 6115−6118.
(55) Kim, J. Y.; Lee, H.; Park, T.; Park, J.; Kim, M.-H.; Cho, H.; Youn, W.; Kang, S. M.; Choi, I. S. Artificial Spores: Cytocompatible Coating of Living Cells with Plant-Derived Pyrogallol. *Chem.—Asian J.* **2016**, *11*, 3183.
(56) Kim, J. Y.; Kim, W. I.; Youn, W.; Seo, J.; Kim, B. J.; Lee, J. K.; Choi, I. S. Enzymatic Film Formation of Nature-Derived Phenolic Amines. *Nanoscale* **2018**, *10*, 13351−13355.
(57) Kim, N.; Lee, H.; Han, S. Y.; Kim, B. J.; Choi, I. S. Enzyme-Mediated Film Formation of Melanin-Like Species from *ortho*-Diphenols: Application to Single-Cell Nanoencapsulation. *Appl. Surf. Sci. Adv.* **2021**, *5*, 100098.
(58) Liu, Y.; Han, Y.; Dong, H.; Wei, X.; Shi, D.; Li, Y. Ca^{2+}-Mediated Surface Polydopamine Engineering to Program Dendritic Cell Maturation. *ACS Appl. Mater. Interfaces* **2020**, *12*, 4163−4173.
(59) Li, J.; Hou, W.; Lin, S.; Wang, L.; Pan, C.; Wu, F.; Liu, J. Polydopamine Nanoparticle-Mediated Dopaminergic Immunoregulation in Colitis. *Adv. Sci.* **2022**, *9*, 2104006.
(60) Wang, L.; Hu, Z.-Y.; Yang, X.-Y.; Zhang, B.-B.; Geng, W.; Van Tendeloo, G.; Su, B.-L. Polydopamine Nanocoated Whole-Cell Asymmetric Biocatalysts. *Chem. Commun.* **2017**, *53*, 6617.
(61) Liu, S.-R.; Cai, L.-F.; Wang, L.-Y.; Yi, X.-F.; Peng, Y.-J.; He, N.; Wu, X.; Wang, Y.-P. Polydopamine Coating on Individual Cells for Enhanced Extracellular Electron Transfer. *Chem. Commun.* **2019**, *55*, 10535−10538.
(62) Yu, Y.-Y.; Wang, Y.-Z.; Fang, Z.; Shi, Y.-T.; Cheng, Q.-W.; Chen, Y.-X.; Shi, W.; Yong, Y.-C. Single Cell Electron Collectors for Highly Efficient Wiring-up Electronic Abiotic/Biotic Interfaces. *Nat. Commun.* **2020**, *11*, 4087.
(63) Chen, W.; Wang, Y.; Qin, M.; Zhang, X.; Zhang, Z.; Sun, X.; Gu, Z. Bacteria-Driven Hypoxia Targeting for Combined Biotherapy and Photothermal Therapy. *ACS Nano* **2018**, *12*, 5995−6005.
(64) Chen, W.; Guo, Z.; Zhu, Y.; Qiao, N.; Zhang, Z.; Sun, X. Combination of Bacterial-Photothermal Therapy with an Anti-PD-1 Peptide Depot for Enhanced Immunity against Advanced Cancer. *Adv. Funct. Mater.* **2020**, *30*, 1906623.
(65) Liu, J.; Wang, Y.; Heelan, W. J.; Chen, Y.; Li, Z.; Hu, Q. Y. Mucoadhesive Probiotic Backpacks with ROS Nanoscavengers Enhance the Bacteriotherapy for Inflammatory Bowel Diseases. *Sci. Adv.* **2022**, *8*, No. eabp8798.
(66) Ai, H.; Fang, M.; Jones, S. A.; Lvov, Y. M. Electrostatic Layer-by-Layer Nanoassembly on Biological Microtemplates: Platelets. *Biomacromolecules* **2002**, *3*, 560−564.
(67) Diaspro, A.; Silvano, D.; Krol, S.; Cavalleri, O.; Gliozzi, A. Single Living Cell Encapsulation in Nano-organized Polyelectrolyte Shells. *Langmuir* **2002**, *18*, 5047−5050.
(68) Li, W.; Lei, X.; Feng, H.; Li, B.; Kong, J.; Xing, M. Layer-by-Layer Cell Encapsulation for Drug Delivery: The History, Technique Basis, and Applications. *Pharmaceutics* **2022**, *14*, 297.
(69) Fakhrullin, R. F.; Lvov, Y. M. "Face-Lifting" and "Make-Up" for Microorganisms: Layer-by-Layer Polyelectrolyte Nanocoating. *ACS Nano* **2012**, *6*, 4557−4564.
(70) Santos, A. C.; Pereira, I.; Ferreira, C.; Veiga, F.; Fakhrullin, R. F. Layer-by-Layer Assembly for Nanoarchitectonics. In *Advanced Supramolecular Nanoarchitectonics*; Ariga, K., Aono, M., Eds.; Elsevier, 2019; pp 89−121.
(71) Franz, B.; Balkundi, S. S.; Dahl, C.; Lvov, Y. M.; Prange, A. Layer-by-Layer Nano-Encapsulation of Microbes: Controlled Cell Surface Modification and Investigation of Substrate Uptake in Bacteria. *Macromol. Biosci.* **2010**, *10*, 164−172.
(72) Oliveira, M. B.; Hatami, J.; Mano, J. F. Coating Strategies Using Layer-by-Layer Deposition for Cell Encapsulation. *Chem.—Asian J.* **2016**, *11*, 1753−1764.
(73) Borges, J.; Zeng, J.; Liu, X. Q.; Chang, H.; Monge, C.; Garot, C.; Ren, K.-F.; Machillot, P.; Vrana, N. E.; Lavalle, P.; Akagi, T.; Matsusaki, M.; Ji, J.; Akashi, M.; Mano, J. F.; Gribova, V.; Picart, C. Recent Developments in Layer-by-Layer Assembly for Drug Delivery and Tissue Engineering Applications. *Adv. Healthc. Mater.* **2024**, *13*, 2302713.
(74) Yang, J.; Li, J.; Li, X.; Wang, X.; Yang, Y.; Kawazoe, N.; Chen, G. Nanoencapsulation of Individual Mammalian Cells with Cytoprotective Polymer Shell. *Biomaterials* **2017**, *133*, 253−262.
(75) Yang, J.; Yang, Y.; Kawazoe, N.; Chen, G. Encapsulation of Individual Living Cells with Enzyme Responsive Polymer Nanoshell. *Biomaterials* **2019**, *197*, 317−326.
(76) Sun, J.; Ren, Y.; Wang, W.; Hao, H.; Tang, M.; Zhang, Z.; Yang, J.; Zheng, Y.; Shi, X. A. Transglutaminase-Catalyzed Encapsulation of Individual Mammalian Cells with Biocompatible and Cytoprotective Gelatin Nanoshells. *ACS Biomater. Sci. Eng.* **2020**, *6*, 2336−2345.
(77) Matsusaki, M.; Kadowaki, K.; Nakahara, Y.; Akashi, M. Fabrication of Cellular Multilayers with Nanometer-Sized Extracellular Matrix Films. *Angew. Chem., Int. Ed.* **2007**, *46*, 4689−4692.
(78) Nishiguchi, A.; Yoshida, H.; Matsusaki, M.; Akashi, M. Rapid Construction of Three-Dimensional Multilayered Tissues with Endothelial Tube Networks by the Cell-Accumulation Technique. *Adv. Mater.* **2011**, *23*, 3506−3510.
(79) Matsuzawa, A.; Matsusaki, M.; Akashi, M. Effectiveness of Nanometer-Sized Extracellular Matrix Layer-by-Layer Assembled Films for a Cell Membrane Coating Protecting Cells from Physical Stress. *Langmuir* **2013**, *29*, 7362−7368.

https://doi.org/10.1021/acs.chemrev.4c00984
Chem. Rev. XXXX, XXX, XXX−XXX

(80) Amano, Y.; Nishiguchi, A.; Matsusaki, M.; Iseoka, H.; Miyagawa, S.; Sawa, Y.; Seo, M.; Yamaguchi, T.; Akashi, M. Development of Vascularized iPSC Derived 3D-Cardiomyocyte Tissues by Filtration Layer-by-Layer Technique and Their Application for Pharmaceutical Assays. *Acta Biomater.* **2016**, *33*, 110−121.
(81) Guerzoni, L. P. B.; Tsukamoto, Y.; Gehlen, D. B.; Rommel, D.; Haraszti, T.; Akashi, M.; De Laporte, L. A Layer-by-Layer Single-Cell Coating Technique to Produce Injectable Beating Mini Heart Tissues via Microfluidics. *Biomacromolecules* **2019**, *20*, 3746−3754.
(82) Gribova, V.; Liu, C.-Y.; Nishiguchi, A.; Matsusaki, M.; Boudou, T.; Picart, C.; Akashi, M. Construction and Myogenic Differentiation of 3D Myoblast Tissues Fabricated by Fibronectin−Gelatin Nanofilm Coating. *Biochem. Biophys. Res. Commun.* **2016**, *474*, 515−521.
(83) Fukuda, Y.; Akagi, T.; Asaoka, T.; Eguchi, H.; Sasaki, K.; Iwagami, Y.; Yamada, D.; Noda, T.; Kawamoto, K.; Gotoh, K.; Kobayashi, S.; Mori, M.; Doki, Y.; Akashi, M. Layer-by-Layer Cell Coating Technique Using Extracellular Matrix Facilitates Rapid Fabrication and Function of Pancreatic β-Cell Spheroids. *Biomaterials* **2018**, *160*, 82−91.
(84) Drachuk, I.; Shchepelina, O.; Harbaugh, S.; Kelley-Loughnane, N.; Stone, M.; Tsukruk, V. V. Cell Surface Engineering with Edible Protein Nanoshells. *Small* **2013**, *9*, 3128−3137.
(85) Hasturk, O.; Sahoo, J. K.; Kaplan, D. L. Synthesis and Characterization of Silk Ionomers for Layer-by-Layer Electrostatic Deposition on Individual Mammalian Cells. *Biomacromolecules* **2020**, *21*, 2829−2843.
(86) Hou, W.; Li, J.; Cao, Z.; Lin, S.; Pan, C.; Pang, Y.; Liu, J. Decorating Bacteria with a Therapeutic Nanocoating for Synergistically Enhanced Biotherapy. *Small* **2021**, *17*, 2101810.
(87) Shi, Y.; Rupa, P.; Jiang, B.; Mine, Y. Hydrolysate from Eggshell Membrane Ameliorates Intestinal Inflammation in Mice. *Int. J. Mol. Sci.* **2014**, *15*, 22728−22742.
(88) Yang, T.; Li, Y.; Ma, M.; Lin, Q.; Sun, S.; Zhang, B.; Feng, X.; Liu, J. Protective Effect of Soluble Eggshell Membrane Protein Hydrolysate on Cardiac Ischemia/Reperfusion Injury. *Food Nutr. Res.* **2015**, *59*, 28870.
(89) Han, S. Y.; Lee, H.; Nguyen, D. T.; Yun, G.; Kim, S.; Park, J. H.; Choi, I. S. Single-Cell Nanoencapsulation of *Saccharomyces cerevisiae* by Cytocompatible Layer-by-Layer Assembly of Eggshell Membrane Hydrolysate and Tannic Acid. *Adv. NanoBiomed Res.* **2021**, *1*, 2000037.
(90) Han, S. Y.; Yun, G.; Nguyen, D. T.; Kang, E. K.; Lee, H.; Kim, S.; Kim, B. J.; Park, J. H.; Choi, I. S. Hydrogen Bonding-Based Layer-by-Layer Assembly of Nature-Derived Eggshell Membrane Hydrolysates and Coffee Melanoidins in Single-Cell Nanoencapsulation. *ChemNanoMat* **2022**, *8*, No. e202100535.
(91) Han, S. Y.; Nguyen, D. T.; Kim, B. J.; Kim, N.; Kang, E. K.; Park, J. H.; Choi, I. S. Cytoprotection of Probiotic *Lactobacillus acidophilus* with Artificial Nanoshells of Nature-Derived Eggshell Membrane Hydrolysates and Coffee Melanoidins in Single-Cell Nanoencapsulation. *Polymers* **2023**, *15*, 1104.
(92) Yang, S. H.; Ko, E. H.; Choi, I. S. Cytocompatible Encapsulation of Individual *Chlorella* Cells within Titanium Dioxide Shells by a Designed Catalytic Peptide. *Langmuir* **2012**, *28*, 2151−2155.
(93) Ko, E. H.; Yoon, Y.; Park, J. H.; Yang, S. H.; Hong, D.; Lee, K.-B.; Shon, H. K.; Lee, T. G.; Choi, I. S. Bioinspired, Cytocompatible Mineralization of Silica−Titania Composites: Thermoprotective Nanoshell Formation for Individual *Chlorella* Cells. *Angew. Chem., Int. Ed.* **2013**, *52*, 12279−12282.
(94) Park, J. H.; Choi, I. S.; Yang, S. H. Peptide-Catalyzed, Bioinspired Silicification for Single-Cell Encapsulation in the Imidazole-Buffered System. *Chem. Commun.* **2015**, *51*, 5523−5525.
(95) Anselmo, A. C.; McHugh, K. J.; Webster, J.; Langer, R.; Jaklenec, A. Layer-by-Layer Encapsulation of Probiotics for Delivery to the Microbiome. *Adv. Mater.* **2016**, *28*, 9486−9490.
(96) Jonas, A. M.; Glinel, K.; Behrens, A.; Anselmo, A. C.; Langer, R. S.; Jaklenec, A. Controlling the Growth of *Staphylococcus epidermidis* by Layer-by-Layer Encapsulation. *ACS Appl. Mater. Interfaces* **2018**, *10*, 16250−16259.
(97) Priya, A. J.; Vijayalakshmi, S. P.; Raichur, A. M. Enhanced Survival of Probiotic *Lactobacillus acidophilus* by Encapsulation with Nanostructured Polyelectrolyte Layers through Layer-by-Layer Approach. *J. Agric. Food Chem.* **2011**, *59*, 11838−11845.
(98) Wang, M.; Yang, J.; Li, M.; Wang, Y.; Wu, H.; Xiong, L.; Sun, Q. Enhanced Viability of Layer-by-Layer Encapsulated *Lactobacillus pentosus* Using Chitosan and Sodium Phytate. *Food Chem.* **2019**, *285*, 260−265.
(99) Moon, H. C.; Han, S.; Borges, J.; Pesqueira, T.; Choi, H.; Han, S. Y.; Cho, H.; Park, J. H.; Mano, J. F.; Choi, I. S. Enzymatically Degradable, Starch-Based Layer-by-Layer Films: Application to Cytocompatible Single-Cell Nanoencapsulation. *Soft Matter* **2020**, *16*, 6063−6071.
(100) Kurisawa, M.; Chung, J. E.; Yang, Y. Y.; Gao, S. J.; Uyama, H. Injectable Biodegradable Hydrogels Composed of Hyaluronic Acid−Tyramine Conjugates for Drug Delivery and Tissue Engineering. *Chem. Commun.* **2005**, *34*, 4312−4314.
(101) Jin, R.; Hiemstra, C.; Zhong, Z.; Feijen, J. Enzyme-Mediated Fast *In Situ* Formation of Hydrogels from Hydrogels from Dextran−Tyramine Conjugates. *Biomaterials* **2007**, *28*, 2791−2800.
(102) Sakai, S.; Liu, Y.; Matsuyama, T.; Kawakami, K.; Taya, M. On-Demand Serum-Degradable Amylopectin-Based *In Situ* Gellable Hydrogel. *J. Mater. Chem.* **2012**, *22*, 1944−1949.
(103) Liu, Y.; Sakai, S.; Taya, M. Impact of the Composition of Alginate and Gelatin Derivatives in Bioconjugated Hydrogels on the Fabrication of Cell Sheets and Spherical Tissues with Living Cell Sheaths. *Acta. Biomater.* **2013**, *9*, 6616−6623.
(104) Kim, M.; Kim, H.; Lee, Y.-S.; Lee, S.; Kim, S.-E.; Lee, U.-J.; Jung, S.; Park, C.-G.; Hong, J.; Doh, J.; Lee, D. Y.; Kim, B.-G.; Hwang, N. S. Novel Enzymatic Cross-Linking-Based Hydrogel Nanofilm Caging System on Pancreatic β Cell Spheroid for Long-Term Blood Glucose Regulation. *Sci. Adv.* **2021**, *7*, No. eabf7832.
(105) Sakai, S.; Taya, M. On-Cell Surface Cross-linking of Polymer Molecules by Horseradish Peroxidase Anchored to Cell Membrane for Individual Cell Encapsulation in Hydrogel Sheath. *ACS Macro Lett.* **2014**, *3*, 972−975.
(106) Liu, Y.; Sakai, S.; Kawa, S.; Taya, M. Identification of Hydrogen Peroxide-Secreting Cells by Cytocompatible Coating with a Hydrogel Membrane. *Anal. Chem.* **2014**, *86*, 11592−11598.
(107) Sakai, S.; Liu, Y.; Sengoku, M.; Taya, M. Cell-Selective Encapsulation in Hydrogel Sheaths via Biospecific Identification and Biochemical Cross-Linking. *Biomaterials* **2015**, *53*, 494−501.
(108) Zhao, Y.; Fan, M.; Chen, Y.; Liu, Z.; Shao, C.; Jin, B.; Wang, X.; Hui, L.; Wang, S.; Liao, Z.; Ling, D.; Tang, R.; Wang, B. Surface-Anchored Framework for Generating RhD-Epitope Stealth Red Blood Cells. *Sci. Adv.* **2020**, *6*, No. eaaw9679.
(109) Choi, D.; Park, J.; Heo, J.; Oh, T. I.; Lee, E. A.; Hong, J. Multifunctional Collagen and Hyaluronic Acid Multilayer Films on Live Mesenchymal Stem Cells. *ACS Appl. Mater. Interfaces* **2017**, *9*, 12264−12271.
(110) Hwang, J.-H.; Han, U.; Yang, M.; Choi, Y.; Choi, J.; Lee, J.-M.; Jung, H.-S.; Hong, J.; Hong, J.-H. Artificial Cellular Nano-Environment Composed of Collagen-Based Nanofilm Promotes Osteogenic Differentiation of Mesenchymal Stem Cells. *Acta Biomater.* **2019**, *86*, 247−256.
(111) Veerabadran, N. G.; Goli, P. L.; Stewart-Clark, S. S.; Lvov, Y. M.; Mills, D. K. Nanoencapsulation of Stem Cells within Polyelectrolyte Multilayer Shells. *Macromol. Biosci.* **2007**, *7*, 877−882.
(112) Hwang, J.; Choi, D.; Choi, M.; Seo, Y.; Son, J.; Hong, J.; Choi, J. Synthesis and Characterization of Functional Nanofilm-Coated Live Immune Cells. *ACS Appl. Mater. Interfaces* **2018**, *10*, 17685−17692.
(113) Choi, D.; Lee, H.; Kim, H.-B.; Yang, M.; Heo, J.; Won, Y.; Jang, S. S.; Park, J. K.; Son, Y.; Oh, T. I.; Lee, E. A.; Hong, J. Cytoprotective Self-Assembled RGD Peptide Nanofilms for Surface Modification of Viable Mesenchymal Stem Cells. *Chem. Mater.* **2017**, *29*, 2055−2065.
(114) Li, W.; Zhang, G.; Guan, T.; Zhang, X.; Khosrozadeh, A.; Xing, M.; Kong, J. Manipulable Permeability of Nanogel Encapsulation on Cells Exerts Protective Effect against TNF-α-Induced Apoptosis. *ACS Biomater. Sci. Eng.* **2018**, *4*, 2825−2835.

https://doi.org/10.1021/acs.chemrev.4c00984
Chem. Rev. XXXX, XXX, XXX−XXX

(115) Nguyen, T. D.; Guyot, S.; Lherminier, J.; Wache, Y.; Saurel, R.; Husson, F. Protection of Living Yeast Cells by Micro-Organized Shells of Natural Polyelectrolytes. *Process Biochem.* **2015**, *50*, 1528−1536.
(116) Nguyen, T. D.; Guyot, S.; Pénicaud, C.; Passot, S.; Sandt, C.; Fonseca, F.; Saurel, R.; Husson, F. Highlighting Protective Effect of Encapsulation on Yeast Cell Response to Dehydration Using Synchrotron Infrared Microspectroscopy at the Single-Cell Level. *Front. Microbiol.* **2020**, *11*, 1887.
(117) Mansouri, S.; Fatisson, J.; Miao, Z.; Merhi, Y.; Winnik, F. M.; Tabrizian, M. Silencing Red Blood Cell Recognition toward Anti-A Antibody by Means of Polyelectrolyte Layer-by-Layer Assembly in a Two-Dimensional Model System. *Langmuir* **2009**, *25*, 14071−14078.
(118) Mansouri, S.; Merhi, Y.; Winnik, F. M.; Tabrizian, M. Investigation of Layer-by-Layer Assembly of Polyelectrolytes on Fully Functional Human Red Blood Cells in Suspension for Attenuated Immune Response. *Biomacromolecules* **2011**, *12*, 585−592.
(119) Lybaert, L.; Ryu, K. A.; De Rycke, R.; Chon, A. C.; De Wever, O.; Vermaelen, K. Y.; Esser-Kahn, A.; De Geest, B. G. Polyelectrolyte-Enrobed Cancer Cells in View of Personalized Immune-Therapy. *Adv. Sci.* **2017**, *4*, 1700050.
(120) Van der Meeren, L.; Verduijn, J.; Li, J.; Verwee, E.; Krysko, D. V.; Parakhonskiy, B. V.; Skirtach, A. G. Encapsulation of Cells in Gold Nanoparticle Functionalized Hybrid Layer-by-Layer (LbL) Hybrid Shells − Remote Effect of Laser Light. *Appl. Surf. Sci. Adv.* **2021**, *5*, 100111.
(121) Li, W.; Guan, T.; Zhang, X.; Wang, Z.; Wang, M.; Zhong, W.; Feng, H.; Xing, M.; Kong, J. The Effect of Layer-by-Layer Assembly Coating on the Proliferation and Differentiation of Neural Stem Cells. *ACS Appl. Mater. Interfaces* **2015**, *7*, 3018−3029.
(122) Chen, P.; Miao, Y.; Zhang, F.; Huang, J.; Chen, Y.; Fan, Z.; Yang, L.; Wang, J.; Hu, Z. Nanoscale Microenvironment Engineering Based on Layer-by-Layer Self-Assembly to Regulate Hair Follicle Stem Cell Fate for Regenerative Medicine. *Theranostics* **2020**, *10*, 11673−11689.
(123) Mei, D.; Xue, Z.; Zhang, T.; Yang, Y.; Jin, L.; Yu, Q.; Hong, J.; Zhang, X.; Ge, J.; Xu, L.; Wang, H.; Zhang, Z.; Zhao, Y.; Zhai, Y.; Tao, Q.; Zhai, Z.; Li, Q.; Li, H.; Zhang, L. Immune Isolation-Enabled Nanoencapsulation of Donor T Cells: A Promising Strategy for Mitigating GVHD and Treating AML in Preclinical Models. *J. Immunother. Cancer* **2024**, *12*, No. e008663.
(124) Zhang, L.; Liu, G.; Lv, K.; Xin, J.; Wang, Y.; Zhao, J.; Hu, W.; Xiao, C.; Zhu, K.; Zhu, L.; Nan, J.; Feng, Y.; Zhu, H.; Chen, W.; Zhu, W.; Zhang, J.; Wang, J.; Wang, B.; Hu, X. Surface-Anchored Nanogel Coating Endows Stem Cells with Stress Resistance and Reparative Potency via Turning Down the Cytokine-Receptor Binding Pathways. *Adv. Sci.* **2021**, *8*, 2003348.
(125) Yang, M.; Kang, E.; Shin, J. W.; Hong, J. Surface Engineering for Mechanical Enhancement of Cell Sheet by Nano-Coatings. *Sci. Rep.* **2017**, *7*, 4464.
(126) Wang, J.; Miao, Y.; Huang, Y.; Lin, B.; Liu, X.; Xiao, S.; Du, L.; Hu, Z.; Xing, M. Bottom-up Nanoencapsulation from Single Cells to Tunable and Scalable Cellular Spheroids for Hair Follicle Regeneration. *Adv. Healthc. Mater.* **2018**, *7*, 1700447.
(127) Rothemund, P. W. K. Folding DNA to Create Nanoscale Shapes and Patterns. *Nature* **2006**, *440*, 297−302.
(128) Zhan, P.; Peil, A.; Jiang, Q.; Wang, D.; Mousavi, S.; Xiong, Q.; Shen, Q.; Shang, Y.; Ding, B.; Lin, C.; Ke, Y.; Liu, N. Recent Advances in DNA Origami-Engineered Nanomaterials and Applications. *Chem. Rev.* **2023**, *123*, 3976−4050.
(129) Gao, T.; Chen, T.; Feng, C.; He, X.; Mu, C.; Anzai, J.-i.; Li, G. Design and Fabrication of Flexible DNA Polymer Cocoons to Encapsulate Live Cells. *Nat. Commun.* **2019**, *10*, 2946.
(130) Hillberg, A. L.; Tabrizian, M. Biorecognition through Layer-by-Layer Polyelectrolyte Assembly: *In-Situ* Hybridization on Living Cells. *Biomacromolecules* **2006**, *7*, 2742−2750.
(131) Davis, B.; Shi, P.; Gaddes, E.; Lai, J.; Wang, Y. Bidirectional Supramolecular Display and Signal Amplification on the Surface of Living Cells. *Biomacromolecules* **2022**, *23*, 1403−1412.
(132) Kato, K.; Itoh, C.; Yasukouchi, T.; Nagamune, T. Rapid Protein Anchoring into the Membranes of Mammalian Cells Using Oleyl Chain and Poly(Ethylene Glycol) Derivatives. *Biotechnol. Prog.* **2004**, *20*, 897−904.
(133) Sarkar, D.; Vemula, P. K.; Zhao, W.; Gupta, A.; Karnik, R.; Karp, J. M. Engineered Mesenchymal Stem Cells with Self-Assembled Vesicles for Systemic Cell Targeting. *Biomaterials* **2010**, *31*, 5266−5274.
(134) Cao, Z.; Wang, X.; Pang, Y.; Cheng, S.; Liu, J. Biointerfacial Self-Assembly Generates Lipid Membrane Coated Bacteria for Enhanced Oral Delivery and Treatment. *Nat. Commun.* **2019**, *10*, 5783.
(135) Cao, Z.; Cheng, S.; Wang, X.; Pang, Y.; Liu, J. Camouflaging Bacteria by Wrapping with Cell Membranes. *Nat. Commun.* **2019**, *10*, 3452.
(136) Yang, S.; Youn, W.; Rheem, H. B.; Han, S. Y.; Kim, N.; Han, S.; Schattling, P.; Städler, B.; Choi, I. S. Construction of Liposome-Based Extracellular Artificial Organelles on Individual Living Cells. *Angew. Chem., Int. Ed.* **2025**, *64*, No. e202415823.
(137) Lybaert, L.; De Vlieghere, E.; De Rycke, R.; Vanparijs, N.; De Wever, O.; De Koker, S.; De Geest, B. G. Bio-Hybrid Tumor Cell-Templated Capsules: A Generic Formulation Strategy for Tumor Associated Antigens in View of Immune Therapy. *Adv. Funct. Mater.* **2014**, *24*, 7139−7150.
(138) Krol, S.; Cavalleri, O.; Ramoino, P.; Gliozzi, A.; Diaspro, A. Encapsulated Yeast Cells Inside *Paramecium primaurelia*: A Model System for Protection Capability of Polyelectrolyte Shells. *J. Microsc.* **2003**, *212*, 239−243.
(139) Krol, S.; Nolte, M.; Diaspro, A.; Mazza, D.; Magrassi, R.; Gliozzi, A.; Fery, A. Encapsulated Living Cells on Microstructured Surfaces. *Langmuir* **2005**, *21*, 705−709.
(140) Svaldo Lanero, T. S.; Cavalleri, O.; Krol, S.; Rolandi, R.; Gliozzi, A. Mechanical Properties of Single Living Cells Encapsulated in Polyelectrolyte Matrixes. *J. Biotechnol.* **2006**, *124*, 723−731.
(141) Svaldo-Lanero, T.; Krol, S.; Magrassi, R.; Diaspro, A.; Rolandi, R.; Gliozzi, A.; Cavalleri, O. Morphology, Mechanical Properties and Viability of Encapsulated Cells. *Ultramicroscopy* **2007**, *107*, 913−921.
(142) Lee, J.; Yang, S. H.; Hong, S.-P.; Hong, D.; Lee, H.; Lee, H.-Y.; Kim, Y.-G.; Choi, I. S. Chemical Control of Yeast Cell Division by Cross-Linked Shells of Catechol-Grafted Polyelectrolyte Multilayers. *Macromol. Rapid Commun.* **2013**, *34*, 1351−1356.
(143) Yang, S. H.; Choi, J.; Palanikumar, L.; Choi, E. S.; Lee, J.; Kim, J.; Choi, I. S.; Ryu, J.-H. Cytocompatible *In Situ* Cross-Linking of Degradable LbL Films Based on Thiol-Exchange Reaction. *Chem. Sci.* **2015**, *6*, 4698−4703.
(144) Eby, D. M.; Harbaugh, S.; Tatum, R. N.; Farrington, K. E.; Kelley-Loughnane, N.; Johnson, G. R. Bacterial Sunscreen: Layer-by-Layer Deposition of UV-Absorbing Polymers on Whole-Cell Biosensors. *Langmuir* **2012**, *28*, 10521−10527.
(145) Wang, G.; Wang, L.; Liu, P.; Yan, Y.; Xu, X.; Tang, R. Extracellular Silica Nanocoat Confers Thermotolerance on Individual Cells: A Case Study of Material-Based Functionalization of Living Cells. *ChemBioChem.* **2010**, *11*, 2368−2373.
(146) Xiong, W.; Yang, Z.; Zhai, H.; Wang, G.; Xu, X.; Ma, W.; Tang, R. Alleviation of High Light-Induced Photoinhibition in Cyanobacteria by Artificially Conferred Biosilica Shells. *Chem. Commun.* **2013**, *49*, 7525−7527.
(147) Wang, B.; Liu, P.; Jiang, W.; Pan, H.; Xu, X.; Tang, R. Yeast Cells with an Artificial Mineral Shell: Protection and Modification of Living Cells by Biomimetic Mineralization. *Angew. Chem., Int. Ed.* **2008**, *47*, 3560−3564.
(148) Wang, B.; Liu, P.; Liu, Z.; Pan, H.; Xu, X.; Tang, R. Biomimetic Construction of Cellular Shell by Adjusting the Interfacial Energy. *Biotechnol. Bioeng.* **2014**, *111*, 386−395.
(149) Lee, H.; Hong, D.; Choi, J. Y.; Kim, J. Y.; Lee, S. H.; Kim, H. M.; Yang, S. H.; Choi, I. S. Layer-by-Layer-Based Silica Encapsulation of Individual Yeast with Thickness Control. *Chem. Asian. J.* **2015**, *10*, 129−132.

https://doi.org/10.1021/acs.chemrev.4c00984
Chem. Rev. XXXX, XXX, XXX−XXX

(150) Yang, S. H.; Lee, T.; Seo, E.; Ko, E. H.; Choi, I. S.; Kim, B.-S. Interfacing Living Yeast Cells with Graphene Oxide Nanosheaths. *Macromol. Biosci.* **2012**, *12*, 61−66.
(151) He, L.; Chang, Y.; Zhu, J.; Bi, Y.; An, W.; Dong, Y.; Liu, J.-H.; Wang, S. A Cytoprotective Graphene Oxide−Polyelectrolytes Nanoshell for Single-Cell Encapsulation. *Front. Chem. Sci. Eng.* **2021**, *15*, 410−420.
(152) Zamaleeva, A. I.; Sharipova, I. R.; Porfireva, A. V.; Evtugyn, G. A.; Fakhrullin, R. F. Polyelectrolyte-Mediated Assembly of Multiwalled Carbon Nanotubes on Living Yeast Cells. *Langmuir* **2010**, *26*, 2671−2679.
(153) Fakhrullin, R. F.; García-Alonso, J.; Paunov, V. N. A Direct Technique for Preparation of Magnetically Functionalised Living Yeast Cells. *Soft Matter* **2010**, *6*, 391−397.
(154) Fakhrullin, R. F.; Shlykova, L. V.; Zamaleeva, A. I.; Nurgaliev, D. K.; Osin, Y. N.; García-Alonso, J.; Paunov, V. N. Interfacing Living Unicellular Algae Cells with Biocompatible Polyelectrolyte-Stabilised Magnetic Nanoparticles. *Macromol. Biosci.* **2010**, *10*, 1257−1264.
(155) Zamaleeva, A. I.; Sharipova, I. R.; Shamagsumova, R. V.; Ivanov, A. N.; Evtugyn, G. A.; Ishmuchametova, D. G.; Fakhrullin, R. F. A Whole-Cell Amperometric Herbicide Biosensor Based on Magnetically Functionalised Microalgae and Screen-Printed Electrodes. *Anal. Methods* **2011**, *3*, 509−513.
(156) Zhang, D.; Fakhrullin, R. F.; Özmen, M.; Wang, H.; Wang, J.; Paunov, V. N.; Li, G.; Huang, W. E. Functionalization of Whole-Cell Bacterial Reporters with Magnetic Nanoparticles. *Microb. Biotechnol.* **2011**, *4*, 89−97.
(157) Dzamukova, M. R.; Zamaleeva, A. I.; Ishmuchametova, D. G.; Osin, Y. N.; Kiyasov, A. P.; Nurgaliev, D. K.; Ilinskaya, O. N.; Fakhrullin, R. F. A Direct Technique for Magnetic Functionalization of Living Human Cells. *Langmuir* **2011**, *27*, 14386−14393.
(158) Konnova, S. A.; Lvov, Y. M.; Fakhrullin, R. F. Nanoshell Assembly for Magnet-Responsive Oil-Degrading Bacteria. *Langmuir* **2016**, *32*, 12552−12558.
(159) Choi, J.; Lee, H.; Choi, I. S.; Yang, S. H. Magnetization of Individual Yeast Cells by *In Situ* Formation of Iron Oxide on Cell Surfaces. *Solid State Sci.* **2017**, *71*, 29−32.
(160) Kahraman, M.; Zamaleeva, A. I.; Fakhrullin, R. F.; Culha, M. Layer-by-Layer Coating of Bacteria with Noble Metal Nanoparticles for Surface-Enhanced Raman Scattering. *Anal. Bioanal. Chem.* **2009**, *395*, 2559−2567.
(161) Fakhrullin, R. F.; Zamaleeva, A. I.; Morozov, M. V.; Tazetdinova, D. I.; Alimova, F. K.; Hilmutdinov, A. K.; Zhdanov, R. I.; Kahraman, M.; Culha, M. Living Fungi Cells Encapsulated in Polyelectrolyte Shells Doped with Metal Nanoparticles. *Langmuir* **2009**, *25*, 4628−4634.
(162) Guo, J.; Suástegui, M.; Sakimoto, K. K.; Moody, V. M.; Xiao, G.; Nocera, D. G.; Joshi, N. S. Light-Driven Fine Chemical Production in Yeast Biohybrids. *Science* **2018**, *362*, 813−816.
(163) Emanet, M.; Fakhrullin, R. F.; Çulha, M. Boron Nitride Nanotubes and Layer-by-Layer Polyelectrolyte Coating for Yeast Cell Surface Engineering. *ChemNanoMat* **2016**, *2*, 426−429.
(164) Chanana, M.; Gliozzi, A.; Diaspro, A.; Chodnevskaja, I.; Huewel, S.; Moskalenko, V.; Ulrichs, K.; Galla, H.-J.; Krol, S. Interaction of Polyelectrolytes and Their Composites with Living Cells. *Nano Lett.* **2005**, *5*, 2605−2612.
(165) Kozlovskaya, V.; Harbaugh, S.; Drachuk, I.; Shchepelina, O.; Kelley-Loughnane, N.; Stone, M.; Tsukruk, V. V. Hydrogen-Bonded LbL Shells for Living Cell Surface engineering. *Soft Matter* **2011**, *7*, 2364−2372.
(166) Hachim, D.; Melendez, J.; Ebensperger, R. Nanoencapsulation of Human Adipose Mesenchymal Stem Cells: Experimental Factors Role to Successfully Preserve Viability and Functionality of Cells. *J. Encapsulation Adsorpt. Sci.* **2013**, *3*, 1−12.
(167) Jonas, A. M.; Glinel, K.; Behrens, A.; Anselmo, A. C.; Langer, R. S.; Jaklenec, A. Controlling the Growth of *Staphylococcus epidermidis* by Layer-by-Layer Encapsulation. *ACS Appl. Mater. Interfaces* **2018**, *10*, 16250−16259.
(168) Hong, D.; Yang, S. H. Cationic Polymers for Coating Living Cells. *Macromol. Res.* **2018**, *26*, 1185−1192.
(169) Carter, J. L.; Drachuk, I.; Harbaugh, S.; Kelley-Loughnane, N.; Stone, M.; Tsukruk, V. V. Truly Nonionic Polymer Shells for the Encapsulation of Living Cells. *Macromol. Biosci.* **2011**, *11*, 1244−1253.
(170) Drachuk, I.; Shchepelina, O.; Lisunova, M.; Harbaugh, S.; Kelley-Loughnane, N.; Stone, M.; Tsukruk, V. V. pH-Responsive Layer-by-Layer Nanoshells for Direct Regulation of Cell Activity. *ACS Nano* **2012**, *6*, 4266−4278.
(171) Kozlovskaya, V.; Zavgorodnya, O.; Chen, Y.; Ellis, K.; Tse, H. M.; Cui, W.; Thompson, J. A.; Kharlampieva, E. Ultrathin Polymeric Coatings Based on Hydrogen-Bonded Polyphenol for Protection of Pancreatic Islet Cells. *Adv. Funct. Mater.* **2012**, *22*, 3389−3398.
(172) Kim, J. Y.; Lee, B. S.; Choi, J.; Kim, B. J.; Choi, J. Y.; Kang, S. M.; Yang, S. H.; Choi, I. S. Cytocompatible Polymer Grafting from Individual Living Cells by Atom-Transfer Radical Polymerization. *Angew. Chem., Int. Ed.* **2016**, *55*, 15306−15309.
(173) Niu, J.; Lunn, D. J.; Pusuluri, A.; Yoo, Y. I.; O'Malley, M. A.; Mitragotri, S.; Soh, H. T.; Hawker, C. J. Engineering Live Cell Surfaces with Functional Polymers via Cytocompatible Controlled Radical Polymerization. *Nat. Chem.* **2017**, *9*, 537−545.
(174) Belluati, A.; Happel, D.; Erbe, M.; Kirchner, N.; Szelwicka, A.; Bloch, A.; Berner, V.; Christmann, A.; Hertel, B.; Pardehkhorram, R.; Reyhani, A.; Kolmar, H.; Bruns, N. Self-Decorating Cells *via* Surface-Initiated Enzymatic Controlled Radical Polymerization. *Nanoscale* **2023**, *15*, 19486−19492.
(175) Yang, J.; Li, J.; Wang, X.; Li, X.; Kawazoe, N.; Chen, G. Single Mammalian Cell Encapsulation by *In Situ* Polymerization. *J. Mater. Chem. B* **2016**, *4*, 7662−7668.
(176) Gottipati, A.; Chelvarajan, L.; Peng, H.; Kong, R.; Cahall, C. F.; Li, C.; Tripathi, H.; Al-Darraji, A.; Ye, S.; Elsawalhy, E.; Abdel-Latif, A.; Berron, B. J. Gelatin Based Polymer Cell Coating Improves Bone Marrow-Derived Cell Retention in the Heart after Myocardial Infarction. *Stem Cell Rev. Rep.* **2019**, *15*, 404−414.
(177) Peng, H.; Chelvarajan, L.; Donahue, R.; Gottipati, A.; Cahall, C. F.; Davis, K. A.; Tripathi, H.; Al-Darraji, A.; Elsawalhy, E.; Dobrozsi, N.; Srinivasan, A.; Levitan, B. M.; Kong, R.; Gao, E.; Abdel-Latif, A.; Berron, B. J. Polymer Cell Surface Coating Enhances Mesenchymal Stem Cell Retention and Cardiac Protection. *ACS Appl. Bio Mater.* **2021**, *4*, 1655−1667.
(178) Davis, K. A.; Peng, H.; Chelvarajan, L.; Abdel-Latif, A.; Berron, B. J. Increased Yield of Gelatin Coated Therapeutic Cells Through Cholesterol Insertion. *J. Biomed. Mater. Res., Part A* **2021**, *109*, 326−335.
(179) Wang, G.; Zhang, K.; Wang, Y.; Zhao, C.; He, B.; Ma, Y.; Yang, W. Decorating an Individual Living Cell with a Shell of Controllable Thickness by Cytocompatible Surface Initiated Graft Polymerization. *Chem. Commun.* **2018**, *54*, 4677−4680.
(180) Wang, K.; Zhao, C.; Ma, Y.; Yang, W. Yolk-Shell Encapsulation of Cells by Biomimetic Mineralization and Visible Light-Induced Surface Graft Polymerization. *Biomacromolecules* **2023**, *24*, 6032−6040.
(181) Lilly, J. L.; Romero, G.; Xu, W.; Shin, H. Y.; Berron, B. J. Characterization of Molecular Transport in Ultrathin Hydrogel Coatings for Cellular Immunoprotection. *Biomacromolecules* **2015**, *16*, 541−549.
(182) Belluati, A.; Harley, I.; Lieberwirth, I.; Bruns, N. An Outer Membrane-Inspired Polymer Coating Protects and Endows *Escherichia coli* with Novel Functionalities. *Small* **2023**, *19*, 2303384.
(183) Xie, X.; Criddle, C.; Cui, Y. Design and Fabrication of Bioelectrodes for Microbial Bioelectrochemical Systems. *Energy Environ. Sci.* **2015**, *8*, 3418−3441.
(184) Wang, S.; Chen, H.; Xu, Z.; Wang, X.; Tao, Z.; Wang, L.; Liu, X.; Huang, X. Engineering Native Cells by TiO_2 Nanoparticles and Polypyrrole for Light-Responsive Manipulation of Collective Behaviors of Unicellular Organisms. *ACS Appl. Nano Mater.* **2023**, *6*, 4626−4635.
(185) Liang, W.; Carraro, F.; Solomon, M. B.; Bell, S. G.; Amenitsch, H.; Sumby, C. J.; White, N. G.; Falcaro, P.; Doonan, C. J. Enzyme Encapsulation in a Porous Hydrogen-Bonded Organic Framework. *J. Am. Soc. Chem.* **2019**, *141*, 14298−14305.

https://doi.org/10.1021/acs.chemrev.4c00984
Chem. Rev. XXXX, XXX, XXX−XXX

(186) Zheng, Y.; Zhang, S.; Guo, J.; Shi, R.; Yu, J.; Li, K.; Li, K.; Li, N.; Zhang, Z.; Chen, Y. Green and Scalable Fabrication of High-Performance Biocatalysts Using Covalent Organic Frameworks as Enzyme Carriers. *Angew. Chem., Int. Ed.* **2022**, *61*, No. e202208744.
(187) Yu, D.; Zhang, H.; Liu, Z.; Liu, C.; Du, X.; Ren, J.; Qu, X. Hydrogen-Bonded Organic Framework (HOF)-Based Single-Neural Stem Cell Encapsulation and Transplantation to Remodel Impaired Neural Networks. *Angew. Chem., Int. Ed.* **2022**, *61*, No. e202201485.
(188) Liang, J.; Chen, Q.; Yong, J.; Suyama, H.; Biazik, J.; Njegic, B.; Rawal, A.; Liang, K. Covalent-Organic Framework Nanobionics for Robust Cytoprotection. *Chem. Sci.* **2024**, *15*, 991−1002.
(189) Zheng, D.; Zheng, Y.; Tan, J.; Zhang, Z.; Huang, H.; Chen, Y. Co-immobilization of Whole Cells and Enzymes by Covalent Organic Framework for Biocatalysis Process Intensification. *Nat. Commun.* **2024**, *15*, 5510.
(190) Wei, Y.; Zhou, F.; Zhang, D.; Chen, Q.; Xing, D. A Graphene Oxide Based Smart Drug Delivery System for Tumor Mitochondria-Targeting Photodynamic Therapy. *Nanoscale* **2016**, *8*, 3530−3538.
(191) Chung, C.; Kim, Y.-K.; Shin, D.; Ryoo, S.-R.; Hong, B. H.; Min, D.-H. Biomedical Applications of Graphene and Graphene Oxide. *Acc. Chem. Res.* **2013**, *46*, 2211−2224.
(192) Kempaiah, R.; Chung, A.; Maheshwari, V. Graphene as Cellular Interface: Electromechanical Coupling with Cells. *ACS Nano* **2011**, *5*, 6025−6031.
(193) Jiang, N.; Ying, G.-L.; Yetisen, A. K.; Montelongo, Y.; Shen, L.; Xiao, Y.-X.; Busscher, H. J.; Yang, X.-Y.; Su, B.-L. A Bilayered Nanoshell for Durable Protection of Single Yeast Cells against Multiple, Simultaneous Hostile Stimuli. *Chem. Sci.* **2018**, *9*, 4730−4735.
(194) Gao, H.; Liu, J.-H.; Anchustegui, V. A. L.; Chang, Y.; Zhang, J.; Dong, Y. The Protective Effects of Graphene Oxide Against the Stress from Organic Solvent by Covering Hela cells. *Curr. Nanosci.* **2019**, *15*, 412−419.
(195) Dong, Y.; Chang, Y.; Gao, H.; León Anchustegui, V. A.; Yu, Q.; Wang, H.; Liu, J.-H.; Wang, S. Characteristic Synergistic Cytotoxic Effects Toward Cells in Graphene Oxide Dressing with Cadmium and Copper Ions. *Toxicol. Res.* **2019**, *8*, 908−917.
(196) Zhou, Z.; Mukherjee, S.; Hou, S.; Li, W.; Elsner, M.; Fischer, R. A. Porphyrinic MOF Film for Multifaceted Electrochemical Sensing. *Angew. Chem., Int. Ed.* **2021**, *60*, 20551−20557.
(197) Liang, K.; Richardson, J. J.; Cui, J.; Caruso, F.; Doonan, C. J.; Falcaro, P. Metal−Organic Framework Coatings as Cytoprotective Exoskeletons for Living Cells. *Adv. Mater.* **2016**, *28*, 7910−7914.
(198) Ejima, H.; Richardson, J. J.; Liang, K.; Best, J. P.; van Koeverden, M. P.; Such, G. K.; Cui, J.; Caruso, F. One-Step Assembly of Coordination Complexes for Versatile Film and Particle Engineering. *Science* **2013**, *341*, 154−157.
(199) Park, J. H.; Kim, K.; Lee, J.; Choi, J. Y.; Hong, D.; Yang, S. H.; Caruso, F.; Lee, Y.; Choi, I. S. A Cytoprotective and Degradable Metal−Polyphenol Nanoshell for Single-Cell Encapsulation. *Angew. Chem., Int. Ed.* **2014**, *53*, 12420−12425.
(200) Liang, K.; Richardson, J. J.; Doonan, C. J.; Mulet, X.; Ju, Y.; Cui, J.; Caruso, F.; Falcaro, P. An Enzyme-Coated Metal−Organic Framework Shell for Synthetically Adaptive Cell Survival. *Angew. Chem., Int. Ed.* **2017**, *56*, 8510−8515.
(201) Ding, M.; Flaig, R. W.; Jiang, H.-L.; Yaghi, O. M. Carbon Capture and Conversion Using Metal−Organic Frameworks and MOF-based materials. *Chem. Soc. Rev.* **2019**, *48*, 2783−2828.
(202) Furukawa, H.; Cordova, K. E.; O'Keeffe, M.; Yaghi, O. M. The Chemistry and Applications of Metal−Organic Frameworks. *Science* **2013**, *341*, 6149.
(203) Mallakpour, S.; Nikkhoo, E.; Hussain, C. M. Application of MOF Materials as Drug Delivery Systems for Cancer Therapy and Dermal Treatment. *Coord. Chem. Rev.* **2022**, *451*, 214262.
(204) Liang, K.; Ricco, R.; Doherty, C. M.; Styles, M. J.; Bell, S.; Kirby, N.; Mudie, S.; Haylock, D.; Hill, A. J.; Doonan, C. J.; Falcaro, P. Biomimetic Mineralization of Metal−Organic Frameworks as Protective Coatings for Biomacromolecules. *Nat. Commun.* **2015**, *6*, 7240.
(205) Liang, K.; Carbonell, C.; Styles, M. J.; Ricco, R.; Cui, J.; Richardson, J. J.; Maspoch, D.; Caruso, F.; Falcaro, P. Biomimetic Replication of Microscopic Metal−Organic Framework Patterns Using Printed Protein Patterns. *Adv. Mater.* **2015**, *27*, 7293−7298.
(206) Gan, L.; Velásquez-Hernández, M. D. J.; Emmerstorfer-Augustin, A.; Wied, P.; Wolinski, H.; Zilio, S. D.; Solomon, M.; Liang, W.; Doonan, C.; Falcaro, P. Multi-Layered ZIF-Coated Cells for the Release of Bioactive Molecules in Hostile Environments. *Chem. Commun.* **2022**, *58*, 10004−10007.
(207) Zhu, L.; Shen, B.; Song, Z.; Jiang, L. Permeabilized TreS-Expressing *Bacillus subtilis* Cells Decorated with Glucose Isomerase and a Shell of ZIF-8 as a Reusable Biocatalyst for the Coproduction of Trehalose and Fructose. *J. Agric. Food Chem.* **2020**, *68*, 4464−4472.
(208) Luzuriaga, M. A.; Herbert, F. C.; Brohlin, O. R.; Gadhvi, J.; Howlett, T.; Shahrivarkevishahi, A.; Wijesundara, Y. H.; Venkitapathi, S.; Veera, K.; Ehrman, R.; Benjamin, C. E.; Popal, S.; Burton, M. D.; Ingersoll, M. A.; De Nisco, N. J.; Gassensmith, J. J. Metal−Organic Framework Encapsulated Whole-Cell Vaccines Enhance Humoral Immunity against Bacterial Infection. *ACS Nano* **2021**, *15*, 17426−17438.
(209) Li, H.; Ma, L.; Zhu, N.; Liang, X.; Tian, X.; Liu, K.; Fu, X.; Wang, X.; Zhang, H.; Chen, H.; Liu, Q.; Yang, J. Mesenchymal Stromal Cells Surface Engineering for Efficient Hematopoietic Reconstruction. *Biomaterials* **2025**, *314*, 122882.
(210) Ji, Z.; Zhang, H.; Liu, H.; Yaghi, O. M.; Yang, P. Cytoprotective Metal−Organic Frameworks for Anaerobic Bacteria. *Proc. Natl. Acad. Sci. U.S.A.* **2018**, *115*, 10582−10587.
(211) Zhu, W.; Guo, J.; Amini, S.; Ju, Y.; Agola, J. O.; Zimpel, A.; Shang, J.; Noureddine, A.; Caruso, F.; Wuttke, S.; Croissant, J. G.; Brinker, C. J. SupraCells: Living Mammalian Cells Protected within Functional Modular Nanoparticle-Based Exoskeletons. *Adv. Mater.* **2019**, *31*, 1900545.
(212) Chen, Q.; Tang, S.; Li, Y.; Cong, Z.; Lu, D.; Yang, Q.; Zhang, X.; Wu, S. Multifunctional Metal−Organic Framework Exoskeletons Protect Biohybrid Sperm Microrobots for Active Drug Delivery from the Surrounding Threats. *ACS Appl. Mater. Interfaces* **2021**, *13*, 58382−58392.
(213) Maciel, M. M.; Correia, T. R.; Gaspar, V. M.; Rodrigues, J. M. M.; Choi, I. S.; Mano, J. F. Partial Coated Stem Cells with Bioinspired Silica as New Generation of Cellular Hybrid Materials. *Adv. Funct. Mater.* **2021**, *31*, 2009619.
(214) He, H.; Yuan, Y.; Wu, Y.; Lu, J.; Yang, X.; Lu, K.; Liu, A.; Cao, Z.; Sun, M.; Yu, M.; Wang, H. Exoskeleton Partial-Coated Stem Cells for Infarcted Myocardium Restoring. *Adv. Mater.* **2023**, *35*, 2307169.
(215) Kim, B. J.; Han, S.; Lee, K.-B.; Choi, I. S. Biphasic Supramolecular Self-Assembly of Ferric Ions and Tannic Acid across Interfaces for Nanofilm Formation. *Adv. Mater.* **2017**, *29*, 1700784.
(216) Lee, H.; Kim, W. I.; Youn, W.; Park, T.; Lee, S.; Kim, T.-S.; Mano, J. F.; Choi, I. S. Iron Gall Ink Revisited: *In Situ* Oxidation of Fe(II)−Tannin Complex for Fluidic-Interface Engineering. *Adv. Mater.* **2018**, *30*, 1805091.
(217) Park, J. H.; Choi, S.; Moon, H. C.; Seo, H.; Kim, J. Y.; Hong, S.-P.; Lee, B. S.; Kang, E.; Lee, J.; Ryu, D. H.; Choi, I. S. Antimicrobial Spray Nanocoating of Supramolecular Fe(III)−Tannic Acid Metal−Organic Coordination Complex: Applications to Shoe Insoles and Fruits. *Sci. Rep.* **2017**, *7*, 6980.
(218) Han, S. Y.; Hong, S.-P.; Kang, E. K.; Kim, B. J.; Lee, H.; Kim, W. I.; Choi, I. S. Iron Gall Ink Revisited: Natural Formulation for Black Hair-Dyeing. *Cosmetics* **2019**, *6*, 23.
(219) Lee, J.; Cho, H.; Choi, J.; Kim, D.; Hong, D.; Park, J. H.; Yang, S. H.; Choi, I. S. Chemical Sporulation and Germination: Cytoprotective Nanocoating of Individual Mammalian Cells with A Degradable Tannic Acid−Fe^{III} Complex. *Nanoscale* **2015**, *7*, 18918−18922.
(220) Park, T.; Kim, J. Y.; Cho, H.; Moon, H. C.; Kim, B. J.; Park, J. H.; Hong, D.; Park, J.; Choi, I. S. Artificial Spores: Immunoprotective Nanocoating of Red Blood Cells with Supramolecular Ferric Ion−Tannic Acid Complex. *Polymers* **2017**, *9*, 140.
(221) Lee, H.; Park, J.; Han, S. Y.; Han, S.; Youn, W.; Choi, H.; Yun, G.; Choi, I. S. Ascorbic Acid-Mediated Reductive Disassembly of Fe^{3+}−Tannic Acid Shells in Degradable Single-Cell Nanoencapsulation. *Chem. Commun.* **2020**, *56*, 13748−13751.

https://doi.org/10.1021/acs.chemrev.4c00984
Chem. Rev. XXXX, XXX, XXX−XXX

(222) Mandsberg, N. K.; Liao, W.; Yamanouchi, Y. A.; Boisen, A.; Ejima, H. Encapsulation of *Chlamydomonas reinhardtii* into a Metal−Phenolic Network. *Algal Res.* **2022**, *61*, 102569.
(223) Li, X.; Liu, H.; Lin, Z.; Richardson, J. J.; Xie, W.; Chen, F.; Lin, W.; Caruso, F.; Zhou, J.; Liu, B. Cytoprotective Metal−Phenolic Network Sporulation to Modulate Microalgal Mobility and Division. *Adv. Sci.* **2024**, *11*, 2308026.
(224) Kim, J. S.; Kim, B. J.; Lee, S. M.; Choi, I. S.; Park, J. H.; Choi, H.-G.; Jin, S. G. Single-Cell Nanoencapsulation Enables Fabrication of Probiotics-Loaded Hydrogel Dressing with Improved Wound Healing Efficacy In Vivo. *J. Pharm. Investig.* **2025**, *55*, 321−331.
(225) Li, W.; Bing, W.; Huang, S.; Ren, J.; Qu, X. Mussel Byssus-Like Reversible Metal-Chelated Supramolecular Complex Used for Dynamic Cellular Surface Engineering and Imaging. *Adv. Funct. Mater.* **2015**, *25*, 3775−3784.
(226) McKenney, P. T.; Driks, A.; Eichenberger, P. The *Bacillus subtilis* Endospore: Assembly and Functions of the Multilayered Coat. *Nat. Rev. Microbiol.* **2013**, *11*, 33−44.
(227) Nguyen, D. T.; Han, S. Y.; Kozlowski, F.; Seisenbaeva, G. A.; Kessler, V. G.; Kim, B. J.; Choi, I. S. Biphasic Water−Oil Systems for Functional Augmentation of Probiotic *Lactobacillus acidophilus* Nanoencapsulated in Luteolin−Fe^{3+} Shells. *Chem. Commun.* **2024**, *60*, 5330−5333.
(228) Lee, H.; Nguyen, D. T.; Kim, N.; Han, S. Y.; Hong, Y. J.; Yun, G.; Kim, B. J.; Choi, I. S. Enzyme-Mediated Kinetic Control of Fe^{3+}−Tannic Acid Complexation for Interface Engineering. *ACS Appl. Mater. Interfaces* **2021**, *13*, 52385−52394.
(229) Lee, J.; Choi, J.; Park, J. H.; Kim, M.-H.; Hong, D.; Cho, H.; Yang, S. H.; Choi, I. S. Cytoprotective Silica Coating of Individual Mammalian Cells through Bioinspired Silicification. *Angew. Chem., Int. Ed.* **2014**, *53*, 8056−8059.
(230) Youn, W.; Ko, E. H.; Kim, M.-H.; Park, M.; Hong, D.; Seisenbaeva, G. A.; Kessler, V. G.; Choi, I. S. Cytoprotective Encapsulation of Individual Jurkat T Cells within Durable TiO_2 Shells for T Cell Therapy. *Angew. Chem., Int. Ed.* **2017**, *56*, 10702.
(231) Fakhrullin, R. F.; Minullina, R. T. Hybrid Cellular−Inorganic Core−Shell Microparticles: Encapsulation of Individual Living Cells in Calcium Carbonate Microshells. *Langmuir* **2009**, *25*, 6617−6621.
(232) Flemke, J.; Maywald, M.; Sieber, V. Encapsulation of Living *E. coli* Cells in Hollow Polymer Microspheres of Highly Defined Size. *Biomacromolecules* **2013**, *14*, 207−214.
(233) Li, W.; Liu, Z.; Liu, C.; Guan, Y.; Ren, J.; Qu, X. Manganese Dioxide Nanozymes as Responsive Cytoprotective Shells for Individual Living Cell Encapsulation. *Angew. Chem., Int. Ed.* **2017**, *56*, 13661−13665.
(234) Oh, J.; Kumari, N.; Kim, D.; Kumar, A.; Lee, I. S. Ultrathin Silica-Tiling on Living Cells for Chemobiotic Catalysis. *Nat. Commun.* **2024**, *15*, 5773.
(235) Bourzac, K. A Conversation with Insung Choi. *ACS Cent. Sci.* **2016**, *2*, 579−580.
(236) Bourzac, K. C&EN Talks with Insung Choi, Cell Protector. *Chem. Eng. News* **2016**, *94*, 23.
(237) Wang, L.; Li, Y.; Yang, X.-Y.; Zhang, B.-B.; Ninane, N.; Busscher, H. J.; Hu, Z.-Y.; Delneuville, C.; Jiang, N.; Xie, H.; Van Tendeloo, G.; Hasan, T.; Su, B.-L. Single-Cell Yolk-Shell Nanoencapsulation for Long-Term Viability with Size-Dependent Permeability and Molecular Recognition. *Natl. Sci. Rev.* **2021**, *8*, No. nwaa097.

https://doi.org/10.1021/acs.chemrev.4c00984
Chem. Rev. XXXX, XXX, XXX−XXX